USGS
science for a changing world

Prepared in cooperation with the U.S. Forest Service

Geologic Framework, Regional Aquifer Properties (1940s–2009), and Spring, Creek, and Seep Properties (2009–10) of the Upper San Mateo Creek Basin near Mount Taylor, New Mexico

Scientific Investigations Report 2012–5019

U.S. Department of the Interior
U.S. Geological Survey

Cover: Cibola San Mateo Creek Basin.

Geologic Framework, Regional Aquifer Properties (1940s–2009), and Spring, Creek, and Seep Properties (2009–10) of the Upper San Mateo Creek Basin near Mount Taylor, New Mexico

By Jeff B. Langman, Jesse E. Sprague, and Roger A. Durall

Prepared in cooperation with the U.S. Forest Service

Scientific Investigations Report 2012–5019

U.S. Department of the Interior
U.S. Geological Survey

U.S. Department of the Interior
KEN SALAZAR, Secretary

U.S. Geological Survey
Marcia K. McNutt, Director

U.S. Geological Survey, Reston, Virginia: 2012

This and other USGS information products are available at http://store.usgs.gov/
U.S. Geological Survey
Box 25286, Denver Federal Center
Denver, CO 80225

To learn about the USGS and its information products visit http://www.usgs.gov/
1-888-ASK-USGS

Any use of trade, product, or firm names is for descriptive purposes only and does not imply endorsement by the U.S. Government.

Although this report is in the public domain, permission must be secured from the individual copyright owners to reproduce any copyrighted materials contained within this report.

Suggested citation:
Langman, J.B., Sprague, J.E., and Durall, R.A., 2012, Geologic framework, regional aquifer properties (1940s–2009), and spring, creek, and seep properties (2009–10) of the upper San Mateo Creek Basin near Mount Taylor, New Mexico: U.S. Geological Survey Scientific Investigations Report 2012–5019, 96 p.

The cooperation of many individuals and organizations was essential for completion of this study. The authors acknowledge the support and help of personnel from the USFS's Cibola National Forest. In particular, Mary Dereske and Livia Crowley who helped guide this study and provided useful insight for completion of study goals. Additionally, the authors wish to thank Harry Lee for allowing access to the springs, creeks, and seeps on the Lee Ranch and his insight into the hydrologic resources of the target area.

Contents

Abstract 1
Introduction 1
Purpose and Scope 2
Description of the Study Area 2
Structural and Surface Geology 3
Subsurface Geology 6
Climate and Surface Hydrology 6
Groundwater Hydrology and Primary Aquifers 6
Valley Alluvium and Menefee Formation 7
Point Lookout, Crevasse Canyon, Gallup, Dakota, and Morrison Formations 8
Chinle Group 9
San Andres and Glorieta Formations 9
Human Influence on Water Resources 9
Previous Studies 10
Study Methods 10
Existing Data 10
New Data 11
Quality-Assurance 14
Geologic Framework and Regional Aquifer Properties 15
San Mateo Creek Basin Geology 15
Hydraulic Properties of Major Aquifers 15
Horizontal Flow 15
Water-Level Elevations 21
Hydraulic Conductivity 22
Groundwater Composition of Major Aquifers 22
Major Elements 22
Trace Elements 25
Contaminants of Concern 25
Spring, Creek, and Seep Properties of the Upper San Mateo Creek Basin, New Mexico, 2009 and 2010 26
Spring, Creek, and Seep Flow 26
Spring, Creek, and Seep Water Composition 27
Water Isotopes and Evaporation 30
Major Elements 31
Saturation Indices 31
Creek Flow Paths and Geochemical Model of Transition from Creek to Seep 32
Summary 35
References 36
Appendixes
1. Historical Groundwater-Elevation Data 41
2. Historical Groundwater Major-Element Data 53
3. Historical Groundwater Trace-Element Data 65
4. Historical Groundwater Contaminants-of-Concern Data 79

Figures

1. Map showing location of the upper San Mateo Creek Basin 2
2. Map showing regional geologic structural areas, study area, and target area 3
3. Map showing San Mateo Creek Basin in the regional landform 4
4. Map showing regional surface geology 5
5. Generalized stratigraphic column of the subsurface geology below the valley forms in the southern San Juan Basin 7
6. Geologic cross section from west to east through the upper San Mateo Creek Basin 8
7. Map showing sampling sites and surface topography of the upper San Mateo Creek Basin 12
8. Map showing surface geology of the upper San Mateo Creek Basin 18
9. Map showing relative differences in water-level elevations for the distribution of water-level data compiled for wells with screens located in the Quaternary alluvium 19
10. Map showing relative differences in water-level elevations for the distribution of water-level data compiled for wells with screens located in Cretaceous, Jurassic, Triassic, and Permian formations 20
11. Trilinear diagrams of major-element relations for groundwater collected from the deposits and formations found in the study area 24
12. Graphs showing landform gradients between sampling sites on El Rito and San Mateo Creeks and underlying geologic formations 27
13. Graph showing dissolved oxygen and pH relation for water from El Rito, San Lucas, and San Mateo Creeks 30
14. Graph showing stable isotope ratios for water from El Rito, San Lucas, and San Mateo Creeks 31
15. Trilinear diagram of major-element relations for water from El Rito, San Lucas, and San Mateo Creeks 32

Tables

1. Information for the spring-, creek-, and seep-sample sites in the upper San Mateo Creek Basin 13
2. Sample analytes and laboratory analysis methods 14
3. Stratigraphic, lithologic, and aquifer characteristics of geologic deposits and formations in the study and target areas 16
4. Water-level elevation statistics for aquifers in consolidated formations in the study area 21
5. Formation characteristics indicative of horizontal hydraulic-conductivity variation among the aquifers in the study area 23
6. Number of detections of frequently detected trace elements in groundwater from the study area 25
7. Number of detections of contaminants of concern in groundwater from the study area 26
8. Physical and chemical properties of springs, creeks, and seeps within the target area, August 2009 28

9. Physical and chemical properties of springs, creeks, and seeps within the target area, May 2010 29
10. Saturation indices of possible common minerals for water collected from the spring, creek, and seep locations along El Rito Creek in the target area 33
11. Saturation indices of possible common minerals for water collected from the spring, creek, and seep locations along San Mateo Creek in the target area 33
12. Geochemical model results for creek to seep locations along El Rito and San Mateo Creeks 34

Conversion Factors, Datums, and Abbreviations

Inch/Pound to SI

Multiply	By	To obtain
inch	2.540	centimeter (cm)
foot (ft)	0.3048	meter (m)
yard (yd)	0.9144	meter (m)
mile (mi)	1.609	kilometer (km)
acre	4,047	square meter (m^2)
gallon (gal)	3.785	liter (L)
foot per day (ft/d)	0.00035	centimeters per second (cm/s)
foot per year (ft/yr)	$9.7xl0^{-7}$	centimeters per second (cm/s)
foot squared per day (ft^2/d)	0.09290	meter squared per day (m^2/d)
cubic feet per second (ft^3/s)	0.0283	cubic meters per minute (m^3/s)
acre-feet per year (acre-ft/yr)	1,233	cubic meter per year (m^3/yr)

Temperature in degrees Celsius (°C) can be converted to degrees Fahrenheit (°F) as follows:

$$°F = (1.8 \times °C) + 32$$

Vertical coordinate information is referenced to the North American Vertical Datum of 1988 (NAVD 88).

Horizontal coordinate information is referenced to the North American Datum of 1983 (NAD 83).

Specific conductance is given in microsiemens per centimeter at 25 degrees Celsius (µS/cm).

Abbreviations

<	less than
>	greater than
%	percent
‰	per mil
±	plus or minus
Ag	silver
Al	aluminum

As	arsenic
B	boron
Ba	barium
Be	beryllium
Br	bromine
C	carbon
CO_2	carbon dioxide
Ca	calcium
Cd	cadmium
Cl	chloride
Cr	chromium
Co	cobalt
Cu	copper
δ	delta, indicates isotopic ratio compared to standard, in per mil units
F	fluoride
Fe	iron
H	hydrogen
HCO_3	bicarbonate
Hg	mercury
IAP	ion activity product
K	potassium
K	hydraulic conductivity
K_{sp}	solubility product
Li	lithium
Ma	million years before present
MDL	method detection level
Mg	magnesium
Mn	manganese
Mo	molybdenum
Na	sodium
Ni	nickel
NO_3	nitrate (may also include nitrate plus nitrite)
NTU	nephelometric turbidity unit
O	oxygen
Pb	lead
Ra	radium
redox	reduction-oxidation
Sb	antimony
Se	selenium
Si	silicon
SO_4	sulfate
TDS	total dissolved solids
Tl	thallium
U	uranium
USEPA	U.S. Environmental Protection Agency
USFS	U.S. Forest Service
USGS	U.S. Geological Survey
V	vanadium
Zn	zinc

Geologic Framework, Regional Aquifer Properties (1940s–2009), and Spring, Creek, and Seep Properties (2009–10) of the Upper San Mateo Creek Basin near Mount Taylor, New Mexico

By Jeff B. Langman, Jesse E. Sprague, and Roger A. Durall

Abstract

The U.S. Geological Survey, in cooperation with the U.S. Forest Service, examined the geologic framework, regional aquifer properties, and spring, creek, and seep properties of the upper San Mateo Creek Basin near Mount Taylor, which contains areas proposed for exploratory drilling and possible uranium mining on U.S. Forest Service land. The geologic structure of the region was formed from uplift of the Zuni Mountains during the Laramide Orogeny and the Neogene volcanism associated with the Mount Taylor Volcanic Field. Within this structural context, numerous aquifers are present in various Paleozoic and Mesozoic sedimentary formations and the Quaternary alluvium. The distribution of the aquifers is spatially variable because of the dip of the formations and erosion that produced the current landscape configuration where older formations have been exhumed closer to the Zuni Mountains.

Many of the alluvial deposits and formations that contain groundwater likely are hydraulically connected because of the solid-matrix properties, such as substantive porosity, but shale layers such as those found in the Mancos Formation and Chinle Group likely restrict vertical flow. Existing water-level data indicate topologically downgradient flow in the Quaternary alluvium and indiscernible general flow patterns in the lower aquifers. According to previously published material and the geologic structure of the aquifers, the flow direction in the lower aquifers likely is in the opposite direction compared to the alluvium aquifer. Groundwater within the Chinle Group is known to be confined, which may allow upward migration of water into the Morrison Formation; however, confining layers within the Chinle Group likely retard upward leakage. Groundwater was sodium-bicarbonate/sulfate dominant or mixed cation-mixed anion with some calcium/bicarbonate water in the study area. The presence of the reduction/oxidation-sensitive elements iron and manganese in groundwater indicates reducing conditions at some time or in some location(s) in most aquifers. Frequent detections of zinc in the alluvium aquifer may represent anthropogenic influences such as mining.

Along the mesas in the upper San Mateo Creek Basin, springs that form various creeks, including El Rito and San Mateo Creeks, discharge from the basalt-cap layer and the upper Cretaceous sedimentary layers. Streamflow in El Rito and San Mateo Creeks flows down steep gradients near the mesas sustained by groundwater discharges, and this streamflow transitions to shallow groundwater contained within the valley alluvium through infiltration where the subsequent groundwater is restricted from downward migration by the shaly Menefee Formation. This shallow groundwater reemerges at seeps where the land surface has been eroded below the groundwater level. Spring- and creek-water samples contained small amounts of dissolved solutes, and seep water contained substantially larger amounts of dissolved solutes. The pH of water within the creeks was neutral to alkaline, and all locations exhibited well-oxygenated conditions, although typically at substantially less than saturated levels. Changes in the stable-isotope ratios of water between spring and summer samples indicate differences in source-water inputs that likely pertain to seasonal recharge sources. Results of the water-isotope analysis and geochemical modeling indicate little evaporation and chemical weathering at the spring and creek sites but stronger evaporation and chemical weathering by the time the water reaches the seep locations in the center of the upper San Mateo Creek Basin.

Introduction

The water resources of the San Mateo Creek Basin (fig. 1) are important to the citizens of New Mexico, in particular, the town of San Mateo and the city of Grants, for potable-water sources. Citizens and tribal groups in this area are concerned about the possible effects on the water resources from exploratory drilling and possible mining of uranium (U) as currently (2011) proposed by various companies. Uranium mining in this region has historically targeted members of the Morrison Formation, and previous mining operations dewatered aquifers at and above the ore. Water generated during dewatering was discharged to natural waterways without

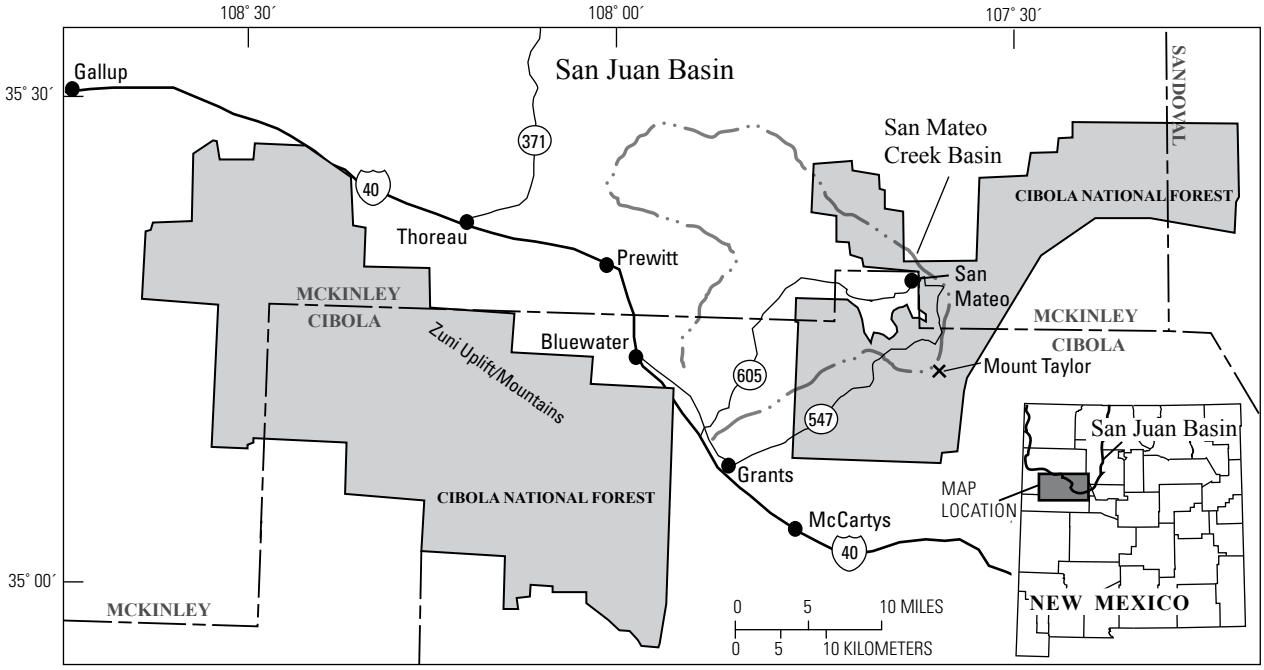

Figure 1. Location of the upper San Mateo Creek Basin.

treatment, because much of the U mining occurred prior to major environmental legislation such as the Clean Water Act. This mine water was a substantial source of contamination of sediment, alluvial aquifers, and deeper aquifers in areas of faulting (Schoeppner, 2008). The New Mexico Environment Department has issued a health advisory for current and future private wells within the San Mateo Creek Basin concerning various contaminants of concern including gross alpha activity, nitrate (NO_3), radium (Ra), and U (New Mexico Environment Department, 2009). The U.S. Geological Survey (USGS), in cooperation with the U.S. Forest Service (USFS), examined the geologic framework; regional aquifer properties; and spring, creek, and seep properties of the upper San Mateo Creek Basin near Mount Taylor, which contains areas proposed for exploratory drilling and possible uranium mining on USFS land.

Purpose and Scope

This report presents the results of a study to characterize the geologic framework; regional aquifer properties; and spring, creek, and seep properties of the upper San Mateo Creek Basin. Existing data (data collected prior to this study; 1940s to 2009) were used to describe groundwater characteristics of major aquifers including general directions of groundwater flow and groundwater composition. New data were collected in 2009 and 2010 to characterize the springs, creeks, and seeps within the upper San Mateo Creek Basin. To evaluate the geologic framework; regional aquifer properties; and spring, creek, and seep properties of the upper San Mateo Creek Basin, the target area of the study (target area) encompasses the upper San Mateo Creek Basin, but a larger study area composed of parts of the Zuni Uplift and Chaco Slope regions was used to ensure sufficient existing data for evaluation of geologic and aquifer properties relevant to the target area (fig. 2).

Description of the Study Area

The study area is composed of the eastern slope of the Zuni Uplift and much of the Chaco Slope region within the southeastern part of the San Juan Basin (fig. 2). The area was a low-lying plain in the late Paleozoic Era and much of the Mesozoic Era, and the landscape was transformed to the current structure mostly because of the Laramide Orogeny during the late Cretaceous age (Woodward and Callender, 1977; Baldwin and Anderholm, 1992; Cather, 2003). Prior to the Laramide Orogeny, the area was part of the Western Interior Basin, a broad foreland basin that subsided partially in response to tectonic loading in the Cordilleran thrust belt, which allowed repeated transgressive-regressive sequences (Cather, 2003). The Zuni Uplift that constitutes the Zuni Mountains was formed during the Ancestral Rockies and Laramide Orogenies (Strickland and others, 2003). The Chaco Slope represents the northeast flank of the Zuni Uplift where formation dip lessens with distance from the apex of the fold.

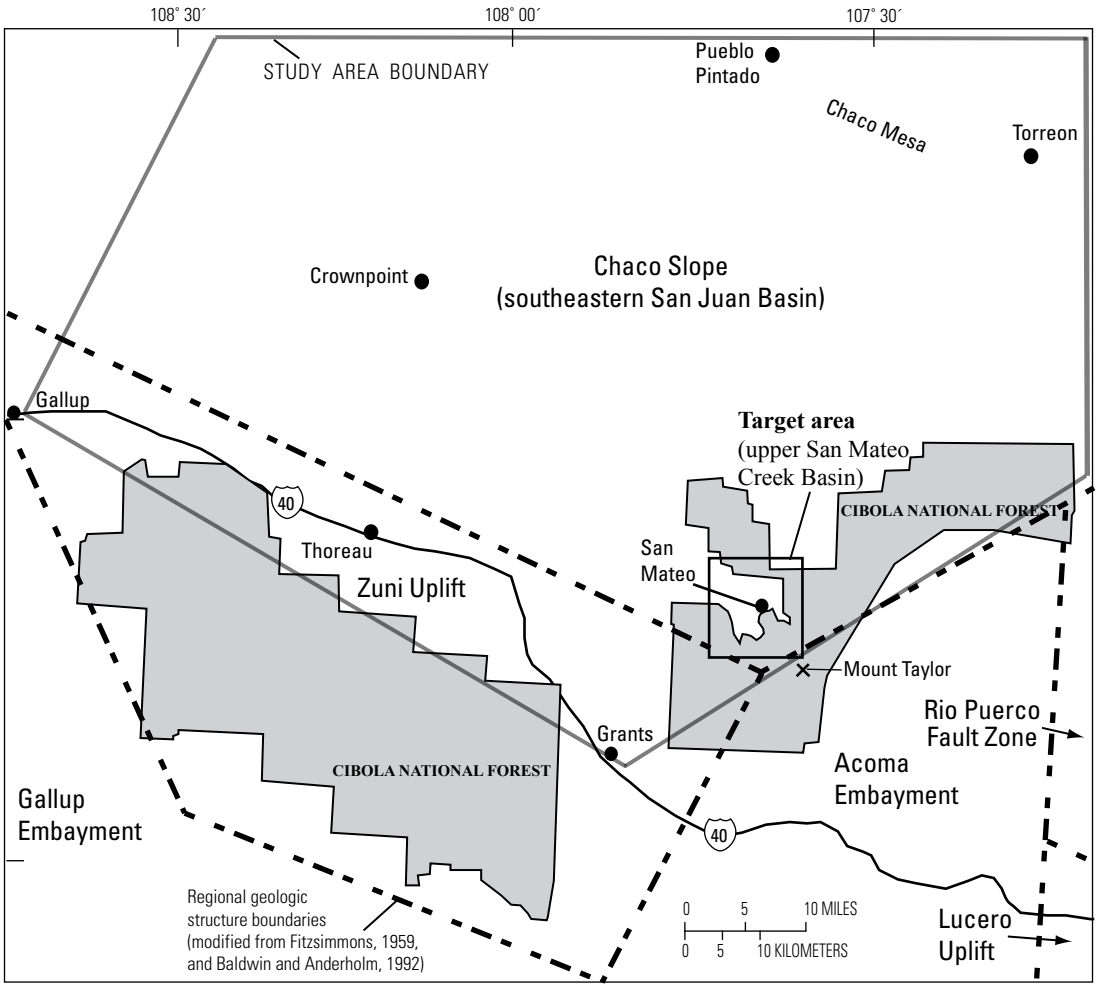

Figure 2. Regional geologic structural areas, study area, and target area.

The Acoma Embayment was a synclinal depositional area east of the Zuni Uplift and now includes Mount Taylor and the Rio Puerco Fault Zone to the east of the mountain (fig. 2). The study area includes valleys and mesas formed from regional folding of the landscape and subsequent erosion of less-resistant strata. The target area of upper San Mateo Creek Basin is the upper, northeast part of the basin above the confluence of San Mateo Creek and Arroyo del Puerto (fig. 3).

Structural and Surface Geology

The Zuni Mountains and Mount Taylor are the major elevated, structural features of the region. The axis of the Zuni Mountains is located about 15 mi west-southwest of Grants and is oriented southeast to northwest. The uplift that formed Zuni Mountains is a monoclinal fold about 75 mi long and 30 mi wide. The study and target areas are located along the east side of the monocline, which has a gentle slope to the north-northeast of about 5 to 10 degrees. The surface geology of the target area is dominated by Mount Taylor and its associated volcanic flows. Mount Taylor is located about 15 mi northeast of Grants and about 8 mi southeast of San Mateo (figs. 3 and 4). The mountain reaches 11,301 ft and is part of a larger, northeast-trending volcanic field. Mount Taylor is primarily an accumulation of thick, viscous trachydacitic and trachyandesitic lavas with a surrounding apron of lava debris and pyroclastics (Crumpler, 2003). This volcanic activity was caused by extensional tectonics that began in the Neogene and continued into the Quaternary period (Laughlin and others, 1994; Keating and Valentine, 1998; WoldeGabriel and others, 1999). Surrounding mesas tend to consist of an upper layer of Neogene rhyolitic domes and pyroclastic deposits with a resistant cap of basalt lava and scoria (Lipman and Mehnert, 1979; Perry and others, 1990; Laughlin and others, 1994).

An erosional period that followed the Neogene volcanism created the valley forms in the study area. It is estimated that the land surface was eroded up to 150 to 200 feet (ft) below current land surface (Gordon, 1961). Following this erosional

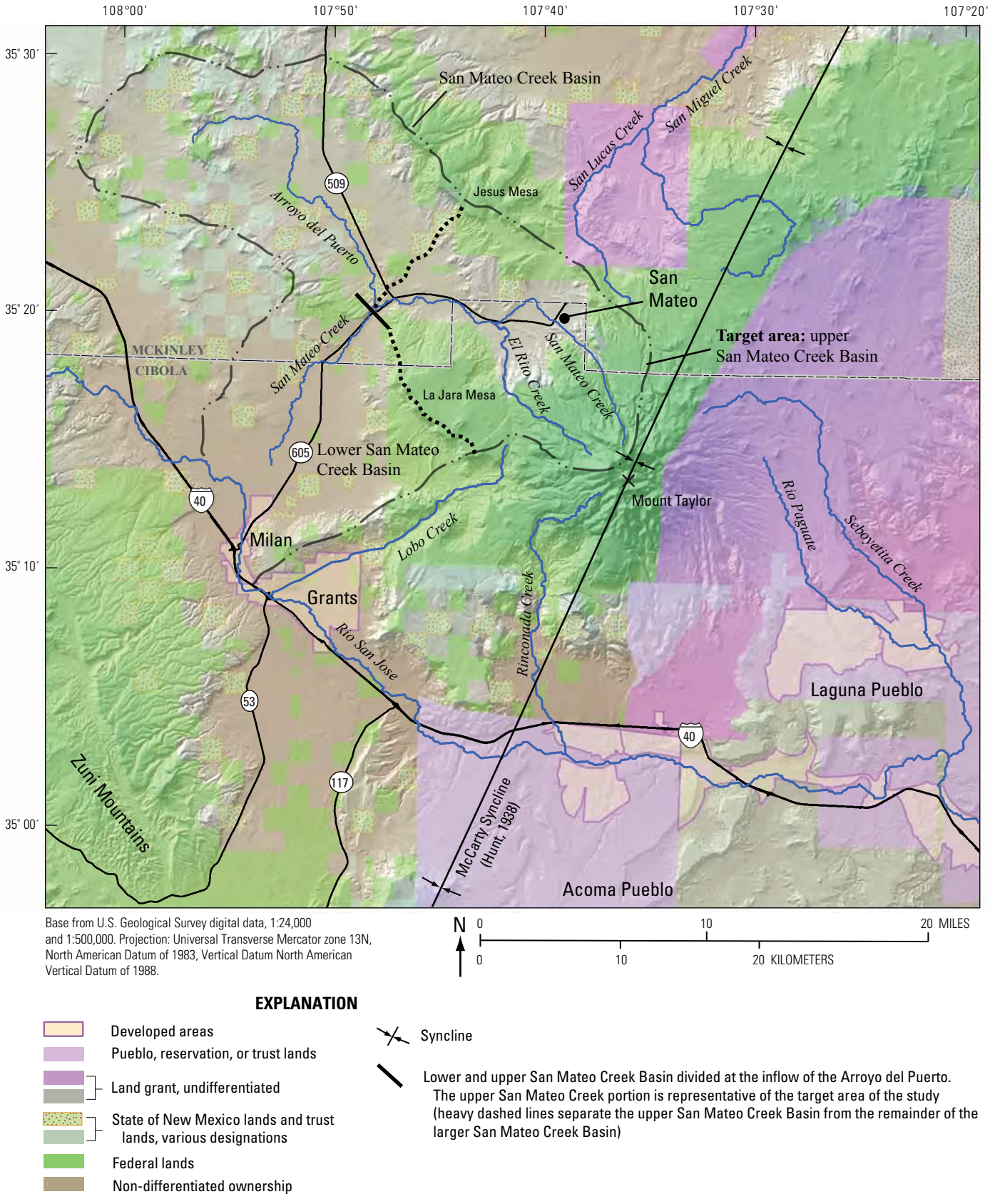

Figure 3. San Mateo Creek Basin in the regional landform.

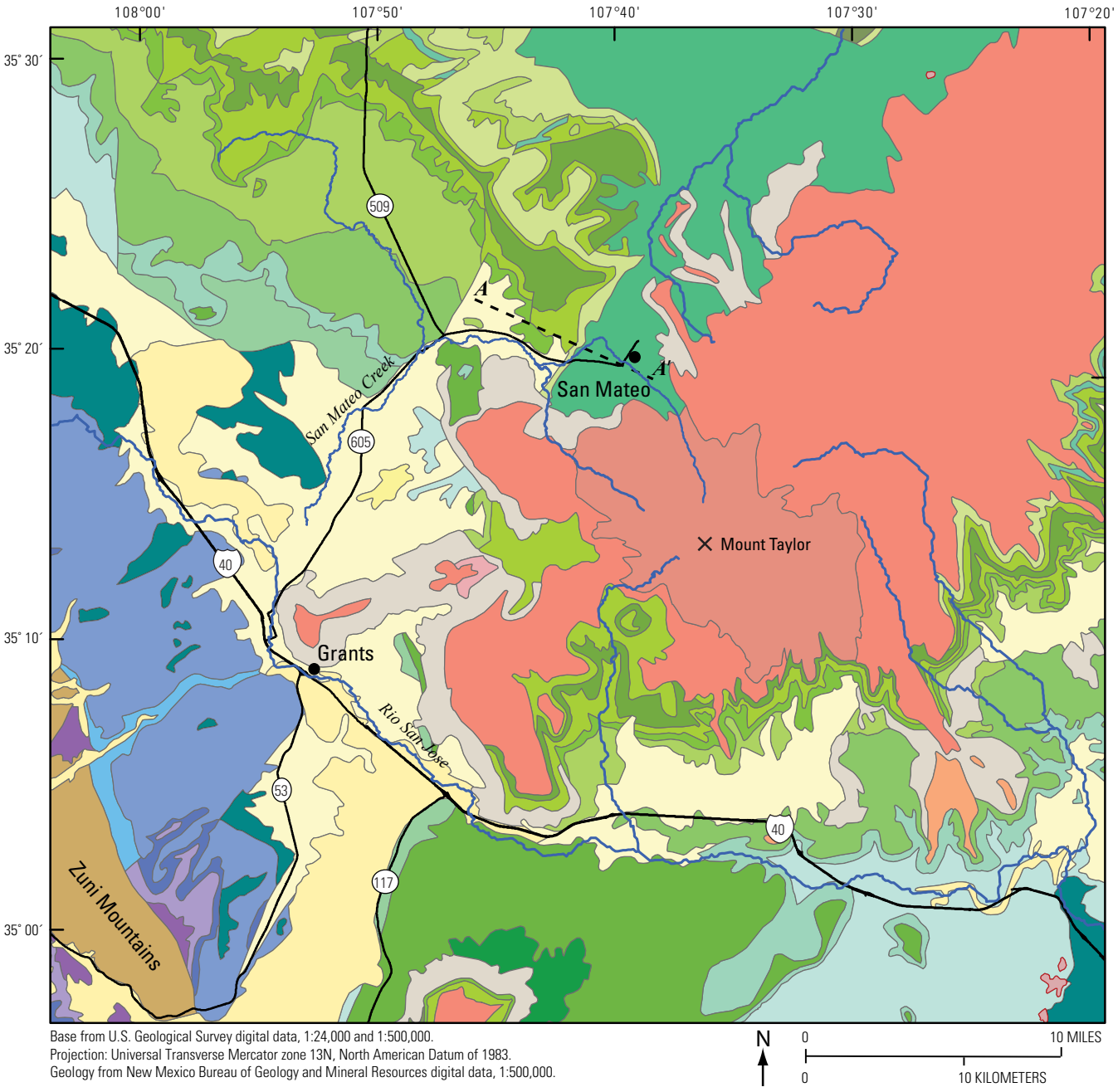

EXPLANATION

Quaternary
- Alluvium
- Landslide deposit
- Eolian deposit
- Basaltic to andesitic lava flows

Neogene
- Basaltic to andesitic lava flows (Pliocene)
- Basaltic to andesitic lava flows (Miocene)
- Silicic to intermediate volcanic rocks
- Intermediate to silicic volcanic rocks
- Intrusive rocks of intermediate to silicic composition

Cretaceous
- Menefee
- Point Lookout
- Satan Tongue, Mancos
- Hasta Tongue, Point Lookout
- Mulatto Tongue, Mancos
- Crevasse Canyon
- Gallup
- Rio Salado Tongue, Mancos
- Mancos
- Mancos, lower
- Mancos and Dakota
- Dakota

Jurassic
- Upper Jurassic, undivided
- Morrison
- Lower Jurassic, undivided, may contain Entrada, Todilto, Summerville, and (or) Bluff

Triassic
- Chinle (Group)

Permian
- Permian, undivided
- San Andres
- Glorieta
- Yeso
- Abo

Precambrian
- Precambrian, undivided

A--*A*′ is a trace for a geologic cross section shown in figure 6.

Figure 4. Regional surface geology.

period, the valleys filled with sediment and additional basalt flows to the present land-surface elevation. Sediment from the eroding highlands of the mesas was deposited in the valleys and formed unconsolidated alluvium mixed with boulder-sized basalt rocks that were transported to the valley floors through either colluvial or alluvial action. In the higher elevations of the target area, the alluvium is about 3 to 6 ft thick with increased thicknesses in the downstream direction; alluvium thicknesses can reach 65 ft or more where San Mateo Creek exits the target area (Brod, 1979). Beneath the basalt caps of the mesas, sedimentary formations are exposed in the target area including the Cretaceous Menefee, Point Lookout, Crevasse Canyon, Gallup, Mancos, and Dakota Formations and small exposures of the Morrison Formation of Jurassic age (New Mexico Bureau of Geology and Mineral Resources, 2003).

Subsurface Geology

Igneous and metamorphic bedrock of Precambrian age underlay younger rock throughout the region, and this bedrock is exposed within the Zuni Mountains (Gordon, 1961). No rocks of Cambrian to Middle Pennsylvanian age are present in the region, because this region was likely a stable paleohighland during that time (Baldwin and Anderholm, 1992). Deposition and preservation of open-marine sediment began in the late Pennsylvanian and transitioned to deposition of continental- and restricted-marine sediment in the early Permian age (Baars, 1962), during which time the Abo, Yeso, Glorieta, and San Andres Formations were deposited (fig. 5). The top of the San Andres Formation was eroded near the end of the Permian or beginning of the Triassic age, then was buried with deposition of the Triassic Chinle Group and Moenkopi Formation (not present in the target area but in the larger study area) when the area was a low plain in a continental and restricted marine environment (Baldwin and Anderholm, 1992). Sedimentary formations overlaying the Chinle Group were deposited during the early Jurassic seas and the Cretaceous Western Interior Seaway by transgressive-regressive sequences (Lipman and others, 1979; Dillinger, 1990) and are exposed at land surface in a stairstep arrangement because of erosion of the Zuni Mountains (fig. 4). The early- to late-Jurassic Entrada, Todilto, Summerville, and Bluff Formations commonly found in northwestern New Mexico are less pervasive in the study area because of erosion and thinning of the deposits, and for this report, these deposits are grouped as the Entrada Complex.

Following deposition of the Mesozoic sediments, the regional area was folded as a result of the Laramide Orogeny starting about 80 million years before present (Ma) (Cather, 2004), forming the Zuni Uplift, Chaco Slope, and Acoma Embayment (includes the McCarty Syncline) (Hunt, 1938; Crumpler, 1982). A cross-section of the San Mateo Creek Basin developed by McCraw and others (2009) indicates a number of confirmed and inferred normal faults bisecting the upper San Mateo Creek Basin (fig. 6). Uranium deposits within the sandstones of the Morrison Formation have been mined since 1948 in the regional area. The origin of the U is not well constrained, but it was likely deposited at the interface between two fluids of different composition and reduction-oxidation (redox) states that emplaced the tabular and lenticular deposits within the Morrison Formation (McLemore and Chenoweth, 2003). The U deposits consist of U-enriched humic matter coated upon sand grains within the host formation (Fitch, 1980).

Climate and Surface Hydrology

The climate of the region is arid to semiarid—precipitation has averaged 8.7 inches per year at San Mateo (1918 to 1988) and 10.3 inches per year at Grants (1953 to 2005) (Western Regional Climate Center, 2009)—although greater precipitation may accumulate on Mount Taylor (Daly and Weisberg, 1997). San Mateo Creek is a tributary to the Rio San Jose and the confluence has been altered from past human development (note the lack of a confluence shown in fig. 3). From 1977 to 1982, the USGS operated a steamflow-gaging station on San Mateo Creek about 5 miles (mi) west of San Mateo just upstream from the confluence with the Arroyo del Puerto (upper to lower San Mateo Creek Basin) where monthly streamflow averaged 0 to 7 cubic feet per second (ft^3/s). Most of the average monthly streamflows were less than 1 ft^3/s (U.S. Geological Survey, 2009). Springs are present in the target area and are concentrated near the confluence of San Mateo Creek and El Rito Creek in the upper San Mateo Creek Basin (fig. 3).

Groundwater Hydrology and Primary Aquifers

Substantial groundwater production in the study area typically is associated with three aquifer types—alluvium, sandstone, and limestone (Stone, 2003), such as the valley alluvium, sandstones of the Morrison and Glorieta Formations, and limestone of the San Andres Formation. Intergranular porosity provides the available space for water storage within the alluvium and poorly to moderately cemented sandstones, whereas fractures and dissolution create available storage space within well-cemented sandstones and limestones. Confining units such as the shales of the Mancos Formation or the Chinle Group can produce some water but typically inhibit flow because of their low permeability (Stone, 2003).

Numerous aquifers are present in the study area and typically are found within the various Paleozoic and Mesozoic sedimentary formations and the Quaternary alluvium. Groundwater flow in the valley alluvium generally parallels the surface flow and likely receives substantial recharge from surface drainages (Baldwin and Anderholm, 1992). The groundwater hydraulic gradient in deeper aquifers such as the San Andres/Glorieta aquifer is away from the Zuni Uplift and steepest closest to the uplift (Baldwin and Anderholm, 1992). Wells typically are located in the valley areas of the successive mesa-valley landscape of the study area, and groundwater

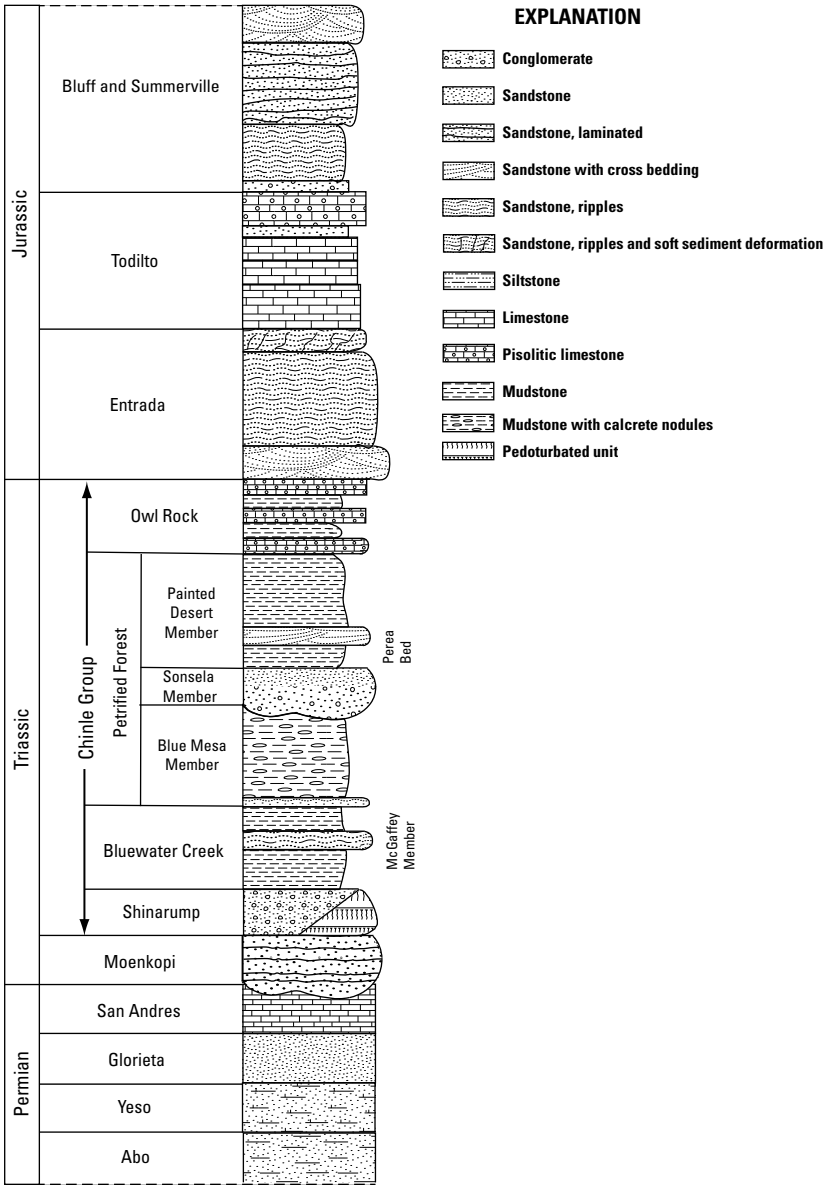

Figure 5. Generalized stratigraphic column of the subsurface geology below the valley forms in the southern San Juan Basin (modified from various figures in Lucas and others, 2003; courtesy of the New Mexico Bureau of Geology and Mineral Resources).

generally is pumped from the valley alluvium or San Andres/Glorieta aquifer (Baldwin and Anderholm, 1992; Agency for Toxic Substances and Disease Registry, 2008). Groundwater in the alluvium is hydraulically connected to groundwater in the San Andres/Glorieta aquifer in areas near the Zuni Uplift, but in other parts of the study area various members of the Chinle Group restrict flow between these two aquifers (Frenzel, 1992). During exploratory drilling in the 1970s north of San Mateo and within the target area, 15 water-bearing units (defined by formations and specific formation members) were encountered between land surface and 3,300 ft below land surface (Gulf Mineral Resources Company, written commun., 1977) indicating that many of the Mesozoic formations in the area likely contain water and may be hydraulically connected.

Valley Alluvium and Menefee Formation

An unconfined aquifer is present in the valley alluvium and the Menefee Formation in the upper San Mateo Creek Basin. The Menefee Formation is present at the surface in the eastern part of the basin in and near the town of San Mateo, and groundwater discharging from the upper Menefee supplies springs that form El Rito, San Lucas, and San Mateo

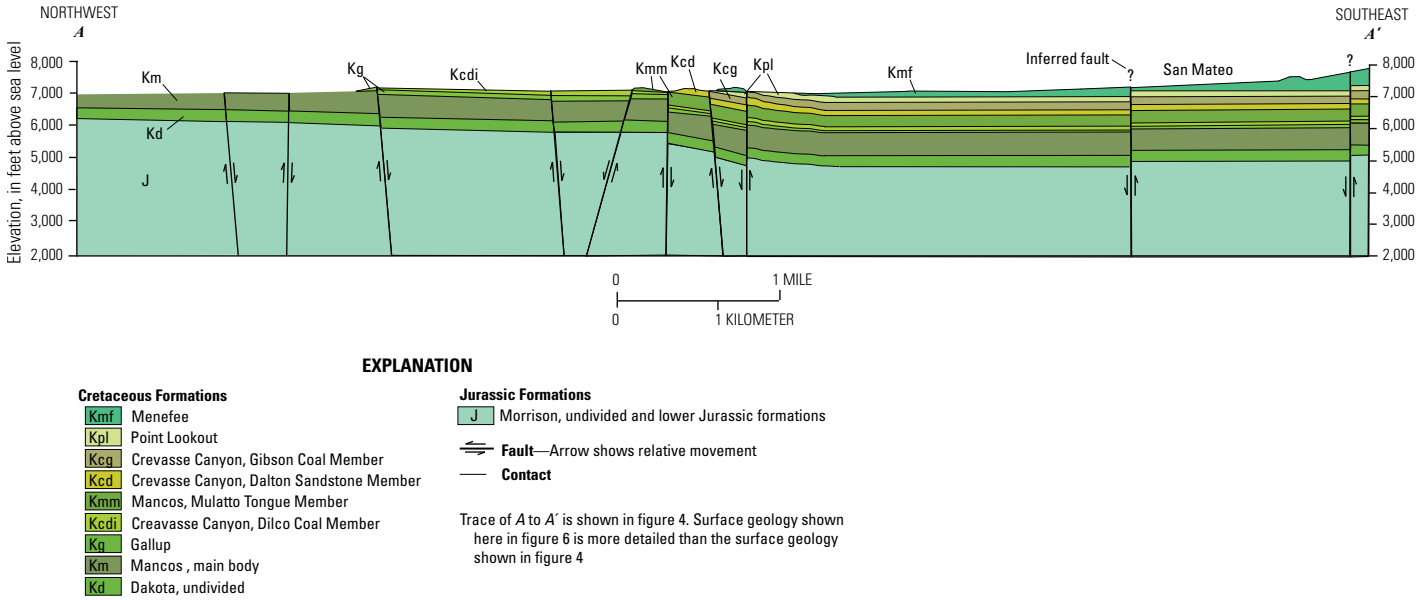

Figure 6. Geologic cross section from west to east through the upper San Mateo Creek Basin (modified from McCraw and others, 2009; courtesy of the New Mexico Bureau of Geology and Mineral Resources).

Creeks in the target area. The upper Menefee has been eroded, and unconsolidated material is present in thin layers in the easternmost part of the valley or along the base of the mesas. The alluvium thickens westward following San Mateo Creek where greater basin area contributes to the deposition of valley alluvium. Near the town of San Mateo, the alluvium aquifer overlies Menefee shales, and numerous intermittent or ephemeral springs and seeps are present in the area of the confluence of El Rito and San Mateo Creeks. West of this location, the Menefee is no longer present as the landscape transitions to older formations exhumed from previous erosion (fig. 4). Within the Rio San Jose Basin, alluvium-aquifer water typically has a specific conductance ranging from 600 to 2,500 microsiemens per centimeter (µS/cm), although values of 6,000 µS/cm have been reported; dissolved-solids concentrations have ranged from 590 to 14,000 milligrams per liter (mg/L) (Brod and Stone, 1981; Stone and others, 1983). Dissolved-solids concentrations in groundwater from the Menefee have ranged from 200 to 1,400 mg/L (Brod and Stone, 1981).

Point Lookout, Crevasse Canyon, Gallup, Dakota, and Morrison Formations

Besides the Menefee, the Cretaceous Point Lookout, Crevasse Canyon, Gallup, and Dakota Formations (predominantly sandstones) likely have the porosity to contain substantial groundwater. Located between the Gallup and Dakota, the Mancos Formation likely contains small amounts of water, but this clay-rich formation probably is more of a confining layer than an aquifer. A review of stratigraphic logs at the New Mexico Bureau of Geology and Mineral Resources (NMBGMR) indicated that the Cretaceous layers can be discontinuous through the area. The Crevasse Canyon Formation can be substantial in thickness and contains two sandstone members (Dalton and Stray) that likely contain water, but these members are spatially variable and not present in many locations across the study area because of erosion (Stone and others, 1983). The underlying Gallup and Dakota sandstones are more likely to be present as aquifers, although deposition of these formations was not prevalent for this area. The southern extent of the Gallup Formation is along the southern boundary of the study area (Stone and others, 1983). Dissolved-solids in the Cretaceous formations have ranged from concentrations of 200 to 700 mg/L for the Point Lookout (Brod and Stone, 1981); 1,200 to 2,200 mg/L for the Gallup (Gulf Mineral Resources Company, written commun., 1979); and 600 to 1,400 mg/L for the Dakota (Brod and Stone, 1981).

Aquifers in the Jurassic formations likely exist in most parts of the study area, and most information is related to U ore extraction from the Morrison Formation. Water was commonly encountered during exploratory drilling and mining of U from the Morrison, and the groundwater was removed for ore extraction (McLemore and Chenoweth, 2003; Yancey and McLemore, 2008). The Morrison Formation is divided into the mudstone, sandstone, conglomerate, and limestone Brushy Basin Member; the conglomerate, sandstone, and mudstone Westwater Canyon Sandstone Member; and interbedded shale and sandstone Recapture Member (Stone and others, 1983). The Brushy Basin Member and Westwater Canyon Member

historically have contained water and were dewatered for U extraction, which caused local water-level declines during mining. Groundwater from the Westwater Canyon Member has contained dissolved-solids concentrations of 360 to 2,200 mg/L (Brod and Stone, 1981). Roca Honda Resources, LLC (2009a) estimated the potentiometric surface of the Morrison aquifer at the Jesus Mesa (fig. 3) to be about 1,000 to 1,300 ft below land surface. Given that groundwater was found in the upper part of the Jurassic formations (Morrison), it can be assumed that the lower Entrada Complex likely contains groundwater.

Chinle Group

The Chinle Group is the only Triassic geologic unit in the study area, but this group can be up to 1,500 ft thick in the region and is composed primarily of mudstone and siltstone with some minor sandstone and limestone components (Stone and others, 1983). A likely discontinuous, confined aquifer(s) is present in the Chinle Group from recharge occurring around the Zuni Uplift, although this aquifer is not considered highly productive (Baldwin and Anderholm, 1992). The Chinle Group tends to act more as a confining unit for the underlying San Andres/Glorieta aquifer (Baldwin and Anderholm, 1992).

San Andres and Glorieta Formations

The confined San Andres/Glorieta aquifer is defined by the Permian San Andres and Glorieta Formations that underlie much of west-central New Mexico and is the primary aquifer of the region. The San Andres consists mostly of limestone and some sandstone and is unconformably overlain by the Chinle Group. The San Andres conformably overlies the Glorieta, which is composed of well-sorted, well-cemented fine- to medium-grained sandstone, and conformably overlies the Yeso Formation. The San Andres and Glorieta are considered to be a single aquifer because of the gradational contact between the formations, and much of the water in this aquifer travels through solution channels within the San Andres (Baldwin and Anderholm, 1992). Joints, fractures, and faults create anisotropic conditions within the San Andres/Glorieta aquifer (Kelley and Clinton, 1960). Groundwater flow is mostly towards the east-northeast away from the Zuni Uplift, and discharge from the aquifer as springs is common (Baldwin and Anderholm, 1992). Dissolved-solids concentrations in the aquifer in the Grants-Bluewater area (fig. 1), typically are less than 1,500 mg/L, and calcium (Ca) and magnesium (Mg) and bicarbonate (HCO_3) and sulfate (SO_4) are the dominant cations and anions (Baldwin and Anderholm, 1992).

Human Influence on Water Resources

Within the study area, municipal, industrial, and agricultural wells were primarily completed in the San Andres/Glorieta aquifer. The city of Grants derives its municipal water from this aquifer. Prior to the 1940s, domestic and stock wells withdrew small amounts of water from the San Andes/Glorieta aquifer, but in the 1940s, new irrigation wells were completed to supply an increasing agricultural area (Baldwin and Anderholm, 1992). By 1955, 22 wells were supplying 13,600 acre-ft/yr for agriculture (85 percent of total withdrawal), municipal, and industrial use in the Grants area (Gordon, 1961). This increase in groundwater withdrawn from the San Andres/Glorieta aquifer is attributed with decreasing flow in the Ojo del Gallo (minor drainage immediately south of Grants) and substantially lowering the potentiometric surface of the aquifer (Baldwin and Anderholm, 1992). Water levels fluctuated with pumpage, and the largest declines were recorded in the early 1960s during the height of agricultural use. These declines recovered following decreases in agricultural use (Baldwin and Anderholm, 1992).

In addition to agricultural uses, mining influenced groundwater levels within the region because of the need to dewater formations containing U ore and water needed for milling operations. Mining and milling operations relied on water from the San Andres/Glorieta aquifer. Substantial U deposits were discovered in 1955 north of Grants, which initiated a boom in mining, increased the local population, and decreased the amount of irrigated land (Baldwin and Anderholm, 1992). The ratio of San Andres/Glorieta water used for agricultural, industrial, and municipal uses began to change with a greater share going to industrial uses (mostly mining or milling or related uses) and a smaller share going to agriculture with an overall drop in the volume of water withdrawn from the aquifer. By 1982, the volume of water withdrawn from the aquifer had decreased to 3,900 acre-ft/yr, and 38 percent of the water was used for industrial operations (Baldwin and Anderholm, 1992). Mining and milling operations decreased through the 1980s and 1990s, and water needs correspondingly decreased. With the decrease in mining and agriculture, municipal water became the primary use of San Andres/Glorieta water.

Within the target area, there is a small population and no major agricultural land use. Most of the private land in the upper San Mateo Creek Basin outside of the town of San Mateo is part of the Lee Ranch (cattle ranch). Surface-water conveyances have been modified to support ranching operations. San Mateo Creek was dammed immediately above the town of San Mateo where incoming creek flow is allowed to infiltrate and discharges below the dam. Smaller retaining structures are present along El Rito and San Mateo Creeks on the valley floor for stock use. According to the New Mexico Water Rights System database managed by the New Mexico Office of the State Engineer (http://nmwrrs.ose.state.nm.us/nmwrrs/index.html; database reviewed in 2010), most of the wells in and around the town of San Mateo draw water from the unconfined aquifer in the valley alluvium and Menefee Formation with the remaining wells drawing water from deeper Cretaceous formations.

Previous Studies

The upper San Mateo Creek Basin has not been studied as an entire hydrologic unit. There are a number of private company reports describing the hydrogeology of various locations in the target area because of the potential for U mining in these locations. These reports are in addition to a substantial amount of geologic work by the New Mexico Bureau of Geology and Mineral Resources such as the recent draft update to the San Mateo quadrangle (McCraw and others, 2009). The New Mexico Environment Department has conducted various monitoring programs in conjunction with regulatory monitoring by the mining companies, but these data have not been compiled by the New Mexico Environment Department to derive an overview of the hydrologic resources within the upper San Mateo Creek Basin.

Study Methods

The characterization of the geologic framework; regional aquifer properties; and springs, creeks, and seeps of the upper San Mateo Creek Basin was performed by compiling and analyzing existing hydrogeologic data supplemented with new data from the analysis of spring-, creek-, and seep-water samples collected as part of this study. Compilation of existing data for the study area consisted of reviewing databases managed by the USGS, U.S. Environmental Protection Agency, and the State of New Mexico along with relevant and readily available journal articles and government and private consultant reports. The data were screened to only include data relevant to deposits and formations found in the target area—upper San Mateo Creek Basin. The larger study area was used to compile sufficient hydraulic and geochemical data to describe the general water-level and geochemical characteristics of the major aquifers that are present in the study and target areas. Most of the existing data compiled for this study ranged from the 1970s to 2009, but some data extend back to the 1940s (date of collection). This large temporal scale was included to allow for comparison of hydraulic and geochemical characteristics of the multiple aquifers relevant to the upper San Mateo Creek Basin.

Existing Data

A review of the study area geology was necessary to establish the geologic framework containing the aquifers. Stratigraphic descriptions were created from existing literature and the review of drilling logs at the New Mexico Bureau of Geology and Mineral Resources. Groundwater hydraulic data (aquifer water levels and hydraulic conductivities) and chemistry data (major and trace elements along with contaminants of concern such as NO_3, Ra, and U) were compiled to analyze basin-wide hydrogeologic characteristics. Water-level differences were interpreted to identify general flow patterns of the major aquifers in the San Mateo Creek Basin where possible. Hydraulic conductivity and transmissivity of aquifers and between aquifers were assessed where available. Aquifers were characterized by comparing concordant data across the various saturated deposits and formations in the study area that were relevant to the target area.

To analyze the data relevant to aquifers in the target area, formation designations were standardized to current (2011) accepted formation nomenclature. This standardization was necessary because of the length of the existing data record (1940s to 2009) during which formation identification has changed with certain formation names dropped from accepted use or added as additional studies continued to update the stratigraphic nomenclature of the region. Although it is a geologic group, the Chinle Group is treated similar to the formation designation because of a lack of discrimination of the Chinle Group's formations in this area regarding hydrogeologic data (it was recently elevated to Group status[1]). In addition to this name standardization, data associated with formation members were grouped under the formation name. This grouping increases the variability of the data subsets because of member differences, but this grouping provides a more consistent discussion with all differences described at the formation level. There are a number of alluvial, colluvial, and landslide Quaternary deposits in the study area, and these unconsolidated deposits were grouped under a Quaternary alluvium (Qa) hydrostratigraphic unit designation with the assumption that these unconsolidated layers should hydraulically behave as a single unit. Similarly, the volcanoclastics of the Mount Taylor Volcanic Field also were grouped as a single unit. It is not assumed that these igneous extrusive rocks have similar hydraulic properties, but these units likely contain only young water recently recharged from the surface. For purposes of this report, data associated with the Entrada, Todilto, Summerville, and Bluff Formations were grouped as a single hydrostratigraphic unit described as the Entrada Complex. These early to mid-Jurassic formations have not been well defined for the study area, and the Entrada Formation likely is the dominant formation of these predominantly sandstone and limestone layers. Additionally, a small percent of data were attributed to multiple formations. These multiple-formation samples were assigned to the uppermost formation for analysis. The uppermost formation was assumed to represent the greater thickness of the saturated interval of the well, because it could not be ascertained as to whether the lower formations were fully penetrated by the wells. Designating individual formations for multiple-formation data mostly affected samples collected from the San Andres/Glorieta aquifer. Some data were attributed to the San Andres Formation and some were attributed to the Glorieta Formation, but a substantial part of the data was attributed to both formations. The single-formation designation of multiple-formation data greatly

[1]The Chinle Group was elevated from formation status by Lucas (1993), but this status change has not been fully accepted (e.g., Dubiel, 1994, and Woody, 2006). The Chinle Group designation is used for purposes of this report.

increased the San Andres Formation data set compared to the Glorieta Formation data set. In most cases, these two data sets can be considered representative of one aquifer because of the gradational contact between these formations and the two data sets are discussed as one regarding certain data.

Existing water-level data were compiled from publicly available sources to evaluate possible groundwater flow patterns. To visualize likely flow patterns of the aquifers, relative differences in water-level elevations are presented through a categorical analysis of the distribution of water-level values for various groups (deposit or geologic time period). Using the statistical program SPlus (Tibco Software, version 8.1; http://spotfire.tibco.com/products/s-plus/statistical-analysis-software.aspx), each water level was assigned to one of seven distribution categories given their relative differences across the entire distribution of the selected group. The presentation is similar to a categorical boxplot but is presented spatially to view relative differences in water-level elevations across the study area. Water levels were not used to construct potentiometric-surface contours because of the substantial length of the temporal record of the data, the variety of collectors of the data, the possible variety of methods for determining depth to water or water-level elevation, and the known anthropogenic and natural influences on water levels in the target and study area during the temporal record of the data. This compilation of data from numerous sources collected over a long temporal record is best viewed from a relativistic perspective than a contoured solution that implies a known hydraulic gradient at some point in time.

The median value and interquartile range (first and third quartiles that encompass 50 percent of the distribution) of water-level elevations were determined for each aquifer to grossly view water-level elevations across the study area. The statistics cannot be used to infer vertical hydraulic relations between aquifers because of a lack of substantial overlap of wells between aquifers within the study area. Erosion of the landscape exposed older formations at the surface in various areas that provides major recharge entry points to the lower aquifer formations. It is assumed that a substantial portion of recharge to the lower, unconfined/semi-confined/confined (depending on restrictive overlying layers) aquifers is occurring at these surface exposures in areas of higher precipitation and concentrated flow that would allow recharge in this semi-arid climate (Zuni Mountains, mesas, Mount Taylor, surface-water bodies), and the groundwater then moves eastward and northeastward in the geologic structure and likely interacts with overlying or underlying aquifers as has been observed for the San Andres/Glorieta aquifer (Baldwin and Anderholm, 1992). The water level of each aquifer reflects the sum of the recharge elevations at any one location. The median of each aquifer's water-level data set represents a center point in the distribution of data that minimizes the influences of local effects such as dewatering from mining or other temporary withdrawals or inputs, and the interquartile range provides an estimation of the similarity or difference in water-level elevation ranges between aquifers across the study area.

Existing major-ion data were screened to eliminate samples missing any of the major cations (Ca, Mg, and Na) or anions (HCO_3 or alkalinity, SO_4, and Cl). A review of pH values indicated that conversion of alkalinity values to HCO_3 was appropriate (majority of all recorded pH values within the range of 7.0 to 8.5), and a single HCO_3 value was determined for each sample that contained an alkalinity value by multiplying the value by 1.22. The total cation content in the samples (in milliequivalents per liter) had to balance within 10 percent of the total anion content in the samples for inclusion in the water-type analysis. The 10-percent acceptable-balance criteria was used instead of the more accepted 5-percent criteria because of the likely variability of sampling and analysis by different data collectors and laboratories. Samples were aggregated by geologic deposit or formation, and average major-element concentrations, along with dissolved-solids concentrations, were calculated for each aquifer. All groupings by deposit or formation balanced within the 10-percent acceptable criteria for the averaged concentrations. Average concentrations were chosen because median concentrations did not meet the ion-balance criteria.

For dissolved trace-elements and contaminants-of-concern data, estimated concentrations (greater than the method detection level (MDL) but less than the reporting level) were accepted as actual concentrations. Some existing data sources presented MDLs and some sources only indicated nondetect data points. No attempts were made to include nondetect data, because of the lack of consistency in available MDLs and substantial presentation of nondetect data points without any indication of a detection level. Analysis of trace-element and contaminants-of-concern data sets were limited to only the detected presence of the constituents because of the lack of control regarding the left-tail of the distribution with the variable MDLs and non-inclusion of nondetect data.

New Data

To supplement the groundwater characterization, surface-water samples were collected from seven spring, creek, and seep locations in the target area in August 2009 and May 2010 (fig. 7 and table 1). Sites were selected by the availability of water. Three springs were flowing in the target area during the sampling periods. The spring sites are located along the southern (El Rito Creek and San Mateo Creek springs) and eastern (San Lucas Creek spring) rims of the basin (fig. 7) where recharge to the discharging aquifer(s) likely occurs from infiltration of precipitation occurring on Mount Taylor. These springs discharged from sandstone layers underlain by shales immediately below the volcanoclastic caps that form the top layers of the mesas. Samples also were collected downgradient from the springs on San Mateo and El Rito Creeks where the creeks transition from the steep gradients of the mesas to the valley floor. The most downstream sampling locations were seeps where ponding water was found along El Rito and San Mateo Creeks on the valley floor. The seeps

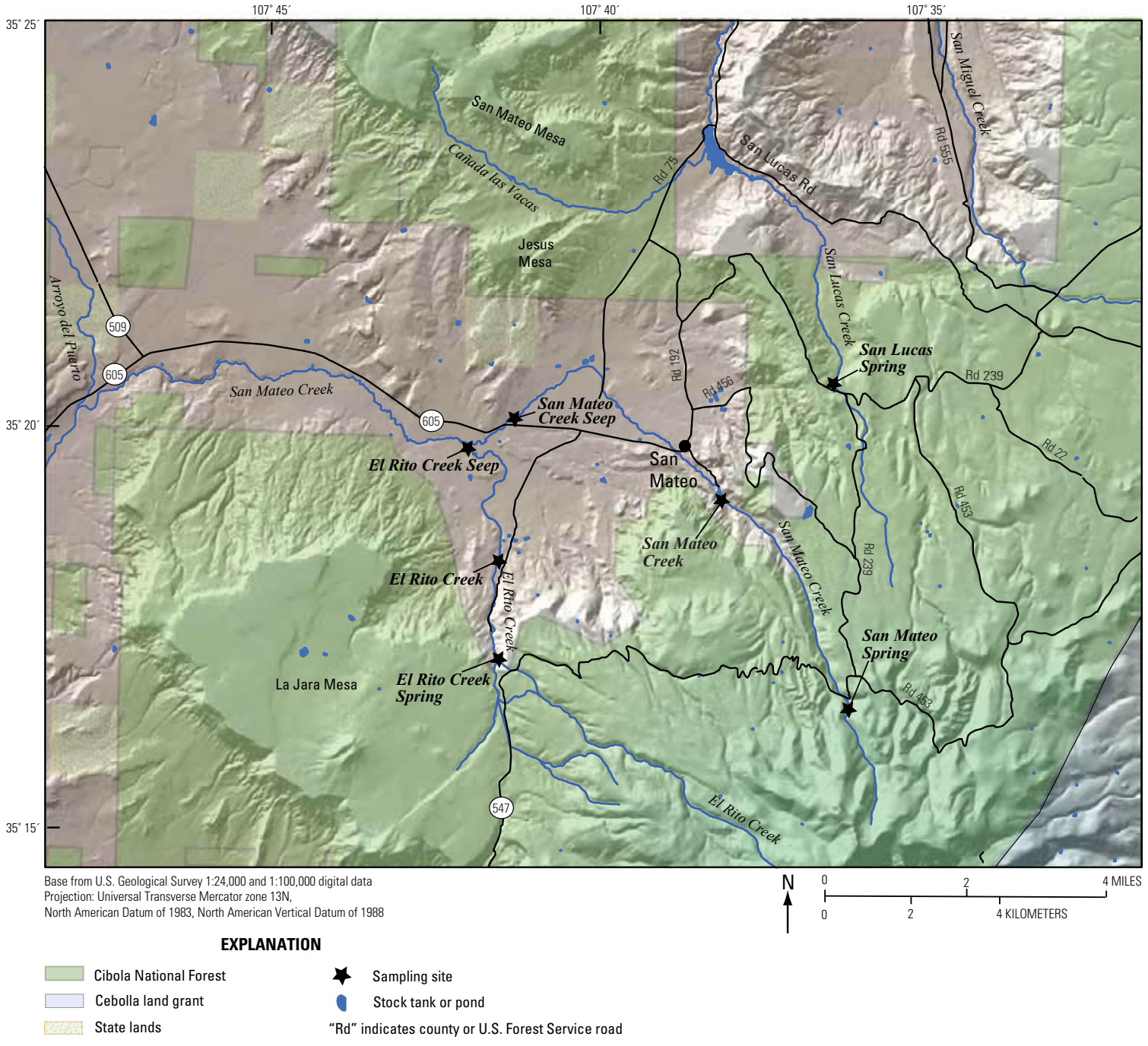

Figure 7. Sampling sites and surface topography of the upper San Mateo Creek Basin.

Table 1. Information for the spring-, creek-, and seep-sample sites in the upper San Mateo Creek Basin.

[USGS, U.S. Geological Survey; NAD 83, North American Datum of 1983; ft, feet; NAVD 88, North American Vertical Datum of 1988]

Local site name (fig. 7)	USGS site name	Latitude (NAD 83)	Longitude (NAD 83)	Land-surface elevation (in ft above NAVD 88)	Exiting or flow through deposit/ formation
El Rito Creek spring	351710107412001	35º17′09.7″	107º41′19.6″	7,935	Volcanoclastic and upper Menefee
El Rito Creek	351828107411301	35º18′28.3″	107º41′13.1″	7,260	Menefee
El Rito Creek seep	351950107413101	35º19′49.5″	107º41′31.4″	7,023	Alluvium
San Mateo Creek spring	351649107355701	35º16′49.0″	107º35′57.4″	8,945	Volcanoclastic
San Mateo Creek	351918107375301	35º19′17.5″	107º37′53.2″	7,520	Menefee
San Mateo Creek seep	352017107410301	35º20′17.4″	107º41′03.2″	7,041	Alluvium
San Lucas Creek spring	352045107361701	35º20′44.7″	107º36′17.3″	7,871	Volcanoclastic and Menefee

were present where shallow groundwater is near the surface as indicated by numerous salt deposits and visible signs of ephemeral or intermittent springs and shallow water levels in nearby piezometers. All samples were analyzed for field properties (water temperature, pH, specific conductance, and dissolved oxygen), dissolved solids, major elements (Ca, Mg, Na, K, HCO_3, SO_4, and Cl), trace elements (Al, Sb, As, Ba, B, Be, Cd, Cr, Co, Cu, Fe, Li, Pb, Mn, Hg, Mo, Ni, Se, Si, Ag, Na, Tl, V, and Zn), stable isotopes of water (δ^2H and $\delta^{18}O$), and contaminants of concern that have historically exceeded maximum contaminant levels in this area (gross alpha activity, NO_3, Ra, and U; table 2). Stable isotopes of hydrogen ($^2H/^1H$) and oxygen ($^{18}O/^{16}O$) composing water are reported as δ^2H and $\delta^{18}O$ per mil (‰), which is the ratio of the stable-isotopic abundances of an element in a sample to those of the Vienna Mean Standard Ocean Water (VSMOW; Révész and Coplen, 2008a; Révész and Coplen, 2008b). All samples were collected as grab samples from atmospherically-exposed surfaces and filtered through a 0.45-micron capsule filter using a peristaltic pump and new, individual Teflon-coated tubing at each site.

The creek- and seep-solute concentrations were used to model potential geochemical mass-balance reactions between the creek sample sites and the seep sample sites on El Rito and San Mateo Creeks. These point-to-point locations represent the evolution of creek flow from groundwater discharged at the mesas to infiltration and flow through the valley alluvium and reappearance at downstream seeps. The reemerged shallow groundwater likely undergoes greater evaporation on the valley floor as it reappears at the surface through seep discharge that produces quiescent shallow ponds. Additionally, relative to water that remains on the surface as creek flow, water that infiltrates into the alluvium would be expected to undergo greater rock-water interactions as it migrates more slowly along the valley floor. This rock-water interaction was visible in the addition of clays and likely associated oxide polymorphs that were apparent in the samples collected from the seep sites. Some of these clays were present in the seep samples following filtration and are considered part of the "dissolved" fraction for concentration analysis because of acid preservation of the samples that draws elements from the clays and oxides into solution. Inclusion of elements associated with the clays that passed through the 0.45-micron filters influences charge balance determination and trace-element concentrations as trace elements sorbed to these very fine particles are not included for determining the charge balance (potential for imbalance with this exclusion) and may increase the concentration of typically low solubility trace elements such as aluminum (Al).

The geochemical model NETPATH (Plummer and others, 1994) was used to model the geochemical reactions between the creek and seep sites using the NETPATH-WIN interface (El-Kadi and Fujiwara, 2009). Each model of the creek to seep flow path for El Rito and San Mateo Creeks was constrained by specific elements that were identified as having substantial mass flux between the creek and seep sites with consideration for the changes in flow type (open channel to shallow groundwater) and the introduction of clays and oxides to the water as shallow groundwater travels through predominantly aluminosilicate alluvium and formations. Mineral phases were chosen based on the local geology, the introduction of aluminosilicate clays and Fe and Mn oxides that passed through the 0.45-micron filter as part of the "dissolved" fraction, and a review of possible mineral phases produced from the calculation of saturation indices (log of the ratio of the ion activity product (IAP) and the solubility product (K_{sp}) from entering all available solute concentrations into PHREEQC (Parkhurst and Appelo, 1999) using the PHREEQCi interface (version 2.17.0); http://wwwbrr.cr.usgs.gov/projects/GWC_coupled/phreeqci/). The selected mineral phases represent the thermodynamically preferred mineral forms given the available element concentrations and general aqueous chemical conditions

Table 2. Sample analytes and laboratory analysis methods.

[ºC, degrees Celsius; %, percent; µS/cm, microsiemens per centimeter at 25 degrees Celsius; NTU, nephelometric turbidity units; mg/L, milligrams per liter; µg/L, micrograms per liter; pCi/L, picocuries per liter; USGS, U.S. Geological Survey; $\delta^x X$ (‰) = ($Ratio_{sample}/Ratio_{standard} - 1$) x 1,000 of specified isotope ratio; ‰, per mil]

Constituent	Description	Method/lab code	Medium	Laboratory	Analytical precision
Field values	Water temperature, pH, conductance, turbidity	Orion 130A, Orion 250A+, Oakton T-100 (field meters)	Water	Field collection	0.1 ºC, 0.02 pH, 0.5% µS/cm, 0.1 NTU
Dissolved solids	Filterable residue	[1]MCAWW 2540C	Water	TestAmerica Labs, Arvada, Co.	5 mg/L
Alkalinity	Alkalinity as $CaCO_3$	[1]MCAWW 2320B	Water	TestAmerica Labs	1.1 mg/L
Major anions	Br, Cl, F, SO_4	[1]MCAWW 300.0A	Water	TestAmerica Labs	0.06 to 1.2 mg/L
Major cations	Ca, Mg, Na, K	[1]SW846 6010B	Water	TestAmerica Labs	0.034 to 1.1 mg/L
Trace elements	[2]24 trace elements	[1]SW846 6010B, 6020, 7470A	Water	TestAmerica Labs	0.01 to 2 µg/L
Nitrate	$NO_3 + NO_2$ as N	[1]USEPA 353.2	Water	TestAmerica Labs	0.05 mg/L
Gross alpha		[3]USEPA 900.0	Water	TestAmerica Labs	1 pCi/L
Radium isotopes	Alpha-emitting isotopes of Ra (^{226}Ra and ^{228}Ra)	[1]USEPA 903.0 and 904.0	Water	TestAmerica Labs	1 pCi/L
Stable isotopes of water	$^2H/^1H$, $^{18}O/^{16}O$	Révész and Coplen, 2008a and b	Water	USGS Reston Stable Isotope Laboratory	2‰ as δ^2H and 0.2‰ $\delta^{18}O$

[1]U.S. Environmental Protection Agency, 2009.

[2]Al, Sb, As, Ba, B, Be, Cd, Cr, Co, Cu, Fe, Li, Pb, Mn, Hg, Mo, Ni, Se, Si, Ag, Tl, U, V, and Zn.

[3]U.S. Environmental Protection Agency, 1993.

(pH, temperature, and dissolved oxygen), but these selected mineral phases are not meant to indicate the only minerals likely to dissolve or precipitate or be available for cation exchange/sorption. These mineral phases are useful for viewing the mass flux of the available solutes between aqueous and solid phases with changes in element compositions and concentrations.

Model results describe the mass transfers of the selected mineral phases that account for the observed changes within the constrained elements. Models were run with creek data representing the initial solution and the seep data representing the final solution. Evaporation was included as an effect along with the dissolution and precipitation of the mineral phases to account for changes in the water chemistry between the initial and final solutions. Cation exchange was attempted in the geochemical models but dismissed as an examinable process because of the leaching of elements from the less than 0.45-micron clays and oxides with acidification of the collected samples that altered the dissolved to exchange-site element ratios. A CO_2 phase did indicate changes between the creek and seep sites, but this phase is not presented because of the lack of organic C data that would hinder this discussion, but this flux is visible in the pH differences between the sites. The mass transfer estimates of the dissolution or precipitation of mineral phases are represented by a positive (dissolution) or negative (precipitation) value in millimoles per kilogram (mmol/kg) of water, and the evaporation effect is quantified through an estimated value of the remaining water solution in grams as indicated by an outputted evaporation factor (concentrations increased by this multiplier through evaporation).

Quality-Assurance

Surface-water data collection was performed according to USGS quality-control and quality-assurance standards described in the USGS *National Field Manual for the Collection of Water-Quality Data* (U.S. Geological Survey, 2006). One sequential replicate sample was collected during each sampling period at a randomly selected site to evaluate laboratory precision, and matrix-spike samples were collected at the same site to ascertain matrix interference for all constituents. All replicate-sample results were within 10 percent of the environmental-sample results for concentrations greater than the reporting level, and matrix-spike sample results were within allowable laboratory limits. Additionally, laboratory-blank samples were analyzed to examine method contamination and no analytes were detected above the reporting level in the laboratory-blank samples.

Geologic Framework and Regional Aquifer Properties

Regional data were used to describe the geologic, hydraulic, and geochemical characteristics of the aquifers of the study area regarding formations relevant to the target area. Geologic and hydraulic characteristics include stratigraphy, formation properties, groundwater-flow patterns derived from existing water-level differences, and published hydraulic conductivities measured in the field or laboratory. Geochemically, groundwater variation among the aquifers was examined by reviewing existing data for differences in pH, dissolved solids, water type defined by the major elements, trace elements, and contaminants of concern.

San Mateo Creek Basin Geology

The geologic framework of the study area consists of the Zuni Uplift, Chaco Slope, and the Mount Taylor Volcanic Field. Within this structural context, the sedimentary formations provide matrices for local and regional aquifers. Information regarding the study area stratigraphy was compiled along with associated aquifer information to present a table of deposit, formation, and aquifer properties that are relevant to the hydrologic resources of the target area (table 3). For this report, aquifers are described by the individual formations or deposits where groundwater is present. These descriptions are used to refer to the saturated portions of deposits or formations but are not meant to discriminate separate aquifers. Many of the aquifers likely are well-connected, but investigation of those connections is beyond the scope of this report. The distribution of the aquifers is spatially variable because of the dip of the formations and erosion that produced the current landscape configuration where older formations have been exhumed closer to the Zuni Mountains.

The thicknesses and range of deposits and formations present a potentially complex interaction of aquifers in the study and target areas. Many of the deposits and formations likely are hydraulically connected because of the solid-matrix properties, such as porosity and permeability (table 3), but the Mancos Formation (including the Mulatto Tongue) and Chinle Group likely restrict vertical flow given the shaly composition of these formations. The Mancos is a near-surface formation that may not be present in parts of the study and target areas because of thinning and erosion. It is more prevalent on the mesas and strongly visible at the surface of Jesus and San Mateo Mesas (fig. 8). The limited presence of the Mancos in the valley areas lessens its role as a potential inhibitor of vertical flow to the lower aquifers. The Chinle Group is a thick sequence of predominantly shale and silt that likely acts as a strong inhibitor to vertical flow between the overlying Jurassic formations and the underlying Permian formations. The Chinle Group is exposed at the surface west of the target area in the lower San Mateo Creek Basin (fig. 4).

Hydraulic Properties of Major Aquifers

Groundwater in the study area occurs in numerous deposits and formations that form unconfined and confined aquifers, and recharge occurs in highlands such as the Zuni Mountains and Mount Taylor. Horizontal flow is driven by these recharge areas and the regional tilt of the landscape, but local effects such as the McCarty Syncline and differences in recharge locations likely influence local conditions. Vertical flow likely is occurring among many of the formations except where restricted by shaly formations such as the Menefee, Mancos, and Chinle. Existing water-level elevations compiled as part of this study are listed in appendix 1.

Horizontal Flow

Available water-level data were evaluated to try and identify general flow patterns within each of the aquifers. Only water-level data from the alluvium aquifer provided an indication of flow direction in the study and target areas. Water-level elevations in the alluvium aquifer decrease in the downstream direction along San Mateo Creek (fig. 9). This observation is consistent with Baldwin and Anderholm's (1992) determination that groundwater flow in the alluvium aquifer generally is the same direction as that of surface water (or land topology) for this region. The water-level data from the lower aquifers in the sedimentary formations did not indicate similar relative differences in water-level elevations across the study area that could be interpreted as prevalent flow directions across the study or target areas. The relative distribution of water-level elevations in the study area for the lower aquifers is presented (fig. 10) as groupings of water levels for formations from geologic periods to indicate the variability in relative water-level elevations among each of the period groupings and no apparent flow directions from differences in relative water-level elevations. The large temporal and spatial extent of the water-level data (fig. 10 and table 1-1) appears to hinder identification of the general flow patterns for these deeper aquifers. In the target area, it is likely that groundwater in these lower aquifers generally flows eastward given the hydrogeologic framework where formation dip is eastward across the target area and the eastward flow direction identified by Baldwin and Anderholm (1992) for the San Andres/Glorieta aquifer. If the flow direction in the underlying aquifers is to the east in the target area, this flow direction is opposite of the flow direction in the alluvium aquifer in the upper San Mateo Creek Basin. Opposing flow directions would be a result of different recharge areas and the unconsolidated alluvium that conforms to the topological gradient compared to the consolidated formations that have a regional opposing gradient.

The influence of faults on groundwater flow was not investigated as part of this study, but the presence of numerous normal faults in the target area (fig. 6) likely influences groundwater flow. Faults can inhibit flow by disconnecting permeable pathways or by reducing porosity from fault gouge,

Table 3. Stratigraphic, lithologic, and aquifer characteristics of geologic deposits and formations in the study and target areas.

[ft, feet; %, percent; NA, not available; <, less than]

Deposit/ formation	Geologic age	[1]Deposit/formation description	Surface location in the target area (figs. 4 and 8)	Thickness (ft)	Porosity/ permeability	[1]Direction of flow	Aquifer present
			Quarternary				
Alluvium (Qa)	Quaternary—upper Pleistocene to Holocene	Alluvium eroded from surrounding formations	Valley floor	Highly variable	Possibly large permeability	Variable	Yes
			Neogene				
Flows and volcanoclastics (Tnv and Tpb)	Neogene	Lava, pyroclastic flows, and associated volcanoclastics from the Mount Taylor Volcanic Field	Forms mesa caps on basin highlands	Highly variable	Possible large porosity in vesicular basalts, but low permeability unless fractured	Away from Mount Taylor	Unlikely as an aquifer. Likely runoff or percolation to underlying formations
			Cretaceous				
Menefee (Kmf)	Late Cretaceous	Interbedded mudstones, siltstones, fine- to medium-grained sandstones, mudstones, and thin coals	Northeastern part of basin	[2]Highly variable (eroded), up to 1,000 ft thick	30% sandstone, 65% shale, decent lense permeability	East to northeast	[3]Discontinuous
Point Lookout (Kpl)	Late Cretaceous	Medium to fine-grained, cross-bedded sandstone	Exposed along northern rim areas	[4,5]120	Likely porous with sandstone dominance	East to northeast	[3]Discontinuous
Crevasse Canyon (Kcc)	Late Cretaceous	Interbedded siltstone, sandstone, and coal with thin conglomerates	Exposed along rim	[5]800	Highly variable	East to northeast	[3]Discontinuous
Mulatto Tongue of Mancos (Kmm)	Late Cretaceous	Thin-bedded, tabular to ripple-laminated sandstone (well to moderately sorted and very fine grained) and black mudstone	Exposed along rim	[5]305	Larger porosity than main body of Mancos shale	East to northeast	[3]Discontinuous
Gallup (Kg)	Late Cretaceous	Cross-bedded, moderately-sorted, very fine- to fine-grained sandstone	Exposed along rim	[5]73–85	Likely porous with sandstone dominance	East to northeast	[3]Discontinuous
Mancos (Km)	Middle Cretaceous	Mudstone and silty mudstone with finely laminated to cross-bedded thin sandstone layers (well sorted and fine grained)	Exposed along base of mesas on northern basin boundary	[5]125–710	Small permeability given dominance of shale layers	East to northeast	[3]Possibly discontinuous
Dakota (Kd)	Middle Cretaceous	[5]Sandstones derived from marine shorefaces, intertongues with Mancos	Exposed along base of mesa on the southwest basin boundary	[5]50–60	Likely porous with sandstone dominance	East to northeast	[3]Possibly discontinuous
			Jurassic				
Morrison (Jm)	Upper Jurassic	Mudstone and sandstone	Minor exposure on La Jara Mesa	[2,5]700	Highly variable	East to northeast	Yes

[5]Entrada Complex—Early to Middle Jurassic composed of the Entrada, Todilto, Summerville, and Bluff Formations

Table 3. Stratigraphic, lithologic, and aquifer characteristics of geologic deposits and formations in the study and target areas.—Continued

[ft, feet; %, percent; NA, not available; <, less than]

Deposit/ formation	Geologic age	[1]Deposit/formation description	Surface location in the target area (figs. 4 and 8)	Thickness (ft)	Porosity/ permeability	[1]Direction of flow	Aquifer present
Bluff (Jb)	Middle Jurassic	Sandstone	Not exposed in the basin	[2]<5–300	Small permeability for a sandstone[2]	East to northeast	Yes
Summerville (Js)	Middle Jurassic	Thin alternating beds of mudstone, siltstone, and sandstone	Not exposed in the basin	NA	NA	East to northeast	Yes
Todilto (Jt)	Early Jurassic	Limestone	Not exposed in the basin	NA	NA	East to northeast	Yes
Entrada (Je)	Early Jurassic	[2]A three member formation consisting of upper and lower sandstones with a middle siltstone	Not exposed in the basin	NA	NA	East to northeast	Yes
			Triassic				
Chinle Group (TRc)	Triassic	[7]Mudstone and siltstone with clayey/silty sandstone lenses	Not exposed in the basin	[7]1,250	[7]Small	East to northeast	[7]Yes, but limited aquifer because of dominance of shales
			Permian				
San Andres (Psa)	Late Permian	[8]Marine, upper and lower massive fossiliferous limestone separated by a sandstone unit	Not exposed in the basin	[7]225 (San Andres and Glorieta)	Large permeability	[7]East	Yes, major aquifer
Glorieta (Pg)	Middle to late Permian	[8]Massive, well-sorted, well-cemented, fine- to medium-grained sandstone	Not exposed in the basin		NA	[7]East	Yes, major aquifer
Yeso (Py)	Early Permian	[7,9]Sandstone, clayey sandstone, and siltstone mixed with carbonates and evaporites deposited under marine conditions	Not exposed in the basin	[1]1,000	[7]Small permeability	Unknown	[7]Leaky basal unit for the San Andres/ Glorieta aquifer
Abo (Pa)	Early Permian	[7]Fine- to coarse-grained sandstone, siltstone, and mudstone with conglomerates in the lower unit deposited during continental conditions	Not exposed in the basin	[7]1,000	[7]Small permeability	Unknown	[7]Leaky confining unit

[1]Descriptions from McCraw and others (2009) and New Mexico Bureau of Geology and Mineral Resources (2003) unless otherwise noted. The flow-direction indication depends on the study area of the cited references. According to the references, flow directions were mostly northeastward closer to the Zuni Mountains and more eastward closer to the McCarty Syncline under Mount Taylor (fig. 3).

[2]Stone and others, 1983.

[3]Given a review of existing local and regional information, a productive aquifer is unlikely present in these formations within the study area but small amounts of groundwater may be present.

[4]Maximum thickness.

[5]Roca Honda Resources, LLC, 2009a.

[6]Entrada Complex—this term is used solely for this report to describe the early to late Jurassic deposits that have not been well discriminated in the study area. The Entrada is the dominant formation and the presence of the Todilto has been identified by the authors from review of driller's notes. The presence of Bluff and Summerville Formations in this area is debatable and beyond the scope of this report.

[7]Baldwin and Anderholm, 1992.

[8]Gordon, 1961.

[9]Baars, 1962.

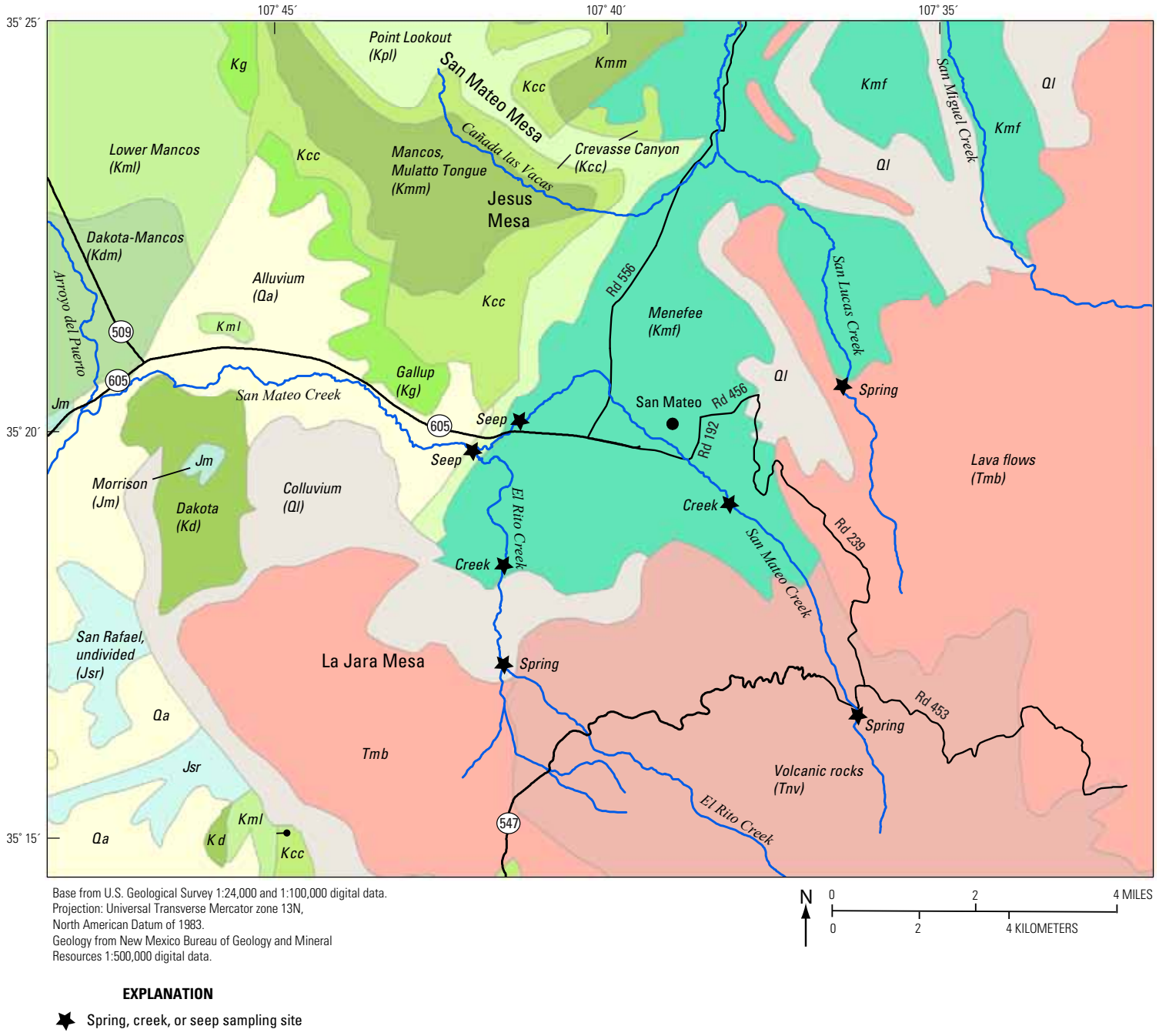

Figure 8. Surface geology of the upper San Mateo Creek Basin.

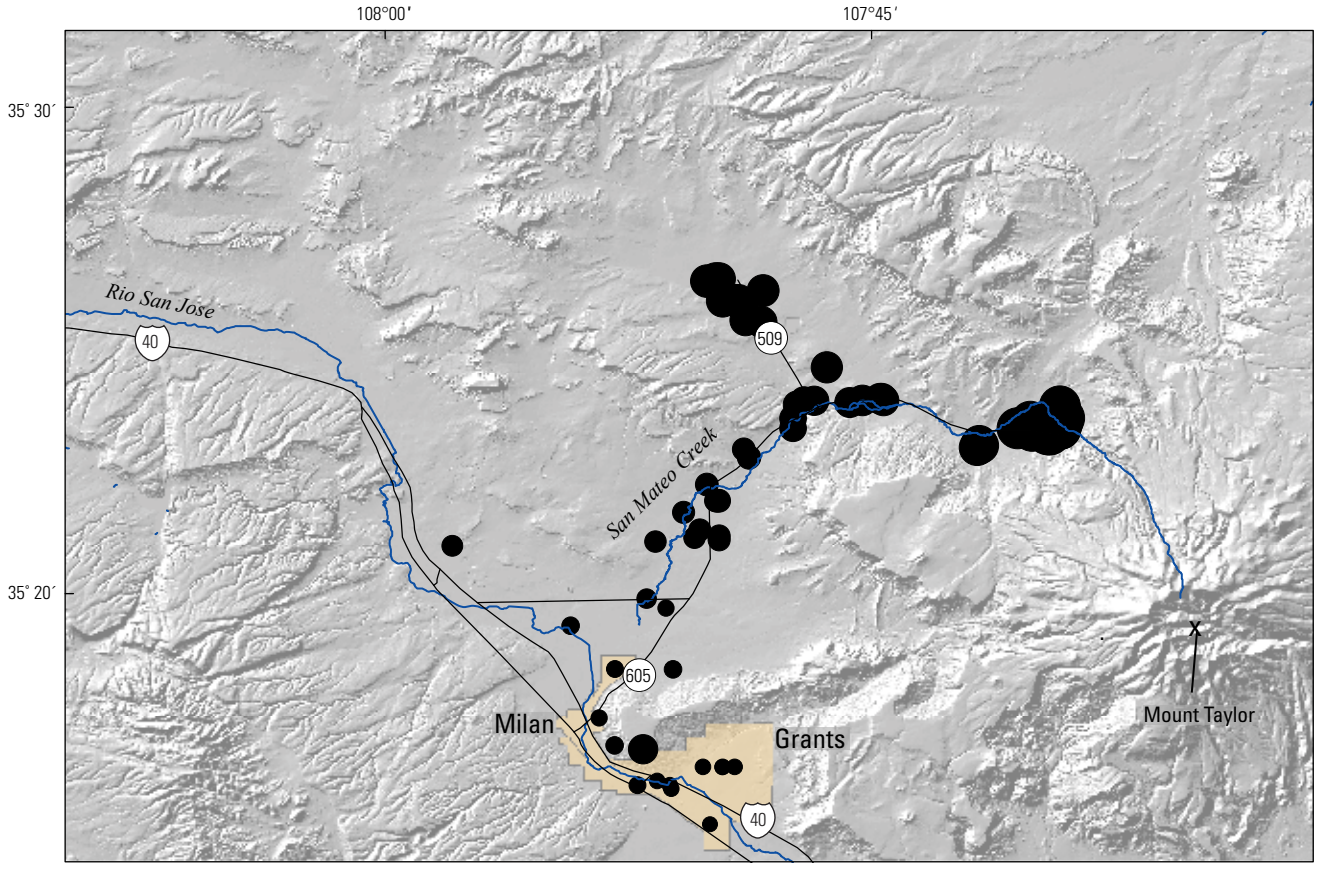

EXPLANATION

Developed area

The relative difference in water levels is presented through a categorical analysis of the distribution of water-level values. Using the statistical program SPlus (Tibco Software, version 8.1), each water level was assigned to one of seven distribution categories as determined by the overall distribution of water levels found in the Quarternary alluivum for the period of record. The presentation is similar to a categorical boxplot

Water-level elevation comparison

Lower water-level elevation Higher water-level elevation

Figure 9. Relative differences in water-level elevations for the distribution of water-level data compiled for wells with screens located in the Quaternary alluvium. Discrete water-level data are presented in appendix 1.

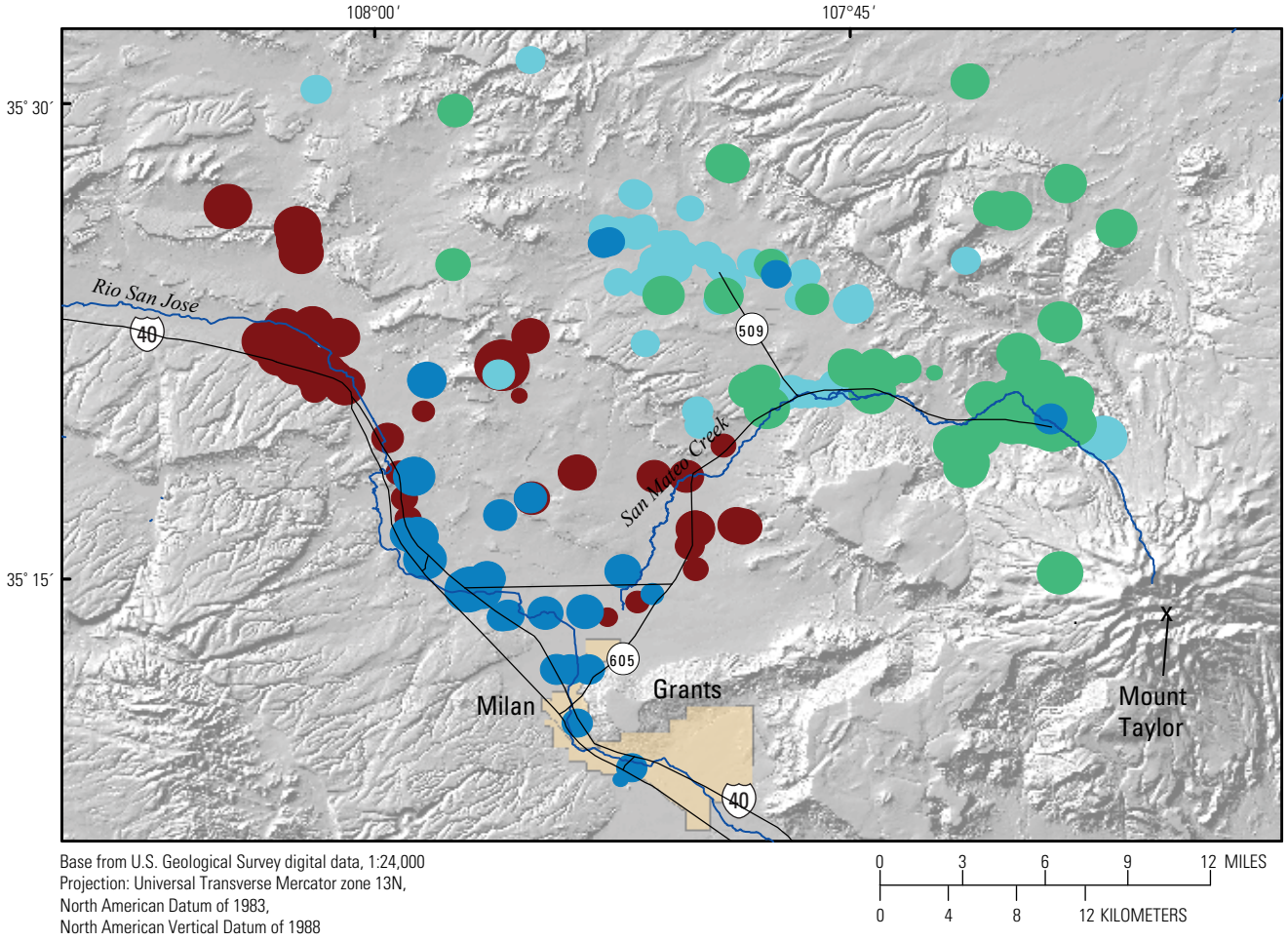

Figure 10. Relative differences in water-level elevations for the distribution of water-level data compiled for wells with screens located in Cretaceous, Jurassic, Triassic, and Permian formations. Discrete water-level data are presented in appendix 1.

but faults also can create higher permeable pathways along the fault trace (Fetter, 2001). The influence of faults is dependent upon the material in the fault zone. There likely is substantial displacement along some of the faults in the target area (fig. 6), but given the consolidated nature and thickness of the sedimentary formations, it is likely that faults in the study area enhance groundwater flow by increasing hydraulic conductivity across the fault zones, as has been observed on regional scales with porous, sedimentary formations (Garven, 1995). Faults as barriers or conduits for groundwater flow, however, depend on the individual nature of a fault (Garven, 1995).

Water-Level Elevations

Median values and the interquartile range of the water-level elevations were ascertained for each aquifer in the study area. These statistics represent the midpoint of the data set and 50 percent of its distribution that allows water levels in the aquifers to be viewed without influence of outliers that may skew inferences about the data. In the San Juan Basin, it is common for there to be substantial differences in the water levels of the various aquifers in the basin and up to 200 ft or more of difference has been identified (Stone and others, 1983). Within the study area, data for the various aquifers indicate 10s to 100s of ft of difference between median water-level elevations with minimal overlap in the range of uncertainty as indicated by the interquartile ranges except between the Dakota and Morrison Formations (table 4). Higher water elevations are found in the upper formations. Water-level elevations generally decrease with depth, although these values cannot be compared directly as the data of each aquifer represents only that discrete area within the study area containing each aquifer's wells (see figs. 9 and 10 for the distribution of wells by age groupings). Insufficient overlap of wells inhibits the interpretation of general vertical flow directions between aquifers in the study area.

The changing basal unit beneath the valley alluvium alters shallow groundwater flow because of differences in permeability of the basal unit that allows or restricts vertical migration of groundwater. In the eastern part of the basin, the presence of the Menefee Formation appears to restrict downward migration of groundwater from the valley alluvium. The Menefee Formation consists of interbedded shales, siltstones, and sandstones and is underlain by the Point Lookout Formation (sandstone) (table 3). It is likely that the portion of the valley alluvium that is underlain by the Point Lookout instead of the Menefee (western part of the target area) allows greater opportunity for downward migration of water from the alluvium aquifer. This geologic transition from the Menefee to Point Lookout has a surface expression of numerous seeps and salt deposits present along the creek from the eastern part of the basin to the confluence of El Rito and San Mateo Creeks. Downgradient or westward of this location, seeps and salt deposits are no longer present, and the Point Lookout Formation underlies the alluvium in this area (figs. 4 and 8).

Groundwater within the Chinle Group is confined (Frenzel, 1992), and upward migration from this aquifer into the Morrison Formation may be possible although the restricted nature of the water-elevation data sets do not allow for such a determination, given the limited overlap of

Table 4. Water-level elevation statistics for aquifers in consolidated formations in the study area.

[All values have been rounded to the nearest 5 feet; values are only shown for aquifers containing nine or more data points; NA, not available]

Deposit/formation	General formation description[1]	Water-level elevation median	Water-level elevation interquartile range[2]	Number of water-level values in the study area
Menefee (Kmf)	Mudstone, siltstone, and sandstone	7,190	7,130–7,240	61
Point Lookout (Kpl)	Sandstone	6,975	6,940–7,045	10
Crevasse Canyon (Kcc)	Siltstone and sandstone	NA	NA	0
Mulatto Tongue of Mancos (Kmm)	Sandstone and mudstone	NA	NA	0
Gallup (Kg)	Sandstone	NA	NA	2
Mancos (Km)	Mudstone and sandstone	6,815	6,710–6,830	9
Dakota (Kd)	Sandstones	6,615	6,495–6,790	13
Morrison (Jm)	Mudstone and sandstone	6,550	6,530–6,585	92
Entrada Complex	Sandstone, siltstone, mudstone, and limestone	NA	NA	3
Chinle Group (TRc)	Mudstone and siltstone	6,685	6,570–6,750	49
San Andres (Psa)	Limestone	6,455	6,440–6,480	30

[1]See table 3 for full formation description.

[2]The interquartile range consists of the first and third quartiles, thereby encompassing 50 percent of the distribution.

water-level elevations between these aquifers. Water-level data for the Entrada Complex consisted of only three data points, and median and interquartile range values of the water-level elevation were not calculated. The Entrada Complex, located between the Morrison and the Chinle, should have sufficient permeability (table 3), given its sandstone dominance, to allow vertical movement of water through this formation. Flow through the Entrada Complex will depend upon available flow paths through the sandstones (or lack of restrictive layers such as thin mudstones that may be present in the Entrada Complex) and the local relation between the various potentiometric surfaces.

Hydraulic Conductivity

Hydraulic conductivity (K) is the capacity of a rock to transmit water and represents the volume of water that will move through a unit area of an aquifer's matrix given a specific unit of time and hydraulic gradient (Heath, 1983). With the substantial variation in composition of the deposits and formations in the study area, K values likely are highly variable, horizontally and vertically, within and between formations. The alluvium aquifer's K likely is highly variable, but published values indicate the possibility for relatively quick groundwater flow through the alluvium aquifer (table 5). The K values of other surficial deposits, such as the volcanoclastics atop the mesas, likely are more site specific and dependent upon depositional characteristics and fracturing as indicated by the large estimated K range for these deposits (table 5).

Few K data are available within the study area for the deeper aquifers, but inferences can be made for the various aquifers, given formation characteristics and the limited K data. Generally, matrices that are unconsolidated, composed of larger grain sizes, well-sorted, less cemented, highly fractured, or strongly weathered would have larger K values compared to matrices with opposing characteristics. Brod and Stone (1981) and Stone and others (1983) compiled characteristics of the study area Neogene, Cretaceous, and Jurassic formations within the San Juan Basin related to aquifer K values (table 5). The characteristics listed in table 5 are highly variable but provide an indicator of the gradation of deposition of the nonmarine sediments composing the Cretaceous and Jurassic formations found in the study area. Fracturing of the formations is not inferred by any of these characteristics, and fracturing can provide substantial pathways for flow. None of the characteristics listed in table 5 can be used to estimate the overall K of an aquifer contained within a formation, but taken together these characteristics can potentially indicate which formations may have larger relative K values. The shale-dominated Chinle Group has relatively small horizontal K values (table 5) and correspondingly small vertical K values of 3×10^{-5} to 1×10^{-4} ft/d (area sampled was north of Milan in the lower San Mateo Creek Basin (Hydro-Engineering, written commun., 1983)). Hydraulic conductivities of the San Andres/Glorieta aquifer can be the largest of all the deeper formation aquifers (table 5).

Groundwater Composition of Major Aquifers

Insufficient data exist to fully describe the geochemical environments of the various aquifers and how they change with time, but sufficient data exist to evaluate overall water types and detections of trace element and contaminants of concern (apps. 2, 3, and 4) in the study area.

Major Elements

Water types in the study area are Na-HCO_3/SO_4 or mixed cation-mixed anion with some Ca-HCO_3 water, and the variation of major elements primarily is between changes in Na and Ca and HCO_3 and SO_4 (fig. 11*A*, *B*, and *C*; app. 2). The major-element variations appear related to typical weathering of silicate minerals and a few common evaporite minerals. Comparison of fresh granitic-type rock to weathered material has shown a possible introduction of the following elements in order of greatest contribution to solution: Na, Ca, Mg, K, Fe (strongly dependent on redox conditions), and Si (Langmuir, 1997). Depending on the level of mineral weathering, clays are primarily aluminosilicates with bound cations that may exchange with groundwater solutes (Bullen and Kendall, 1998). For an aqueous environment in a siliciclastic matrix, major anions primarily are influenced by atmospheric precipitation and soil concentrations because of the lack of these elements in igneous minerals. Bicarbonate is primarily influenced by atmospheric and soil gas inputs (carbon dioxide) and subsequent redox reactions that can decrease HCO_3 in aquifers, although increases in HCO_3 can indicate weathering of CO_3-rich minerals such as limestone ($CaCO_3$), which are not present in any substantial amount in the study area. The change from a water type of Ca–Mg–HCO_3 to larger dissolved-solids concentrations and Na–SO_4–Cl groundwater is common with dissolution of evaporite minerals such as gypsum ($CaSO_4 \cdot H_2O$) and halite (NaCl) (Vengosh, 2003), which also are not present in the study area in substantial amounts. Very little Cl is present in the aquifers in the study area except for a sample from the Chinle Group, which also indicated SO_4-dominant samples and groundwater with the largest dissolved-solids concentrations. The possible addition of Cl or SO_4 with evaporite mineral dissolution in the Chinle aquifer is difficult to attribute to any specific flow path and interaction with a certain formation in the Chinle Group given the gross nature of this analysis, but evaporite deposits have been observed in the Chinle Group in the region (Heckert and Lucas, 2003). Additionally, the shaly nature of much of the Chinle Group provides ample opportunity for cation exchange that can alter groundwater composition such as the exchange of Ca or Mg for Na (loss of Ca or Mg in solution with gain of Na in solution) (Appelo and Postma, 2005) that may account for some of the Na input instead of just silicate mineral weathering.

Table 5. Formation characteristics indicative of horizontal hydraulic-conductivity variation among the aquifers in the study area (from Brod and Stone, 1981; Stone and others, 1983, unless otherwise indicated).

[S/M, sand to mud ratio; T, transmissivity; ft^2/d, square feet per day; K, hydraulic conductivity; ft/d, feet per day; NA, not available]

Formation	Median grain size	Sorting	S/M ratio	Porosity (percent)	Horizontal T[1] (ft^2/d)	Horizontal K (ft/d)
			Quaternary			
Alluvium (Qa)	NA	NA	NA	NA	NA	[2]2–300
			Neogene			
Flows and volcanoclastics (Tnv and Tpb)	NA	NA	NA	NA	NA	[3]1–1,000+
			Cretaceous			
Menefee (Kmf)	Very fine to fine sand	Poor to moderate	4.6	9	2.7–112	.005–.01
Point Lookout (Kpl)	Fine to medium sand	Moderate to moderately well	19.1	2–9	.4–240	.002–.02
Crevasse Canyon (Kcc), sandstone unit	Fine sand	Poor to well	8.4	4	3–250	NA
Mulatto Tongue (Kmm)	Fine sand	Moderate to very well	5.7	11	NA	NA
Gallup (Kg)	Fine to coarse sand	Moderate	13.7–33.5	4–9	[4]15–390	.1–1.0
Dakota (Kd)	Fine to medium sand	Moderate	6.1–18.2	2–6	[4]44–370	.0004–1.5
			Jurassic			
Morrison (Jm)	Fine sand	Moderate to very well	15.7–101.1	0–10	2–480	[5]0.1
Entrada Complex: Early to Middle Jurassic composed of the Bluff, Summerville, Todilto, and Entrada Formations						
Bluff (Jb)	Medium sand	Poor to well	12	7	3–50	NA
Summerville (Js)	Very fine sand	Moderate to moderately well	6.7–10.8	5–6	8.2	NA
Entrada (Je)	Very fine to fine sand	Extremely poor to very well	1.3–9.8	5–11	.84–400	.5–5
			Triassic			
Chinle Group (TRc)	Mudstone mixed with sandstone and limestone		NA	NA	4.7–100	[6]10^{-8}–10^{-1}
			Permian			
San Andres and Glorieta (Psa and Pg)	Micritic limestone and fine to medium sand		NA	NA	[7]10–450,000	[3]40–60

[1]Transmissivity is the rate at which water is transmitted through a unit width of an aquifer under a unit hydraulic gradient. It equals the hydraulic conductivity multiplied by the aquifer thickness (Heath, 1983).

[2]Frenzel, 1992; Risser and Lyford, 1983.

[3]Dames and Moore, written commun., 1986.

[4]Possible overlap of test interval between the Gallup and Dakota Formations.

[6]Roca Honda Resources, LLC, 2009b.

[6]Wolff, 1981.

[7]Brod and Stone, 1981; Brod and Stone, 1983; Frenzel, 1992.

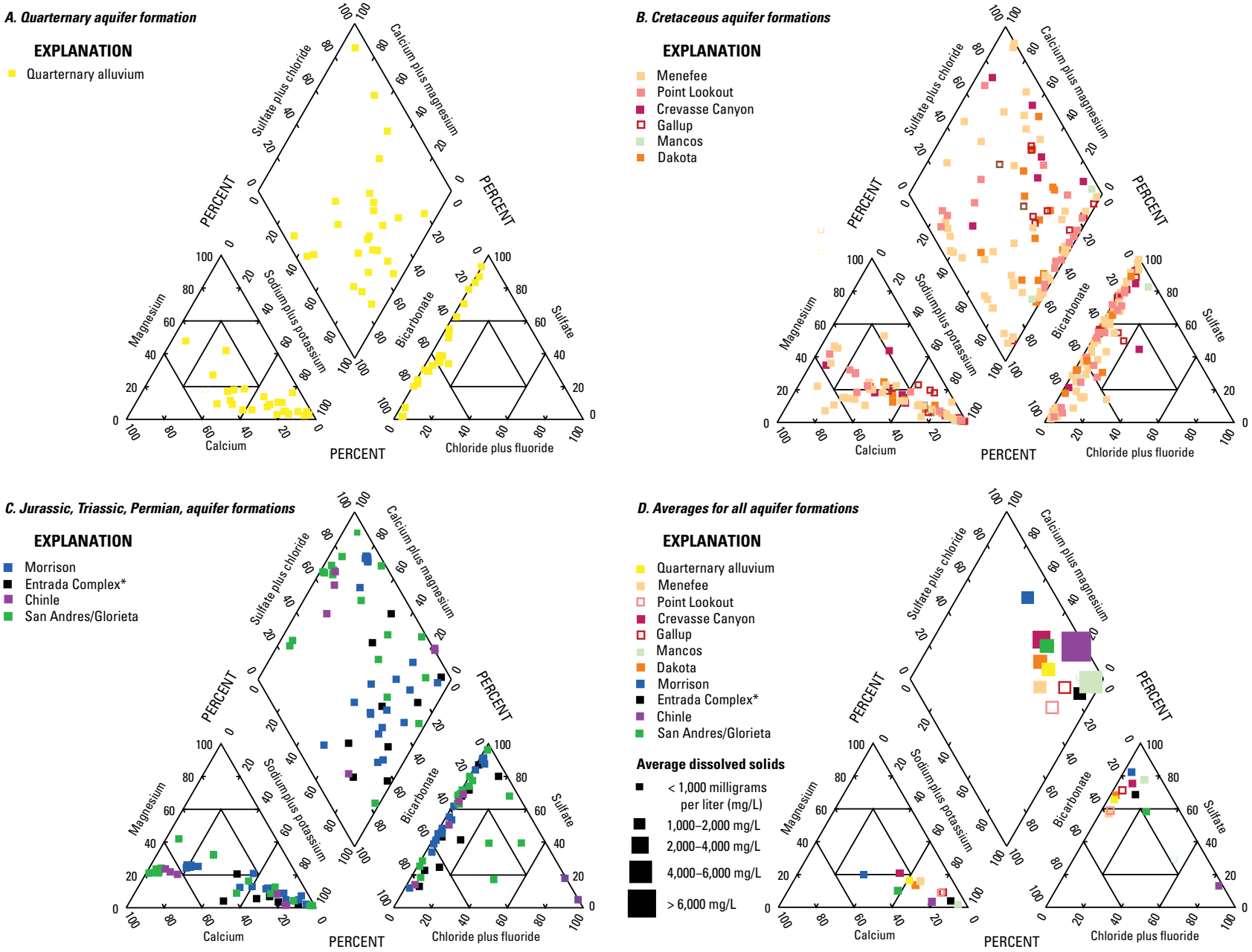

*Entrada Complex represents the combined formations of the Bluff, Summerville, Todilto, and Entrada Formations that are difficult to discriminate in this area and combined for purposes of this report.

Figure 11. Trilinear diagrams of major-element relations for groundwater collected from the deposits and formations found in the study area. The data are a composite of available major-element concentrations collected in the study area from 1958 to 2009.

Trace Elements

A search of existing trace-element data in the study area produced data for Al, Sb, As, Ba, Be, B, Br, Cd, Cr, Co, Cu, Fe, Pb, Li, Mn, Mo, Ni, Se, Ag, Tl, V, and Zn. Very few of these elements were consistently detected in any aquifer, and only Ba, B, Fe, Li, Mn, V, and Zn were detected with any frequency. All existing data sources indicated some data where the elements were not detected at concentrations greater than the MDL(s), although MDLs were not regularly presented in the literature. Nondetect data were not included for analysis in this report because of missing MDLs, which severely limits the statistical analysis of the data because of the bias from this exclusion. The elements of Ba, B, Fe, Li, Mn, V, and Zn are abundant in the Earth's crust and can be mobile in natural waters, and each element can indicate certain characteristics of mineral weathering and redox-environment changes (Hem, 1989; Nimz, 1998). The presence of the redox-sensitive elements Fe and Mn (and to a lesser degree V) indicates reducing conditions at some time in some location in most formations (table 6). Fe is present in the aquifers in various concentrations (app. 3), and it can enter solution under reducing conditions that substantially increase its solubility (Hem, 1989). As part of the USGS National Water-Quality Assessment Program redox classification system, McMahon and Chapelle (2008), proposed a reducing condition threshold 50 µg/L for Mn and 100 µg/L for Fe. As shown in appendix 3, each aquifer contained groundwater at some time that met one or both of the thresholds for reducing conditions. Given the gross nature of this analysis and data compilation and interconnectedness of the aquifers, persistence of reducing conditions in any aquifer at any specific location is unknown.

Boron is the most common trace element detected and had the largest concentrations except for Fe in specific aquifers (table 6 and app. 3). Boron is an abundant element in the Earth's crust and is highly mobile in natural waters (Bullen and Kendall, 1998; Nimz, 1998). Chemical weathering appears strongest in the upper formations because of the frequency of detections of B and Li and the presence of the other common trace elements (table 6), although this could be attributed to sampling frequency. Lithium is common in pegmatites, substitutes for Mg in some minerals, and tends to remain in solution as it is less favored in common-ion exchange compared to other ions (Kelly, 1948; Heier and Billings, 1970). Because of the nature of the data and the likely interconnectedness of the aquifers, the larger presence of these elements cannot be attributed to any characteristic of the upper formations. It is possible that chemical weathering of minerals containing these elements is occurring in overlying formations, such as the Menefee Formation, and being transported into lower formations, such as the Point Lookout Formation. Zinc was most commonly detected in the upper aquifers and the Morrison aquifer, which could represent anthropogenic influences such as mining, where mined water or materials containing Zn were brought to the surface from the Morrison Formation and Zn was transported to the upper aquifers.

Contaminants of Concern

Groundwater in the San Mateo Creek Basin has been contaminated by past mining and milling operations, and a health advisory has been issued for existing and future private wells within the basin concerning contaminant concentrations in excess of Federal drinking-water standards for gross alpha, NO_3, Ra, and U (New Mexico Environment Department, 2009). The sources of contamination are suspected to be naturally occurring ore deposits and former U mines and mills (New Mexico Environment Department, 2009). For purposes

Table 6. Number of detections of frequently detected trace elements in groundwater from the study area.

[Concentrations of the detected occurrence are presented in appendix 3; NA, not available]

Deposit/formation	Barium	Boron	Iron	Lithium	Manganese	Vanadium	Zinc
Alluvium (Qa)	4	39	22	1	7	1	6
Menefee (Kmf)	8	50	40	7	13	5	21
Point Lookout (Kpl)	12	21	16	NA	4	1	11
Crevasse Canyon (Kcc)	NA	7	7	NA	NA	NA	NA
Gallup (Kg)	NA	13	13	1	3	NA	2
Mancos (Km)	NA	2	2	1	1	NA	NA
Dakota (Kd)	1	12	14	1	2	NA	2
Morrison (Jm)	4	22	11	5	5	NA	11
Entrada Complex (Je)	NA	11	15	2	2	1	1
Chinle Group (TRc)	1	9	11	NA	1	NA	NA
San Andres (Psa)	NA	26	27	NA	3	NA	1

of this report, estimated concentrations of contaminants of concern in groundwater (above the MDL but below the reporting level) were accepted as valid detections of the contaminant. All nondetections or less than method detection level indicators were disregarded because of the variety of laboratory analysis methods and MDLs. An estimate of the number of nondetections from analysis of groundwater in the area is difficult to ascertain given the variety of data compiled for this report. For this reason, this discussion only references detected values and only the number of detections is presented with no discussion of concentration levels. A number of negative values were reported for ^{226}Ra, ^{228}Ra, and gross alpha. A negative value implies that the number of alpha emissions detected was smaller than the count of background alpha emissions. These values were disregarded because their negative value implies relatively small concentrations and possible nondetections. The detection counts by formation for the contaminants of concern are shown in table 7. Overall, the contaminants were detected more frequently in the upper aquifers (alluvium, Menefee, and Point Lookout) likely because of sampling frequency targeting mining contamination from surface activities.

Spring, Creek, and Seep Properties of the Upper San Mateo Creek Basin, New Mexico, 2009 and 2010

Snowmelt and precipitation on Mount Taylor and the surrounding mesas provide groundwater to the Neogene volcanoclastics, which recharge the underlying Cretaceous formations. The recharge areas around Mount Taylor and dip of the Cretaceous layers direct groundwater along layers that restrict vertical flow (formation contacts and bedding layers in the volcanoclastics and sedimentary layers) and produce discharges at springs that form El Rito, San Mateo, and San Lucas Creeks, all of which are oriented northward and exit the mesas within or just below the Neogene volcanoclastics. No active springs were found along Jesus and San Mateo Mesas in the northern part of the target area, because of lack of an upgradient watershed (such as Mount Taylor) to catch sufficient precipitation and provide concentrated flow for recharge in this semiarid environment.

Spring, Creek, and Seep Flow

Discharge was occurring in August 2009 and May 2010 from the springs that form El Rito, San Mateo, and San Lucas Creeks. Late spring and summer discharges were about 1 to 2 ft^3/s at all three locations (flows were estimated by determining the cross-sectional area and estimating the streamflow velocity by the float method; Rantz and others, 1983), although quantifying the flow rate was imprecise because of the diffuse nature of the springs. Flow in El Rito and San Mateo Creeks increased between the spring and creek sampling sites. The amount of flow increase varied between the late summer and late spring sampling events, but increased flow was observed in the downgradient direction during both sampling events. This increase in creek streamflow likely is from additional discharges from the underlying Menefee Formation (fig. 12). The spring locations indicate an inhibitor to vertical flow that drives water laterally to a spring, and downslope contributions that increase flow indicate lower saturated layers with similar restrictions to vertical flow and subsequent lateral discharge. Some vertical hydraulic connectivity is likely between the volcanoclastics and formations that compose the mesas, and lateral flow occurs at changes in vertical permeability.

Table 7. Number of detections of contaminants of concern in groundwater from the study area.

[Concentrations of the detected occurrence are presented in appendix 4; NA, not available]

Deposit/formation	Nitrate	Uranium	Radium 226	Radium 228	Radium 226 + 288	Gross alpha
Quaternary alluvium (Qa)	61	13	6	14	14	15
Menefee (Kmf)	52	19	10	15	15	20
Point Lookout (Kpl)	14	NA	9	10	11	11
Crevasse Canyon (Kcc)	17	NA	NA	NA	NA	NA
Gallup (Kg)	37	NA	5	4	5	5
Mancos (Km)	2	NA	NA	NA	NA	NA
Dakota (Kd)	33	1	NA	NA	NA	NA
Morrison (Jm)	34	13	10	10	11	11
Entrada Complex (Je)	28	NA	NA	NA	NA	NA
Chinle (TRc)	28	NA	NA	NA	NA	NA
San Andres/Glorieta (Psa/Pg)	78	NA	NA	NA	NA	NA

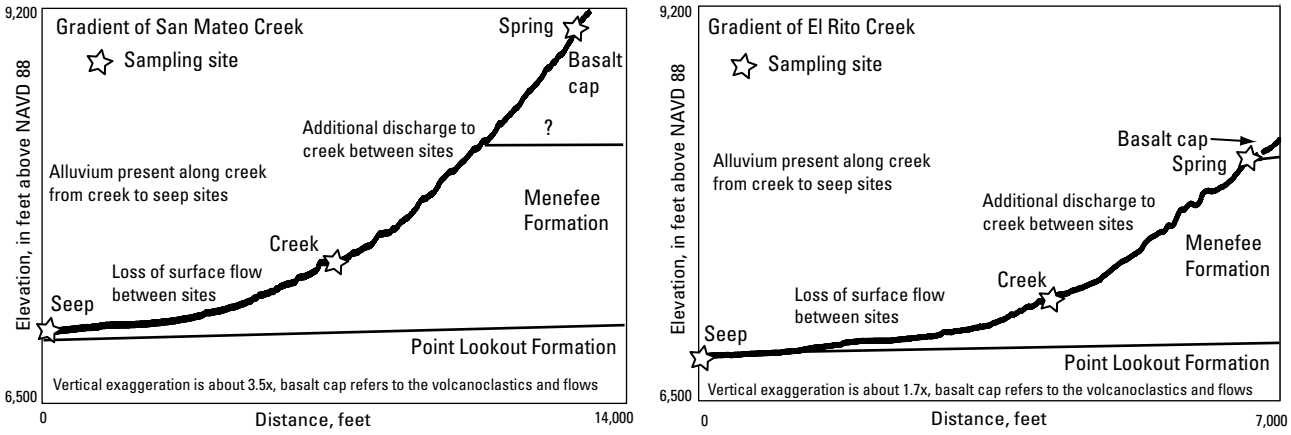

Figure 12. Landform gradients between sampling sites on El Rito and San Mateo Creeks and underlying geologic formations.

Differences in downstream flow of El Rito and San Mateo Creeks were observed between the August 2009 and May 2010 sampling events. Streamflows were larger in El Rito Creek during the May event than the August event, but streamflow was larger in San Mateo Creek during the August event than the May event. El Rito Creek appears to react more quickly to snowmelt from Mount Taylor as compared to San Mateo Creek. This difference may be a result of location and timing of spring snowmelt around Mount Taylor and the watershed orientation of each creek. El Rito Creek drains the western part of Mount Taylor, and San Mateo Creek drains the northern part of the mountain. Remaining snowpack was observed during the May event in the San Mateo Creek watershed but not in the El Rito Creek watershed. The difference in watershed orientation likely is the reason the larger flow was observed in El Rito Creek in May and in San Mateo Creek in August.

Water from El Rito and San Mateo Creeks is captured by man-made diversions for livestock purposes as the creeks exit the higher elevations where the landscape transitions to the valley floor. The creeks were dry below these diversions during both sampling events as the diverted water and remaining creek flow infiltrate into the alluvium aquifer. Springs previously have been mapped in the area and indicators of spring flow (dry discharge points and associated salt crusts) were present along the valley floor near El Rito and San Mateo Creeks. Seeps were present in both creek beds along the valley floor as stagnant water that supported wetlands and small wetted depressions. During both sampling events, there was no flowing water in San Mateo or El Rito Creeks along the valley floor in the upper San Mateo Creek Basin.

Spring, Creek, and Seep Water Composition

Spring- and creek-water samples from the target area contained small amounts of dissolved solutes, and seep water contained substantially larger amounts of dissolved solutes (tables 8 and 9). The specific conductance of water exiting the springs and within the creeks was less than 200 µS/cm, and dissolved-solids concentrations were less than or equal to 150 mg/L during August 2009 and May 2010. Dissolved solids did not substantially increase between the spring and creek locations, although a larger increase was present between the spring and creek locations on San Mateo Creek as compared to El Rito Creek (tables 8 and 9), which may be because of the greater distance between these locations on San Mateo Creek (figs. 8 and 12). The small difference in dissolved solids and similar composition between the spring and creek locations in each system (tables 8 and 9) indicates similar composition for water discharging from the Menefee Formation (indicated by increased downstream flow) as compared to the upper volcanoclastics supplying the springs. Dissolved-solids concentrations substantially increased at the downstream seep sites for El Rito and San Mateo Creeks (tables 8 and 9) indicating mineral dissolution and likely evaporation that concentrated solutes in the water. Samples collected from the seep locations contained particulates less than 0.45-micron in diameter (after filtering), which likely were clay particles and various oxide complexes as indicated by their tannish color. The presence of the small-sized particulates contributes to the "dissolved" concentrations listed in tables 8 and 9. Such particulates were not present in the water from the creek and spring sites following filtering.

The pH of water within the creeks was neutral to alkaline, and all locations indicated oxygenated conditions (dissolved oxygen concentrations were greater than 3 mg/L for all samples; although nearly all samples were undersaturated) that reflects atmospheric exposure (fig. 13, tables 8 and 9). The pH of El Rito Creek did not substantially change from site to site or between August 2009 and May 2010, but the pH of San Mateo Creek changed substantially from site to site and between August 2009 and May 2010. Water in El Rito Creek

Table 8. Physical and chemical properties of springs, creeks, and seeps within the target area, August 2009.

[cond., conductance; µS/cm, microsiemens per centimeter at 25ºC; mg/L, milligrams per liter; ºC, degrees Celsius; %, percent; NTU, nephelometric turbidity unit; <, less than; µg/L, micrograms per liter; $\delta^x X$ (‰) = ($Ratio_{sample}/Ratio_{standard}$ − 1) x 1,000 of specified isotope ratio; ‰, per mil; pCi/L, picocurie per liter]

Constituent	Units	El Rito Creek Spring	El Rito Creek	El Rito Creek Seep	San Mateo Creek Spring	San Mateo Creek	San Mateo Creek Seep	San Lucas Creek Spring
General properties								
pH		8.34	8.29	8.38	7.49	8.1	7.29	7.27
Specific cond.	µS/cm	151	159	600	119	129	1,009	181
Dissolved O_2	mg/L	6.07	8.2	3.79	5.43	5.22	3.86	5.61
O_2 saturation	%	60	78	39	53	55	47	55
Temperature	ºC	14.7	13.1	16.5	14.2	17.5	24.8	13.8
Turbidity	NTU	1.1	4.1	850	4.9	6.3	NA	4.3
Dissolved solids	mg/L	130	130	1,300	72	120	590	130
Major elements								
Calcium	mg/L	14	14	8.2	13	11	42	17
Magnesium	mg/L	4	4.2	3.3	3.6	3.1	26	6.4
Sodium	mg/L	9.7	9.7	130	3.8	8.9	140	9.6
Potassium	mg/L	3.6	3.4	6.3	*1.2	3.4	4.1	3.4
Silica	mg/L	53	51	26	23	47	21	45
Alkalinity	mg/L	72	77	380	36	62	440	89
Sulfate	mg/L	*1.5	*1.4	24	6.9	*1.5	60	*1.6
Chloride	mg/L	*2.1	*2	21	*1.7	*1.7	29	*2.5
Fluoride	mg/L	*.24	*.29	1.3	<.06	*.18	1.7	*.12
Trace elements								
Aluminum	µg/L	<18	<18	700	<18	<18	<18	<18
Antimony	µg/L	<3.1	<3.1	<3.1	*3.2	<3.1	<3.1	<3.1
Arsenic	µg/L	<4.4	<4.4	17	<4.4	<4.4	<4.4	<4.4
Barium	µg/L	19	33	28	39	26	170	24
Beryllium	µg/L	<.47	<.47	<.47	<.47	<.47	<.47	<.47
Boron	µg/L	*8.4	*10	190	*6.3	*8.3	110	*11
Bromide	µg/L	<110	<110	*170	<110	<110	230	<110
Cadmium	µg/L	<.45	<.45	<.45	<.45	<.45	<.45	<.45
Chromium	µg/L	<.66	<.66	<.66	<.66	<.66	<.66	<.66
Cobalt	µg/L	<1.2	<1.2	*1.8	<1.2	<1.2	<1.2	<1.2
Copper	µg/L	<1.4	<1.4	*12	<1.4	<1.4	<1.4	<1.4
Iron	µg/L	<22	*54	790	610	*27	<22	<22
Lead	µg/L	<2.6	*2.6	<2.6	<2.6	<2.6	<2.6	<2.6
Lithium	µg/L	*8.5	*8.9	17	*4	*9	66	*7
Manganese	µg/L	<.25	*1.7	39	100	*2	310	*1.8
Molybdenum	µg/L	<3.1	<3.1	*7.6	<3.1	<3.1	*8.6	<3.1
Nickel	µg/L	<1.3	<1.3	*3.4	<1.3	<1.3	<1.3	<1.3
Selenium	µg/L	<4.9	<4.9	<4.9	<4.9	<4.9	<4.9	<4.9
Silver	µg/L	*1.4	*1.6	*1.4	*1.4	*1.6	*1.6	*1.2
Strontium	µg/L	93	110	120	87	76	1,000	120
Thallium	µg/L	<4.9	<4.9	<4.9	<4.9	<4.9	<4.9	<4.9
Vanadium	µg/L	*3.7	*3.4	57	<1.1	*2.2	*1.5	*4.8
Zinc	µg/L	*5.8	<4.5	*7.6	*6.1	*5.4	<4.5	*8.9
Isotopes								
δ^2H ($^2H/^1H$)	‰	-89.10	-88.46	-39.39	-83.79	-90.14	-81.92	-90.13
$\delta^{18}O$ ($^{18}O/^{16}O$)	‰	-12.58	-12.48	-5.16	-11.81	-12.52	-11.02	-12.47
Local contaminants of concern								
Nitrate, as N	mg/L	.44	*.036	*.036	*.045	*.069	*.044	.19
Uranium	µg/L	*.59	*.39	2.7	<.02	*.25	4.2	*.49
Mercury	µg/L	<.027	<.027	<.027	<.027	<.027	<.027	<.027
Radium-226	pCi/L	*.19	*.28	*.21	<.15	<.15	*.2	<.15
Radium-228	pCi/L	<.4	<.4	<.4	<.4	*.76	*.46	<.4
Gross alpha	pCi/L	<1.5	<1.5	3.5	<1.5	<1.5	3.4	<1.5

*Estimated value—concentration was detected below the reporting level but above the method detection level.

Table 9. Physical and chemical properties of springs, creeks, and seeps within the target area, May 2010.

[cond., conductance; µS/cm, microsiemens per centimeter at 25ºC; mg/L, milligrams per liter; ºC, degrees Celsius; %, percent; NTU, nephelometric turbidity unit; <, less than; µg/L, micrograms per liter; $\delta^{x}X$ (‰) = ($Ratio_{sample}/Ratio_{standard}$ − 1) x 1,000 of specified isotope ratio; ‰, per mil; pCi/L, picocurie per liter]

Constituent	Units	El Rito Creek Spring	El Rito Creek	El Rito Creek Seep	San Mateo Creek Spring	San Mateo Creek	San Mateo Creek Seep	San Lucas Creek Spring
General properties								
pH		8.16	8.19	8.57	6.98	8.09	9.23	7.98
Specific cond.	µS/cm	151	178	1,027	58.7	134	2,460	191
Dissolved O_2	mg/L	6.80	9.84	6.03	7.98	7.83	9.66	7.39
O_2 saturation	%	64	78	69	69	79	>100	68
Temperature	ºC	12.7	5.4	21.8	8.7	15.8	25.0	11.6
Turbidity	NTU	.8	11	1.8	2.2	9.8	74	8.7
Dissolved solids	mg/L	130	150	690	63	130	1,600	140
Major elements								
Calcium	mg/L	13	16	29	5	10	12	18
Magnesium	mg/L	3.5	4.4	22	1.3	2.8	7.9	6.2
Sodium	mg/L	9.6	12	190	2.9	9.8	590	10
Potassium	mg/L	3.8	3.8	9.5	*.99	3.7	6.8	3.7
Silica	mg/L	51	51	54	17	45	7.5	45
Alkalinity	mg/L	71	85	550	15	64	840	96
Sulfate	mg/L	*1.5	*2	27	7.6	*2.6	380	*1.6
Chloride	mg/L	*2.2	*2.7	14	*1.6	*2.2	130	*2.8
Fluoride	mg/L	*.27	*.3	2.4	*.08	*.23	2.9	*.16
Trace elements								
Aluminum	µg/L	<18	<18	<18	410	*78	190	*52
Antimony	µg/L	<3.1	<3.1	<3.1	<3.1	<3.1	<3.1	<3.1
Arsenic	µg/L	<4.4	<4.4	*13	<4.4	<4.4	21	<4.4
Barium	µg/L	18	37	73	14	25	48	33
Beryllium	µg/L	<.47	<.47	<.47	<.47	<.47	<.47	<.47
Boron	µg/L	*9.9	*11	220	*4.4	*10	280	*12
Bromide	µg/L	<110	<110	240	<110	<110	1,000	<110
Cadmium	µg/L	<.45	<.45	<.45	<.45	<.45	<.45	<.45
Chromium	µg/L	<.66	<.66	<.66	<.66	<.66	<.66	<.66
Cobalt	µg/L	<.12	<.12	<.12	<.12	<.12	*.98	<.12
Copper	µg/L	*1	*1.1	*4.4	*1.2	*.62	23	*1.0
Iron	µg/L	<22	*52	<22	200	*68	340	*39
Lead	µg/L	<.26	<.26	<.26	<.26	<.26	<.26	<.26
Lithium	µg/L	*7.9	*5.1	78	<.26	*4	51	*2.3
Manganese	µg/L	<.25	<.25	*.51	*2	*.79	*7.2	*.95
Molybdenum	µg/L	<3.1	<3.1	*7.8	<3.1	<3.1	42	<3.1
Nickel	µg/L	<1.3	<1.3	*1.9	<1.3	<1.3	*5.8	<1.3
Selenium	µg/L	<4.9	<4.9	<4.9	<4.9	<4.9	<4.9	<4.9
Silver	µg/L	<.93	<.93	<.93	<.93	<.93	<.93	<.93
Strontium	µg/L	86	120	510	32	69	280	120
Thallium	µg/L	<4.9	<4.9	<4.9	<4.9	<4.9	<4.9	<4.9
Vanadium	µg/L	*2.7	*2.6	13	<1.1	*2.4	38	*4.3
Zinc	µg/L	<4.5	<4.5	<4.5	<4.5	<4.5	<4.5	<4.5
Isotopes								
$\delta^{2}H$ ($^{2}H/^{1}H$)	‰	-89.51	-88.18	-73.49	-88.77	-88.67	-48.08	-89.14
$\delta^{18}O$ ($^{18}O/^{16}O$)	‰	-12.68	-12.46	-9.15	-12.59	-12.39	-3.51	-12.46
Local contaminants of concern								
Nitrate, as N	mg/L	.37	*.17	<.042	<.042	*.09	<.042	*.16
Uranium	µg/L	*.63	*.54	7.1	*.025	*.37	26	*.58
Mercury	µg/L	<.027	<.027	<.027	<.027	<.027	<.027	<.027
Radium-226	pCi/L	<.15	<.15	<.15	<.15	<.15	*.34	<.15
Radium-228	pCi/L	<.67	<.67	<.67	<.67	*.92	.77	<.67
Gross alpha	pCi/L	<1.5	<1.5	*2.8	<1.5	<1.5	29	<1.5

*Estimated value—concentration was detected below the reporting level but above the method detection level.

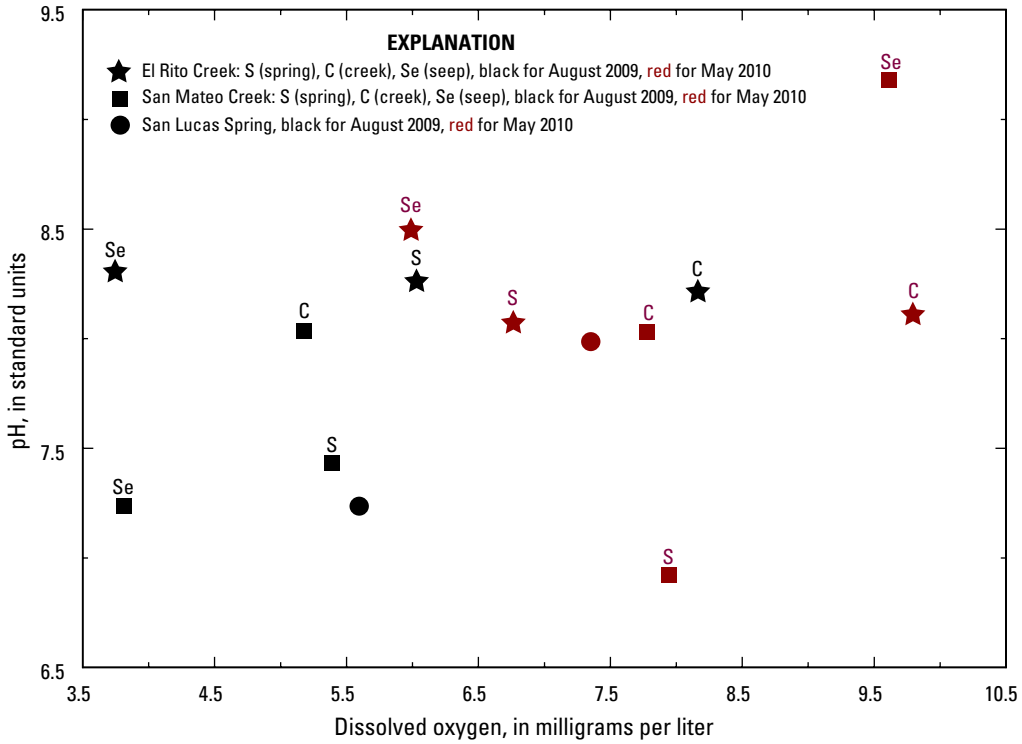

Figure 13. Dissolved oxygen and pH relation for water from El Rito, San Lucas, and San Mateo Creeks.

indicated a greater increase in dissolved-oxygen percent saturation with flow from the spring to creek locations as compared to San Mateo Creek, likely because of the larger topological gradient on El Rito Creek between the spring and creek locations (more turbulent flow). Dissolved-oxygen concentrations and percent saturation were equal or greater during the May 2010 sampling as compared to the August 2009 sampling for all locations.

Water Isotopes and Evaporation

The variation in isotopic composition of precipitation may allow discrimination of recharge because of changes in the isotopic composition from temperature changes during formation of precipitation and additional evaporation (Genereux and Hooper, 1998; Ingraham, 1998). The δ^2H and $\delta^{18}O$ values in the two creek systems generally plot near the global meteoric water line (GMWL) (fig. 14), which is atypical of the southwestern United States, where the semiarid climate generally produces values for any surface water or groundwater that plot below the GMWL with a reduced trend slope (evaporation line) because of a greater fractionation influence on H than O (Friedman and others, 1992; Kendall and Coplen, 2001). Only the seep samples indicate values below the GMWL. The larger values of the seeps indicate heavier isotope ratios or greater loss of the lighter isotopes likely from fractionation during evaporation, assuming no other water sources of different isotopic composition (no identifiable upward leakage sources given the geologic framework and likely vertical flow directions).

The water isotopes also indicate differences in source waters and (or) evaporative effect between El Rito and San Mateo Creeks. The seep in El Rito Creek contained water with a heavier isotopic value for the August sample compared to the May sample, which is expected given the higher rate of evaporation during August. This seasonal influence was different for the seep in San Mateo Creek, which contained a heavier isotopic value for the May sample. This contrast in seasonal influences between the two creeks, indicates differences in source-water inputs between the two sampling events that likely pertain to differences in source-water mixing (winter precipitation and snowmelt compared to summer thunderstorms) and evaporation during snowmelt. This difference may be the quicker melt in the El Rito Creek watershed, given the observed lack of snow in this watershed and the presence of snow in the San Mateo Creek watershed during the May sampling event, as discussed in the Spring, Creek, and Seep Flow section. Such seasonal differences in the stable isotopes of water is common for shallow groundwater where the isotope signal is not attenuated (seasonal sources are not mixed) prior to discharge from the springs or seeps (Leibundgut and others, 2009). A lack of attenuation of the seasonal isotopic signal indicates that seasonal changes in flow or solutes will be visible in the spring, creek, and seep discharges.

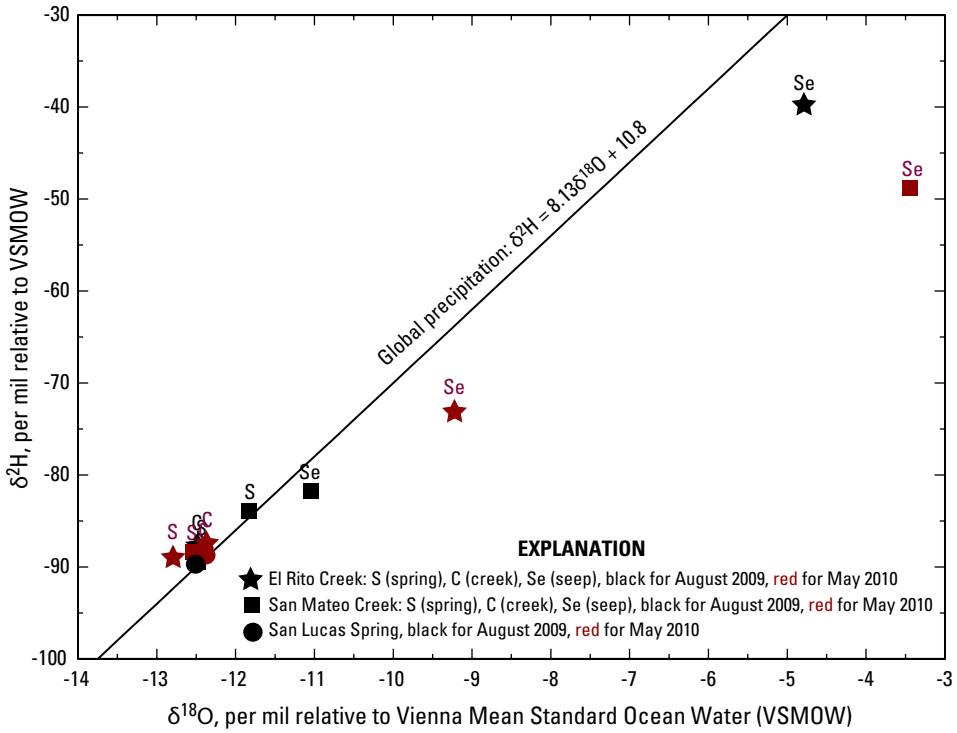

Figure 14. Stable isotope ratios for water from El Rito, San Lucas, and San Mateo Creeks.

Major Elements

The ion-exchange pool at any location in a flow path exemplifies water-rock interactions and atmospheric inputs, and ions will exchange at the mineral surfaces at relatively constant rates that reflect clay mineralogy, water pH, and water chemistry (Bullen and Kendall, 1998); although, water-rock interactions that produce mineral dissolution or adsorption can result in nonconservative solute behavior that limits the utility of major-element and trace-element concentrations for identifying source waters and flow paths (Langmuir, 1997). Results from the creek sampling indicated similarities in composition between the El Rito and San Mateo Creeks at comparable sampling sites (spring to spring or creek to creek) and large changes in downstream composition in each creek, mostly as a result of changes in Na and smaller changes in SO_4 between the creek and seep sites (fig. 15 and tables 8 and 9). These changes alter the composition in El Rito and San Mateo Creeks from a mixed cation-HCO_3 water type at the spring and creek locations to Na-HCO_3 at the seeps, which can occur with silicate weathering or cation exchange (Stumm and Morgan, 1996).

The major-element data indicated a strong electrical (cation-anion) imbalance for the sample from the seep along El Rito Creek in August 2009 (14 percent greater anion charge). Water at the seep along El Rito Creek in 2009 appears to contain additional buffering compounds such as hydroxides (largest pH value of all samples), borates (largest boron value of all samples), aluminosilicates (largest aluminum value of all samples), and organic ligands (largest concentrations for many of the trace elements) (table 8), which resulted from the inclusion of very fine suspended particles passing through the 0.45-micron filter and were visible to the naked eye. The major cations and anions also did not balance for the sample collected from the spring at San Mateo Creek during the August 2009 sampling event, but this unbalanced charge was positive. This location appears to be influenced by a change in oxidation conditions. Water from the spring was oxygenated (5.43 mg/L dissolved oxygen at a saturation level of 53 percent), but the water contained relatively large concentrations of Fe (610 µg/L) and Mn (100 µg/L). It appears that reducing conditions may be present in the aquifer contained within the young, cap-forming basalts. The water chemistry of the aquifer may not be fully represented by the spring sample site as the water becomes oxygenated and kinetic reactions of various soluble or insoluble solutes occur at different rates with the transition from reduced to oxygenated conditions.

Saturation Indices

The presence of the major elements and trace elements in surface water in the upper San Mateo Creek Basin may allow various mineral compounds and phases to either dissolve in or precipitate from solution given the elements' concentrations.

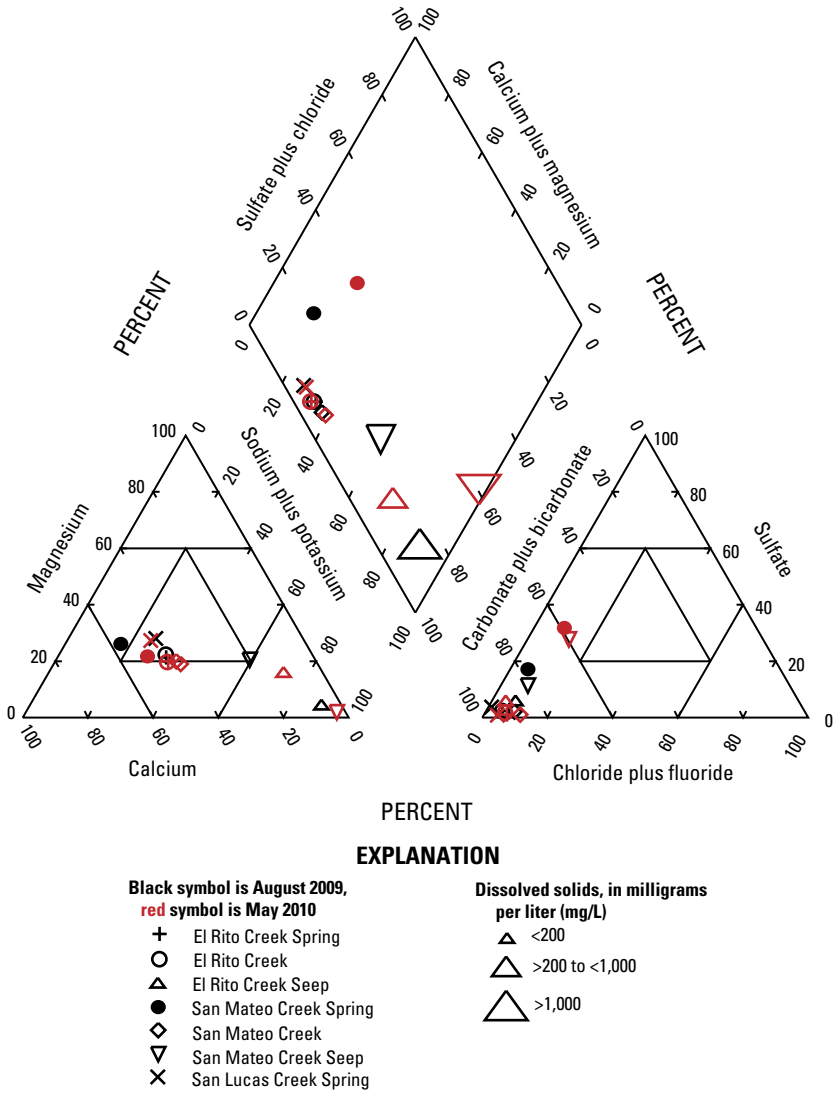

Figure 15. Trilinear diagram of major-element relations for water from El Rito, San Lucas, and San Mateo Creeks.

The saturation indices of possible common mineral forms were determined for the water samples from the August 2009 and May 2010 sampling events (tables 10 and 11). Negative values indicate undersaturation where a mineral might dissolve in the water and positive values indicate supersaturation where a mineral may precipitate from the water. The saturation indices indicate similar water composition and solute concentrations for spring to creek flow paths indicating no inputs of different water chemistries (tables 10 and 11). The increased flow between the spring and creek sites that was observed for El Rito and San Mateo Creeks is a result of the addition of water that is similar in composition to that discharging from the springs. The change from an open channel flow to infiltration into the alluvium from the creek to seep sites allows increased mineral weathering and provides available surfaces for sorption and cation exchange as seen with the substantial differences in mineral phases (tables 10 and 11). Such a change in the flow system can induce large changes in the aqueous chemical environment as the elemental composition is altered with new inputs/outputs from weathering, cation exchange, and possible precipitation of various minerals along with sorbed elements (Bullen and Kendall, 1998).

Creek Flow Paths and Geochemical Model of Transition from Creek to Seep

El Rito and San Mateo Creeks are fed by precipitation (seasonal snow and rain) around Mount Taylor that feed the springs forming these creeks near the base of the mountain.

Table 10. Saturation indices of possible common minerals for water collected from the spring, creek, and seep locations along El Rito Creek in the target area.

[Saturation indices were calculated in PHREEQC (2.17.0) and represent the log of the ratio of the ion activity product (IAP) and the solubility product (K_{sp})]

Phase	Mineral composition	August 2009			May 2010		
		Spring	Creek	Seep	Spring	Creek	Seep
Anhydrite	$CaSO_4$	-4.14	-4.17	-7.68	-4.16	-3.95	-2.88
Barite	$BaSO_4$	-1.72	-1.48	-10.67	-1.7	-1.11	-.31
Calcite	$CaCO_3$	-.1	-.14	-8.11	-.34	-.26	1.2
Celestite	$SrSO_4$	-4.36	-4.32	-9.84	-4.39	-4.1	-2.67
Chalcedony	SiO_2	.61	.62	-3.37	.62	.72	.52
Chrysotile	$Mg_3Si_2O_5(OH)_4$	-1.24	-1.72	31.32	-2.78	-3.33	2.76
Dolomite	$CaMg(CO_3)_2$	-.54	-.63	-16.4	-1.07	-1.06	2.61
Fluorite	CaF_2	-2.67	-2.49	-12.32	-2.57	-2.29	-.72
Gypsum	$CaSO_4 \cdot 2H_2O$	-3.89	-3.91	-7.68	-3.91	-3.69	-2.65
Halite	NaCl	-9.2	-9.22	-5.56	-9.18	-8.98	-7.16
Sepiolite	$Mg_2Si_3O_7.5OH \cdot 3H_2O$	.37	.12	15.26	-.55	-.46	2.62
Strontianite	$SrCO_3$	-1.77	-1.73	-10.27	-1.99	-1.81	-.06

Table 11. Saturation indices of possible common minerals for water collected from the spring, creek, and seep locations along San Mateo Creek in the target area.

[Saturation indices were calculated in PHREEQC (2.17.0) and represent the log of the ratio of the ion activity product (IAP) and the solubility product (K_{sp})]

Phase	Mineral composition	August 2009			May 2010		
		Spring	Creek	Seep	Spring	Creek	Seep
Anhydrite	$CaSO_4$	-3.48	-4.22	-2.33	-3.79	-4.02	-2.46
Barite	$BaSO_4$	-.72	-1.62	.33	-.95	-1.36	.26
Calcite	$CaCO_3$	-1.26	-.45	.1	-2.7	-.51	1.3
Celestite	$SrSO_4$	-3.71	-4.43	-2.03	-4.02	-4.23	-2.06
Chalcedony	SiO_2	.26	.53	.1	.2	.53	-.46
Chrysotile	$Mg_3Si_2O_5(OH)_4$	-7.21	-2.72	-5.03	-12.54	-3.17	3.15
Dolomite	$CaMg(CO_3)_2$	-2.88	-1.2	.34	-5.9	-1.36	2.83
Gypsum	$CaSO_4 \cdot 2H_2O$	-3.23	-3.97	-2.11	-3.53	-3.77	-2.25
Halite	NaCl	-9.7	-9.34	-6.99	-9.81	-9.18	-5.77
Manganite	MnOOH	-4.73	-4.72	-5.18	-7.9	-5.15	-2.37
Rhodochrosite	$MnCO_3$	-.88	-1.82	.26	-3.58	-2.25	-.67
Sepiolite	$Mg_2Si_3O_7.5OH \cdot 3H_2O$	-4.17	-.86	-3.39	-7.6	-1.09	1.12
Strontianite	$SrCO_3$	-2.92	-2.12	-1.07	-4.35	-2.17	.22

El Rito and San Mateo Creeks transition from steep gradients along the mesas where flow is sustained by groundwater discharges from mesa volcanoclastics and the Menefee Formation to low gradients in the valleys where surface flow has infiltrated into to the valley alluvium. The subsequent shallow groundwater is restricted (or retarded) from downward migration by a shaly layer in the Menefee Formation. This change from open-channel flow to shallow groundwater substantially alters the influences on the chemistry of the water. The upper creek flow that originates at the springs is influenced by infiltration of precipitation from Mount Taylor that remains dilute indicating relatively quick entry into the surface-water system without substantial addition of dissolved solutes that could occur with longer residence times in these upper layers of the mesas (additionally shown with the lack of isotopic signal attenuation for seasonal inputs described in the Water Isotopes and Evaporation section). With transition to the lower gradient valley floor of upper San Mateo Creek Basin, creek flow infiltrates into the valley alluvium but does not progress to substantial depths because of an apparent shale layer within the underlying Menefee found near the surface in the eastern part of the basin. The transitions from the mesa to the valley floor were geochemically modeled to compare the potential evaporation and water-rock influences on the water chemistry of the creeks.

All geochemical data were entered into NETPATH for the El Rito and San Mateo creek and seep locations. Each model was constrained by changes in Al, C, Ca, Fe, K, Mg, Mn, Na, and S, which were the elements that indicated large changes in concentration between the creek and seep sites in each system. Each model also was constrained by mineral phases that were chosen according to the local geology and changes in typical minerals according to the saturation indices derived for each location (tables 10 and 11). Results of the geochemical modeling (table 12) are indicative of changes in water chemistry from the dissolution and precipitation of various minerals (including the presence of very fine clay particles from weathering) and cation exchange/sorption as solutes enter the system from water-rock interaction and the increase in concentration of solutes from evaporation. As visible in the concentrations (tables 8 and 9) and saturation indices (tables 10 and 11), elements of the selected minerals typically increase in groundwater concentration from creek to seep locations, which conforms to the conceptual model of chemical weathering and inputs of additional elements between these locations; although, certain minerals decrease in prevalence (become more undersaturated), such as gypsum in the August 2009 El Rito Creek samples, reflecting the changing element composition and preferred mineral forms. The mineral phases presented in table 12 are not meant to represent the entire chemical environment, but are common minerals that are thermodynamically preferred given the elemental composition of the waters. The mineral phases do reflect the presence of clays (thermodynamically preferred phases of montmorillinite and kaolinite possible in these solutions) that were observed in the filtered solution from the seeps. These clay phases do not represent the only clays present, but reflect the presence of very fine weathered aluminosilicate particles in solution. In addition to the likely substantial chemical weathering from creek to seep locations, the model results indicate a strong evaporative effect between the creek and seep locations (table 12). The evaporative effect was stronger in the May 2010 results

Table 12. Geochemical model results for creek to seep locations along El Rito and San Mateo Creeks.

[Aug 2009, August 2009 sampling event; May 2010, May 2010 sampling event; positive value represents an addition of the elements composing the mineral phase to the solution through dissolution in millimoles per kilogram of water (mmol/kg); negative value represents a subtraction of the elements composing the mineral phase to the solution through precipitation (mmol/kg); evaporation values are based on 1 kilogram of solution; <, less than]

Phase	Mineral composition	El Rito Creek		San Mateo Creek	
		Aug 2009	May 2010	Aug 2009	May 2010
Albite	$NaAlSi_3O_8$	2.37*	2.78	4.03	13.54
Calcite	$CaCO_3$	2.54	2.53	6.76	6.64
Ca-Montmorillonite	$Ca_{0.165}Al_{2.33}Si_{3.67}O_{10}(OH)_2$	-17.37	-16.35	-39.94	-53.03
Goethite	FeOOH	.01	<-.01	<-.01	<.01
Gypsum	$CaSO_4 \cdot 2H_2O$	.12	.09	.50	2.13
Halite	NaCl	.26	<.01	.63	<.01
Kaolinite	$Al_2Si_2O_5(OH)_4$	19.05	17.65	44.51	55.02
Rhodochrosite	$MnCO_3$	<.01	.00	.01	<.01
Talc	$Mg_3Si_4O_{10}(OH)_2$	-.03	.06	.25	.02
Grams of water (H_2O) remaining after evaporation		539	400	829	543
Evaporation factor (divisor)		1.85	2.50	1.21	1.84

*A secondary model was run with cation exchange (Ca substitution of Na on clay surfaces) as an additional influence. Results of this model were similar to the model results shown in the table except for the lack of albite dissolution and proportional decreases in Ca-montmorillonite and kaolinite (silicate layered clays).

(2.50 and 1.84 evaporation factors) as compared to the August 2009 results (1.85 and 1.21 evaporation factors). These results support the conceptual model of substantial mineral dissolution with increased water-rock interaction because of the entrance of the creek flow into the subsurface with the transition to the valley floor followed by substantial evaporation of the water as it reappears at the surface from seeps near the confluence of El Rito and San Mateo Creeks.

Summary

The water resources of the San Mateo Creek Basin are important to the citizens of New Mexico, in particular, the town of San Mateo and the city of Grants, for potable water sources. Citizens and tribal groups in this area are concerned about the possible effects on the water resources from exploratory drilling and possible mining of uranium as currently (2011) proposed by various companies for U.S. Forest Service land in the upper San Mateo Creek Basin. Existing data were used to describe the geologic framework and regional aquifer properties, and new data were collected to characterize the springs, creeks, and seeps in the upper San Mateo Creek Basin. The geologic framework of the study area consists of the Zuni Uplift, Chaco Slope, and the Mount Taylor Volcanic Field. The major landscape features of the San Mateo Creek Basin are a result of folding and tilting during the Laramide Orogeny and the Neogene volcanism associated with the Mount Taylor Volcanic Field. Within this structural context, the sedimentary formations provide matrices for local and regional aquifers.

Groundwater in the study area occurs in numerous deposits and formations that form unconfined and confined aquifers, and recharge occurs in highlands such as the Zuni Mountains and Mount Taylor. Existing water-level data indicate topologically downgradient flow in the Quaternary alluvium aquifer and indiscernible general flow patterns in lower aquifers. According to previously published material and the geologic structure of the aquifers, the flow direction in the lower aquifers likely is in the opposite direction compared to the alluvium aquifer. These opposing horizontal-flow directions are a result of different recharge areas, the unconsolidated alluvium that follows the topological gradient, and a regional opposing gradient of the lower sedimentary formations.

Insufficient data exist to fully describe the geochemical environments of the various aquifers and how they change with time, but sufficient data exist to evaluate general water types in the study area. Water types in the study area are sodium-bicarbonate/sulfate or mixed cation-mixed anion with some calcium-bicarbonate water, and the variation of major elements is primarily between changes in sodium and calcium and bicarbonate and sulfate. The major-element variations appear related to typical weathering of silicate minerals and a few common evaporite minerals and cation-exchange processes. The presence of the reduction/oxidation-sensitive elements iron and manganese indicates reducing conditions at some time or in some location in most formation aquifers. The large concentrations of zinc in the alluvium aquifer could represent anthropogenic influences such as mining.

Snowmelt and precipitation on Mount Taylor and the surrounding mesas provide groundwater to the Neogene volcanoclastics, which recharge the underlying Cretaceous formations. The upgradient recharge areas and regional dip of the Cretaceous layers towards the north-northeast direct groundwater along likely bedding planes that restrict vertical flow and cause discharges at springs that form El Rito, San Mateo, and San Lucas Creeks. Streamflows were larger in El Rito Creek during May 2010 compared to August 2009, but streamflow was larger in San Mateo Creek during August 2009 compared to May 2010. El Rito Creek appears to react more quickly to snowmelt from Mount Taylor than does San Mateo Creek. This difference may be a result of location and timing of spring snowmelt around Mount Taylor because of differences in watershed orientation. Water from El Rito and San Mateo Creeks is captured by man-made diversions for livestock purposes as the creeks exit the higher elevations where the landscape transitions to the valley floor. The creeks were dry below these diversions during the sampling events in 2009 and 2010. The diverted water and remaining creek flow infiltrate into the alluvium aquifer, but some of this water did reemerge in seeps in the center of the upper San Mateo Creek Basin near the confluence of El Rito and San Mateo Creeks.

Spring- and creek-water samples from the target area contained small amounts of dissolved solutes, and seep water contained substantially larger amounts of dissolved solutes. The specific conductance of water exiting the springs and within the creeks was less than 200 microsiemens per centimeter and dissolved-solids concentrations were less than or equal to 150 milligrams per liter during August 2009 and May 2010. The pH of water within the creeks was neutral to alkaline, and all locations indicated oxygenated conditions with nearly all samples being undersaturated for dissolved oxygen. Results of water-isotope analyses indicate limited evaporation at the spring and creek sites but greater evaporation by the time the water reaches the seep locations in the center of upper San Mateo Creek Basin. Variations in water isotopes between El Rito and San Mateo Creeks indicate differences in source-water inputs between the two sampling events that likely pertain to spring snowmelt compared to summer-thunderstorm precipitation.

Results from the creek sampling indicated similarities in composition between the El Rito and San Mateo Creeks at the comparable sampling sites (spring to spring or creek to creek) and large changes in downstream composition in each creek, mostly as a result of changes in sodium and smaller changes in sulfate between the creek and seep sites. These changes alter the composition in El Rito and San Mateo Creeks from mixed cation-bicarbonate water type at the spring and creek locations to sodium-bicarbonate water type at the seeps. Geochemical modeling of the transition from creek to seep locations along El Rito and San Mateo Creeks indicates chemical weathering

and additional element inputs through water-rock interactions and possible element composition changes from cation exchange. Additionally, the model results indicate an evaporative effect between the creek and seep locations and differences in the chemical weathering and evaporation effects by season.

References

Agency for Toxic Substances and Disease Registry, 2008, Health Consultation, Homestake Mining Company Mill Site, Milan, Cibola County, New Mexico: Division of Health Assessment and Consultation, Agency for Toxic Substances and Disease Registry, Department of Health and Human Services, 26 p., accessed July 6, 2010, at http://www.epa.gov/region6/6sf/newmexico/homestake_mining/nm_homestake_mining_atsdr_rpt.pdf.

Appelo, C.A.J., and Postma, D., 2005, Geochemistry, groundwater, and pollution, 2d edition: AA Balkema Publishers, Rotterdam, 638 p.

Baars, D.L., 1962, Permian system of the Colorado Plateau: American Association of Petroleum Geologists Bulletin, v. 46, no. 2, p. 149–218.

Baldwin, J.A., and Anderholm, S.K., 1992, Hydrogeology and ground-water chemistry of the San Andres/Glorieta aquifer in the Acoma embayment and eastern Zuni uplift, west-central New Mexico: U.S. Geological Survey Water-Resources Investigations Report 91–4033, 304 p.

Brod, R.C., 1979, Hydrogeology and water resources of the Ambrosia Lake–San Mateo area, McKinley and Valencia counties, New Mexico: Socorro, N. Mex., M.S. thesis, New Mexico Institute of Mining and Technology, 194 p.

Brod, R.C., and Stone, W.J., 1981, Hydrogeology of Ambrosia Lake–San Mateo area, McKinley and Cibola Counties, New Mexico: New Mexico Bureau of Mines and Mineral Resources, HS–2, text and map, scale 1:62,500.

Bullen, T.D., and Kendall, C., 1998, Tracing of weathering reactions and water flowpaths, a multi-isotope approach, *in* Kendall, C., and McDonnell, J.J., eds., Isotope tracers in catchment hydrology: Amsterdam, Elsevier Science B.V., chap. 18, p. 611–643.

Cather, S.M., 2003, Polyphase Laramide tectonism and sedimentation in the San Juan Basin, New Mexico, *in* Lucas, S.G., Semken, S.C., Berglof, W.R., and Ulmer-Scholle, D.S., eds., Geology of the Zuni Plateau: New Mexico Geological Society, Fifty-Fourth Annual Field Conference, Las Vegas, New Mexico, New Mexico Highlands University, September 24–27, 2003, p. 119–132.

Cather, S.M., 2004, The Laramide Orogeny in central and northern New Mexico and southern Colorado, *in* Mack, G.H., and Giles, K.A., eds., The geology of New Mexico, a geologic history: Socorro, New Mexico Geological Society Special Publication 11, p. 203–248.

Crumpler, L.S., 1982, Volcanism in the Mount Taylor region: New Mexico Geological Society Guidebook 33, p. 291–298.

Crumpler, L.S., 2003, The Mount Taylor Volcanic Field, *in* Lucas, S.G., Semken, S.C., Berglof, W.R., and Ulmer-Scholle, D.S., eds., Geology of the Zuni Plateau: New Mexico Geological Society, Fifty-Fourth Annual Field Conference, Las Vegas, New Mexico, New Mexico Highlands University, September 24–27, 2003, p. 75–77.

Daly, C., and Weisburg, J., 1997, Average annual precipitation, New Mexico: U.S. Department of Agriculture, Natural Resources Conservation Service, National Water and Climate Center, accessed July 25, 2011, at http://www.wrcc.dri.edu/pcpn/nm.gif.

Dillinger, J.K., 1990, Geologic map of the Grants 30' x 60' quadrangle, west-central New Mexico: U.S. Geological Survey Coal Investigations map C–118–A, scale 1:100,000.

Dubiel, R.F., 1994, Triassic deposystems, paleogeography, and paleoclimate of the Western Interior, *in* Caputo, M.V., Peterson, J.A., and Franczyk, K.J., eds., Mesozoic systems of the Rocky Mountain region, USA: Rocky Mountain Section, Society of Economic Paleontologists and Mineralogists, p. 133–168.

El–Kadi, A., and Fujiwara, K., 2009, NETPATH-WIN—Windows version of NETPATH based on original model of Plummer and others (2009), distributed by the Isotope Hydrology Section of the International Atomic Energy Agency, Vienna, Austria.

Fetter, C.W., 2001, Applied hydrogeology: New Jersey, Prentice Hall, Inc., 598 p.

Fitch, D.C., 1980, Exploration for uranium deposits, Grants Mineral Belt, *in* Rautman, C.A., ed., Geology and mineral technology of the Grants uranium region 1979: New Mexico Bureau of Mines and Mineral Resources, Memoir 38, p. 40–51.

Fitzsimmons, J.P., 1959, The structure and geomorphology of west-central New Mexico, *in* Weir, Jr., J.E., Baltz, E.H., and Cardwell, W.D.E., eds., Guidebook of west-central New Mexico: Socorro, New Mexico Geological Society, 10th Field Conference, p. 112–116.

Frenzel, P.F., 1992, Simulation of ground-water flow in the San Andres/Glorieta aquifer in the Acoma Embayment and eastern Zuni Uplift, west-central New Mexico: U.S. Geological Survey Water-Resources Investigations Report 91–4099, 381 p.

Friedman, I., Smith, G.I., Gleason, J.D., Warden, A., and Harris, J.M., 1992, Stable isotope composition of waters in southeastern California—modern precipitation: Journal Geophysical Research, v. 97, p. 5795–5812.

Garven, G., 1995, Continental-scale groundwater flow and geologic processes: Annual Review of Earth and Planetary Sciences, v. 23, p. 89–118.

Genereux, D.P., and Hooper, R.P., 1998, Oxygen and hydrogen isotopes in rainfall-runoff studies, *in* Kendall, C., and McDonnell, J.J., eds., Isotope tracers in catchment hydrology: Amsterdam, Elsevier Science B.V., p. 319–346.

Gordon, E.D., 1961, Geology and ground-water resources of the Grants–Bluewater area, Valencia County, New Mexico: New Mexico State Engineer Technical Report 20, 109 p.

Heath, R.C., 1983, Basic ground-water hydrology: U.S. Geological Survey Water-Supply Paper 2220, 84 p.

Heckert, A.B., and Lucas, S.G., 2003, Triassic stratigraphy in the Zuni Mountains, west-central New Mexico, *in* Lucas, S.G., Semken, S.C., Berglof, W.R., and Ulmer-Scholle, D.S., eds., Geology of the Zuni Plateau: New Mexico Geological Society, Fifty-Fourth Annual Field Conference, September 24–27, 2003, p. 245–262.

Heier, K.S., and Billings, G.K., 1970, Lithium, *in* Wedepohl, K.H., ed., Handbook of geochemistry: Berlin, Springer–Verlag, v. II–1, p. 3I1–3I3.

Hem, J.D., 1989, Study and interpretation of the chemical characteristics of natural water: U.S. Geological Survey Water-Supply Paper 2254, 263 p.

Hunt, C.B., 1938, Igneous geology and structure of the Mount Taylor Volcanic Field, New Mexico: U.S. Geological Survey Professional Paper 189–B, p. 51–80.

Ingraham, N.L., 1998, Isotopic variations in precipitation, *in* Kendall, C., and McDonnell, J.J., eds., Isotope tracers in catchment hydrology: Amsterdam, Elsevier Science B.V., p. 87–118.

Keating, G.N., and Valentine, G.A., 1998, Proximal stratigraphy and syn-eruptive faulting in rhyolitic Grants Ridge Tuff, New Mexico, USA: Journal of Volcanology and Geothermal Research, v. 81, no. 1–2, p. 37–49.

Kelley, V.C., and Clinton, N.J., 1960, Fracture systems and tectonic elements of the Colorado Plateaus: Albuquerque, University of New Mexico Press, Publications in Geology, no. 6, 104 p.

Kelly, W.P., 1948, Cation exchange in soils: New York, Reinhold Publishing Corporation, 114 p.

Kendall, C., and Coplen, T.B., 2001, Distribution of oxygen-18 and deuterium in river waters across the United States: Hydrological Processes, v. 15, no. 7, p. 1363–1393.

Langmuir, D., 1997, Aqueous environmental geochemistry: New Jersey, Prentice Hall, Inc., 600 p.

Laughlin, A.W., Perry, F.V., Damon, P.E., Shafiqullah, M., WoldeGabriel, G., McIntosh, W., Harrington, C.D., Wells, S.G., and Drake, P.G., 1994, Geochronology of Mount Taylor, Cebollita Mesa, and Zuni–Bandera volcanic fields, Cibola County, New Mexico: New Mexico Geology, v. 15, no. 4, p. 81–92.

Leibundgut, C., Maloszewski, P., and Külls, C., 2009, Tracers in hydrology: West Sussex, United Kingdom, Wiley-Blackwell, 415 p.

Lipman, P.W., and Mehnert, H.H., 1979, Potassium-argon ages from the Mount Taylor Volcanic Field, New Mexico: U.S. Geological Survey Professional Paper 1124–B, 8 p.

Lipman, P.W., Pallister, J.S., and Sargent, K.A., 1979, Geologic map of the Mount Taylor quadrangle, Valencia County, New Mexico: U.S. Geological Survey Map GQ–1523, scale 1:24,000.

Lucas, S.G., 1993, The Chinle Group—revised stratigraphy and biochronology of upper Triassic nonmarine strata in the western United States: Museum of Northern Arizona Bulletin, v. 59, p. 27–50.

Lucas, S.G., Semken, S.C., Berglof, W.R., and Ulmer–Scholle, D.S., eds., 2003, Geology of the Zuni Plateau: New Mexico Geological Society, Fifty-Fourth Annual Field Conference, Las Vegas, New Mexico, New Mexico Highlands University, September 24–27, 2003, variously paged.

McCraw, D.J., Read, A.S., Lawrence, J.R., Goff, F., and Goff, C.J., 2009, Preliminary geologic map of the San Mateo quadrangle, McKinley and Cibola Counties, New Mexico: New Mexico Bureau of Geology and Mineral Resources, Open-file Digital Geologic Map OF–GM 194, map.

McLemore, V.T., and Chenoweth, W.L, 2003, Uranium resources in the San Juan Basin, New Mexico*, in* Lucas, S.G., Semken, S.C., Berglof, W.R., and Ulmer–Scholle, D.S., eds., Geology of the Zuni Plateau: New Mexico Geological Society, Fifty-Fourth Annual Field Conference, Las Vegas, New Mexico, New Mexico Highlands University, September 24–27, 2003, p. 165–177.

McMahon, P.B., and Chapelle, F.H., 2008, Redox processes and water quality of selected principal aquifer systems: Ground Water, v. 46, no. 2, p. 259–271.

New Mexico Bureau of Geology and Mineral Resources, 2003, Geologic map of New Mexico, 1:500,000: New Mexico Bureau of Geology and Mineral Resources, map with explanation.

New Mexico Environment Department, 2009, Health advisory for the private wells within the San Mateo Creek Basin: New Mexico Environment Department, 3 p., accessed July 1, 2010, at http://www.nmenv.state.nm.us/OOTS/documents/wellhealthadvisory01072009final.pdf.

Nimz, G.J., 1998, Lithogenic and cosmogenic tracers, *in* Kendall, C., and McDonnell, J.J., Isotope tracers in catchment hydrology: Amsterdam, Elsevier Science B.V., chapter 8, p. 247–289.

Parkhurst, D.L., and Appelo, C.A.J., 1999, User's guide to PHREEQC (version 2)—A computer program for speciation, batch-reaction, one-dimensional transport, and inverse geochemical calculations: U.S. Geological Survey Water-Resources Investigations Report 99–4259, 310 p.

Perry, F.V., Baldridge, W.S., DePaolo, J., and Shafiqullah, M., 1990, Evolution of a magmatic system during continental extension: the Mount Taylor Volcanic Field, New Mexico: Journal of Geophysical Research, v. 95, p. 19327–19348.

Plummer, L.N., Prestemon, E.C., and Parkhurst, D.L., 1994, An interactive code (NETPATH) for modeling NET geochemical reactions along a flowpath—Version 2.0: U.S. Geological Survey Water-Resources Investigations Report 94–4169, 130 p.

Rantz, S.E., and others, 1982, Measurement and computation of streamflow, volume 1— Measurement of stage and discharge: U.S. Geological Survey Water-Supply Paper 2175, 284 p.

Révész, K., and Coplen, T.B., 2008a, Determination of the δ(2H/1H) of water—RSIL Lab Code 1574, *in* Révész, K., and Coplen, T.B., eds., Methods of the Reston Stable Isotope Laboratory: U.S. Geological Survey Techniques and Methods, book 10, section C, chapter 1, 27 p.

Révész, K., and Coplen, T.B., 2008b, Determination of the δ(18O/16O) of water—RSIL Lab Code 489, *in* Révész, K., and Coplen, T.B., eds., Methods of the Reston Stable Isotope Laboratory: U.S. Geological Survey Techniques and Methods, book 10, section C, chapter 2, 28 p.

Risser, D.W., and Lyford, F.P., 1983, Water resources on the Pueblo of Laguna, west-central New Mexico: U.S. Geological Survey Water-Resources Investigations Report 83–4038, 308 p.

Roca Honda Resources, LLC, 2009a, 11-20-2009 permit application, Phase II of a new mine application—Baseline data report: Permit application to the Mining and Minerals Division of the New Mexico Energy, Minerals, and Natural Resources Department, variously paged, accessed January 3, 2011, at http://www.emnrd.state.nm.us/MMD/MARP/permits/MARP_Permits.htm.

Roca Honda Resources, LLC, 2009b, 11-20-2009 permit application, Phase II of a new mine application—Sampling and analysis plan revision, phase I of new mine application: Permit application to the Mining and Minerals Division of the New Mexico Energy, Minerals, and Natural Resources Department, variously paged, accessed January 3 , 2011, at http://www.emnrd.state.nm.us/MMD/MARP/permits/MARP_Permits.htm.

Schoeppner, J., 2008, Groundwater remediation from uranium mining in New Mexico: Southwest Hydrology, November/December issue, p. 22–23.

Stone, W.J., 2003, Hydrostratigraphy, hydrodynamics, and hydrochemistry—Geologic controls of groundwater phenomena in the San Juan Basin, *in* Lucas, S.G., Semken, S.C., Berglof, W.R., and Ulmer–Scholle, D.S., eds., Geology of the Zuni Plateau: New Mexico Geological Society, Fifty-Fourth Annual Field Conference, Las Vegas, New Mexico, New Mexico Highlands University, September 24–27, 2003, p. 191–195.

Stone, W.J., Lyford, F.P., Frenzel, P.F., Mizell, N.H., and Padgett, E.T., 1983, Hydrogeology and water resources of San Juan Basin, New Mexico: Socorro, New Mexico Bureau of Mines and Mineral Resources, Hydrologic Report 6, 70 p.

Strickland, D., Heizler, M.T., Selverstone, J., and Karlstrom, K.E., 2003, Proterozoic evolution of the Zuni Mountains, western New Mexico—Relationship to the Jemez Lineament and implications for a complex cooling history, *in* Lucas, S.G., Semken, S.C., Berglof, W.R., and Ulmer–Scholle, D.S., eds., Geology of the Zuni Plateau: New Mexico Geological Society, Fifty-Fourth Annual Field Conference, Las Vegas, New Mexico, New Mexico Highlands University, September 24–27, 2003, p. 109–117.

Stumm, W., and Morgan J.J., 1996, Aquatic chemistry—Chemical equilibria and rates in natural waters, (3d): New York, Wiley-Interscience, 1,022 p.

U.S. Environmental Protection Agency, 1993, Methods for the determination of inorganic substances in environmental samples: EPA/600/R–93/100, including updates, variously paged.

U.S. Environmental Protection Agency, 2009, Methods and guidance for the analysis of water (official EPA versions) including updates, variously paged on CD-ROM.

U.S. Geological Survey, 2006, Collection of water samples (ver. 2.0): U.S. Geological Survey Techniques of Water-Resources Investigations, book 9, chap. A4, variously paged, accessed July 1, 2010, at http://pubs.water.usgs.gov/twri9A4/.

U.S. Geological Survey, 2009, USGS surface-water monthly statistics for New Mexico, USGS 08342600 San Mateo Creek near San Mateo, NM: U.S. Geological Survey National Water Information System Web interface, http://waterdata.usgs.gov/nm/nwis/nwisman/?site_no=08342600&agency_cd=USGS.

Vengosh, A., 2003, Salinization and saline environments, *in* Holland, H.D., Turekian, K.K., and Sherwood Lollar, B., eds., Treatise on geochemistry: Elsevier Sciences, v. 9.09, p. 333–365.

Western Regional Climate Center, 2009, New Mexico climate summaries for cooperator stations, variously paged, accessed September 9, 2010, at http://weather.nmsu.edu/cooperator1/index.htm.

WoldeGabriel, G., Keating, G.N., and Valentine, G.A., 1999, Effects of shallow basaltic intrusion into pyroclastic deposits, Grants Ridge, New Mexico, USA: Journal of Volcanology and Geothermal Research, v. 92, no. 3–4, p. 389–411.

Wolff, R.G., 1981, Porosity, permeability, distribution coefficients, and dispersivity, *in* Touloukian, Y.S., Judd, W.R., and Roy, R.F., eds., 1981, Physical properties of rocks and minerals: New York, McGraw Hill/CINDAS, v. II–2, p. 45–81.

Woodward, L.A., and Callender, J.F., 1977, Tectonic framework of the San Juan Basin, *in* Fassett, J.E., and James, H.L., eds., 1977, Guidebook of San Juan Basin III, northwestern New Mexico: New Mexico Geological Society, 28th Field Conference, p. 209–212.

Woody, D.T., 2006, Revised stratigraphy of the lower Chinle Formation (upper Triassic) of Petrified Forest National Park, Arizona, *in* Parker, W.G., Ash, S.R., and Irmis, R.B., eds., A century of research at Petrified Forest National Park, 1906–2006: Museum of Northern Arizona Bulletin 62, p. 17–45.

Yancey, C.L., and McLemore, V.T., 2008, Uranium geology of the West: Southwest Hydrology, November/December 2008, p. 20–34.

Appendix 1.—Historical Groundwater-Elevation Data

Existing groundwater-elevation data in the study area are presented in table 1-1. The spatial distribution of the associated wells across the study area is shown in fig. 1-1 (individual well locations can be located through latitude and longitude coordinates presented in table 1-1). The water-level data set is a compilation of multiple sources and is presented in order of increasing geologic age of the associated formation. Initial formation designations were determined by the authors/data collectors of the source references (references listed following the table). Groundwater-elevation data without formation designations were not included for analysis in this study. For this study, formation designations were homogenized to currently (2011) accepted formation nomenclature. This homogenization was necessary because of the long data record (1940s onward) during which formation identification has changed with certain formation names dropped from the lexicon or added as additional studies continued to update the stratigraphic nomenclature of the region (see Methods section).

Table 1-1. Historical groundwater-elevation data in the study area, 1946–2009.

[NAD 83, North American Datum of 1983; ft, feet; NAVD 88, North American Vertical Datum of 1988; Qa, Quaternary alluvium; NA, a specific date is not available, but the data are associated with documents that place the date within the range of 1946–2009; Kmf, Cretaceous Menefee Formation; Kpl, Cretaceous Point Lookout Formation; Kg, Cretaceous Gallup Formation; Km, Cretaceous Mancos Formation; Kd, Cretaceous Dakota Formation; Jm, Jurassic Morrison Formation; Je, Jurassic Entrada Complex (includes Entrada, Todilto, Summerville, and Bluff Formations); TRc, Triassic Chinle Group; Psa, Permian San Andres Formation (including Glorieta Formation)]

Line no.	Formation	Data source*	Data identifier**	Latitude (NAD 83)	Longitude (NAD 83)	Date	Water elevation (in ft above NAVD 88)	Land-surface elevation (in ft above NAVD 88)
1	Qa	RHR	21	35.323	107.684	03/23/78	7,062	7,077
2	Qa	RHR	23	35.325	107.683	03/23/78	7,055	7,070
3	Qa	RHR	24	35.324	107.682	03/23/78	7,055	7,070
4	Qa	RHR	28	35.337	107.654	NA	7,144	7,224
5	Qa	RHR	33	35.334	107.657	06/17/78	7,122	7,152
6	Qa	RHR	36	35.335	107.649	07/03/80	7,194	7,224
7	Qa	RHR	40	35.344	107.637	NA	7,274	7,279
8	Qa	RHR	43	35.342	107.637	NA	7,277	7,285
9	Qa	RHR	53	35.339	107.637	NA	7,303	7,307
10	Qa	RHR	54	35.336	107.637	NA	7,310	7,349
11	Qa	RHR	59	35.333	107.637	NA	7,362	7,470
12	Qa	RHR	60	35.333	107.637	NA	7,362	7,470
13	Qa	RHR	69	35.338	107.635	NA	7,326	7,328
14	Qa	RHR	70	35.336	107.636	NA	7,326	7,354
15	Qa	RHR	76	35.330	107.644	09/01/62	7,303	7,339
16	Qa	RHR	79	35.331	107.645	09/01/62	7,267	7,287
17	Qa	RHR	85	35.330	107.643	06/22/81	7,250	7,300
18	Qa	RHR	87	35.330	107.643	08/18/80	7,352	7,402
19	Qa	RHR	88	35.331	107.653	05/29/05	7,181	7,215
20	Qa	RHR	96	35.331	107.647	12/12/79	7,238	7,274
21	Qa	RHR	106	35.364	107.769	08/31/89	6,863	6,900
22	Qa	RHR	115	35.347	107.776	03/01/75	6,797	6,834
23	Qa	RHR	116	35.345	107.786	05/10/05	6,744	6,824
24	Qa	RHR	119	35.346	107.756	03/01/76	6,816	6,867
25	Qa	RHR	120	35.348	107.738	12/01/57	6,856	6,913
26	Qa	RHR	121	35.348	107.739	12/01/57	6,856	6,913
27	Qa	Stone	15.10.32.214	35.491	107.914	09/18/62	7,451	7,460
28	Qa	Stone	13.09.24.221a	35.347	107.737	12/06/57	6,853	6,910
29	Qa	Stone	13.08.25.111	35.333	107.661	09/11/62	7,276	7,295
30	Qa	Stone	12.09.06.312	35.296	107.831	07/25/56	6,599	6,673

Table 1-1. Historical groundwater-elevation data in the study area, 1946–2009.—Continued

[NAD 83, North American Datum of 1983; ft, feet; NAVD 88, North American Vertical Datum of 1988; Qa, Quaternary alluvium; NA, a specific date is not available, but the data are associated with documents that place the date within the range of 1946–2009; Kmf, Cretaceous Menefee Formation; Kpl, Cretaceous Point Lookout Formation; Kg, Cretaceous Gallup Formation; Km, Cretaceous Mancos Formation; Kd, Cretaceous Dakota Formation; Jm, Jurassic Morrison Formation; Je, Jurassic Entrada Complex (includes Entrada, Todilto, Summerville, and Bluff Formations); TRc, Triassic Chinle Group; Psa, Permian San Andres Formation (including Glorieta Formation)]

Line no.	Formation	Data source*	Data identifier**	Latitude (NAD 83)	Longitude (NAD 83)	Date	Water elevation (in ft above NAVD 88)	Land-surface elevation (in ft above NAVD 88)
31	Qa	Stone	12.09.07.3431	35.278	107.830	11/30/55	6,582	6,640
32	Qa	Stone	12.11.15.214	35.273	107.981	NA	6,550	6,630
33	Qa	Stone	12.10.27.222	35.246	107.871	09/01/58	6,520	6,570
34	Qa	Stone	12.10.32.211	35.232	107.914	01/04/47	6,480	6,555
35	Qa	Stone	11.10.04.422	35.210	107.889	07/26/56	6,462	6,538
36	Qa	Stone	11.10.02.421	35.210	107.856	03/01/59	6,468	6,598
37	Qa	Stone	11.10.16.142a	35.185	107.898	10/15/57	6,450	6,530
38	Qa	Stone	11.10.21.242	35.171	107.889	06/12/49	6,467	6,515
39	Qa	Stone	11.10.22.243	35.169	107.873	10/01/58	6,800	6,910
40	Qa	Stone	11.09.30.211	35.160	107.821	NA	6,437	6,475
41	Qa	Stone	11.09.30.122a	35.160	107.828	NA	6,429	6,470
42	Qa	Stone	11.09.30.122	35.160	107.828	05/11/49	6,417	6,470
43	Qa	Stone	11.10.25.221	35.160	107.839	08/26/56	6,429	6,440
44	Qa	Stone	11.10.26.321a	35.153	107.865	09/05/57	6,431	6,465
45	Qa	Stone	11.10.26.441	35.149	107.857	09/20/57	6,435	6,450
46	Qa	Stone	11.10.27.414	35.151	107.876	01/03/47	6,459	6,495
47	Qa	Stone	12.10.26.23	35.241	107.860	03/05/54	6,450	6,550
48	Qa	Stone	11.10.26.414	35.151	107.858	09/28/56	6,435	6,450
49	Qa	Stone	10.09.06.111	35.131	107.835	11/27/58	6,426	6,430
50	Qa	USGS	351638107495001	35.277	107.831	11/30/55	6,585	6,643
51	Qa	USGS	351640107494801	35.278	107.831	03/29/84	6,603	6,645
52	Qa	USGS	351722107502001	35.289	107.840	03/29/84	6,623	6,655
53	Qa	USGS	351745107495301	35.296	107.832	07/25/56	6,603	6,677
54	Qa	Brod	A3	35.290	107.850	07/01/56	6,589	6,657
55	Qa	Brod	A5	35.281	107.841	08/01/77	6,585	6,640
56	Qa	Brod	A4	35.277	107.844	07/01/56	6,567	6,625
57	Qa	Brod	A6	35.275	107.866	07/01/56	6,571	6,621
58	Qa	Brod	A1	35.296	107.830	07/01/56	6,593	6,673
59	Qa	Brod	A2	35.276	107.830	11/01/55	6,582	6,640
60	Qa	Brod	A10	35.338	107.788	03/01/75	6,721	6,829
61	Qa	Brod	A11	35.347	107.782	12/01/57	6,743	6,830
62	Qa	Brod	A12	35.347	107.749	12/01/57	6,584	6,910
63	Qa	Brod	A3	35.347	107.749	12/01/57	6,853	6,910
64	Qa	Brod	A14	35.333	107.788	08/05/77	6,722	6,780
65	Qa	Brod	A8	35.387	107.806	03/01/75	6,876	6,896
66	Qa	Brod	A9	35.388	107.815	03/01/75	6,880	6,904
67	Qa	Brod	A16	35.408	107.837	02/01/75	6,925	6,958
68	Qa	Brod	A17	35.409	107.832	02/01/75	6,923	6,947
69	Qa	Brod	A18	35.409	107.830	02/01/75	6,915	6,952
70	Qa	Brod	A19	35.398	107.828	03/01/75	6,923	6,926

Table 1-1. Historical groundwater-elevation data in the study area, 1946–2009.—Continued

[NAD 83, North American Datum of 1983; ft, feet; NAVD 88, North American Vertical Datum of 1988; Qa, Quaternary alluvium; NA, a specific date is not available, but the data are associated with documents that place the date within the range of 1946–2009; Kmf, Cretaceous Menefee Formation; Kpl, Cretaceous Point Lookout Formation; Kg, Cretaceous Gallup Formation; Km, Cretaceous Mancos Formation; Kd, Cretaceous Dakota Formation; Jm, Jurassic Morrison Formation; Je, Jurassic Entrada Complex (includes Entrada, Todilto, Summerville, and Bluff Formations); TRc, Triassic Chinle Group; Psa, Permian San Andres Formation (including Glorieta Formation)]

Line no.	Formation	Data source*	Data identifier**	Latitude (NAD 83)	Longitude (NAD 83)	Date	Water elevation (in ft above NAVD 88)	Land-surface elevation (in ft above NAVD 88)
71	Qa	Brod	A20	35.403	107.805	02/01/75	6,890	6,936
72	Qa	Brod	A21	35.396	107.817	02/01/75	6,907	6,910
73	Qa	Brod	A22	35.398	107.819	02/01/75	6,901	6,922
74	Qa	Brod	A23	35.398	107.821	02/01/75	6,895	6,924
75	Kmf	RHR	5	35.384	107.637	08/18/79	7,159	7,231
76	Kmf	RHR	7	35.368	107.659	NA	7,121	7,198
77	Kmf	RHR	9	35.353	107.646	09/10/62	7,114	7,185
78	Kmf	RHR	20	35.342	107.664	10/23/62	7,066	7,103
79	Kmf	RHR	27	35.335	107.657	02/01/78	7,138	7,178
80	Kmf	RHR	31	35.334	107.651	10/17/72	7,170	7,205
81	Kmf	RHR	34	35.335	107.655	06/03/05	6,915	7,175
82	Kmf	RHR	42	35.342	107.640	10/01/72	7,198	7,257
83	Kmf	RHR	45	35.340	107.637	NA	7,290	7,303
84	Kmf	RHR	47	35.348	107.737	NA	7,335	7,425
85	Kmf	RHR	48	35.343	107.631	06/02/73	7,138	7,323
86	Kmf	RHR	57	35.333	107.642	09/10/62	7,207	7,297
87	Kmf	RHR	31	35.335	107.637	NA	7,301	7,316
88	Kmf	RHR	61	35.333	107.642	02/01/78	7,196	7,297
89	Kmf	RHR	62	35.334	107.643	05/29/05	7,209	7,297
90	Kmf	RHR	63	35.335	107.640	03/01/78	7,141	7,280
91	Kmf	RHR	37	35.335	107.637	NA	7,301	7,316
92	Kmf	RHR	66	35.339	107.633	NA	7,092	7,352
93	Kmf	RHR	75	35.331	107.642	09/10/62	7,260	7,303
94	Kmf	RHR	77	35.329	107.642	10/01/72	7,259	7,339
95	Kmf	RHR	80	35.329	107.642	10/11/72	7,312	7,339
96	Kmf	RHR	82	35.329	107.640	07/31/71	7,317	7,392
97	Kmf	RHR	84	35.328	107.641	09/08/80	7,229	7,349
98	Kmf	RHR	89	35.334	107.653	08/01/73	7,179	7,215
99	Kmf	RHR	91	35.331	107.641	10/24/72	7,221	7,254
100	Kmf	RHR	92	35.331	107.646	02/01/78	7,255	7,277
101	Kmf	RHR	94	35.330	107.648	04/21/89	7,200	7,270
102	Kmf	RHR	98	35.325	107.680	08/01/77	7,046	7,070
103	Kmf	RHR	100	35.320	107.693	01/01/47	7,050	7,070
104	Kmf	RHR	104	35.309	107.687	01/01/67	7,142	7,192
105	Kmf	Stone	13.08.14.422	35.354	107.646	09/10/62	7,109	7,180
106	Kmf	Stone	13.08.24.223	35.345	107.631	09/10/62	7,189	7,330
107	Kmf	Stone	13.08.22.242	35.344	107.664	10/23/62	7,073	7,110
108	Kmf	Stone	13.08.23.432	35.336	107.651	NA	7,142	7,180
109	Kmf	Stone	13.08.24.334	35.335	107.643	NA	7,240	7,290
110	Kmf	Stone	13.08.24.334a	35.335	107.643	09/10/62	7,210	7,300

Table 1-1. Historical groundwater-elevation data in the study area, 1946–2009.—Continued

[NAD 83, North American Datum of 1983; ft, feet; NAVD 88, North American Vertical Datum of 1988; Qa, Quaternary alluvium; NA, a specific date is not available, but the data are associated with documents that place the date within the range of 1946–2009; Kmf, Cretaceous Menefee Formation; Kpl, Cretaceous Point Lookout Formation; Kg, Cretaceous Gallup Formation; Km, Cretaceous Mancos Formation; Kd, Cretaceous Dakota Formation; Jm, Jurassic Morrison Formation; Je, Jurassic Entrada Complex (includes Entrada, Todilto, Summerville, and Bluff Formations); TRc, Triassic Chinle Group; Psa, Permian San Andres Formation (including Glorieta Formation)]

Line no.	Formation	Data source*	Data identifier**	Latitude (NAD 83)	Longitude (NAD 83)	Date	Water elevation (in ft above NAVD 88)	Land-surface elevation (in ft above NAVD 88)
111	Kmf	Stone	13.08.24.334b	35.334	107.642	09/10/62	7,205	7,295
112	Kmf	Stone	13.08.26.211	35.333	107.653	09/11/62	7,182	7,215
113	Kmf	Stone	13.08.25.114	35.331	107.642	09/11/62	7,274	7,310
114	Kmf	Stone	15.08.21.4414	35.509	107.685	09/20/62	6,747	6,857
115	Kmf	USGS	352004107383001	35.334	107.642	09/10/62	7,259	7,299
116	Kmf	Brod	MF9	35.254	107.637	05/15/05	7,240	7,290
117	Kmf	Brod	MF1	35.354	107.654	10/01/72	7,124	7,180
118	Kmf	Brod	MF1	35.354	107.654	09/01/62	7,108	7,180
119	Kmf	Brod	MF2	35.343	107.676	10/01/72	7,077	7,110
120	Kmf	Brod	MF2	35.343	107.676	10/01/62	7,073	7,110
121	Kmf	Brod	MF4	35.336	107.658	02/01/78	7,132	7,169
122	Kmf	Brod	MF5	35.336	107.652	09/01/62	7,142	7,180
123	Kmf	Brod	MF6	35.344	107.632	02/01/78	7,189	7,248
124	Kmf	Brod	MF8	35.345	107.645	09/01/62	7,179	7,320
125	Kmf	Brod	MF8	35.345	107.645	10/01/72	7,125	7,320
126	Kmf	Brod	MF10	35.335	107.643	09/01/62	7,211	7,300
127	Kmf	Brod	MF10	35.335	107.643	02/01/78	7,207	7,295
128	Kmf	Brod	MF14	35.336	107.641	03/01/78	7,186	7,325
129	Kmf	Brod	MF15	35.331	107.632	09/01/62	7,277	7,320
130	Kmf	Brod	MF16	35.331	107.630	10/01/72	7,263	7,290
131	Kmf	Brod	MF17	35.331	107.630	09/01/62	7,274	7,310
132	Kmf	Brod	MF18	35.331	107.630	10/01/72	7,230	7,310
133	Kmf	Brod	MF19	35.332	107.656	09/01/62	7,182	7,215
134	Kmf	Brod	MF20	35.332	107.656	08/01/73	7,171	7,207
135	Kmf	Brod	MF21	35.332	107.663	02/01/78	7,246	7,267
136	Kpl	RHR	25	35.333	107.664	06/15/00	7,049	7,136
137	Kpl	RHR	50	35.340	107.631	NA	6,899	7,369
138	Kpl	RHR	83	35.332	107.640	05/29/05	7,044	7,313
139	Kpl	RHR	90	35.332	107.651	09/11/62	6,973	7,254
140	Kpl	RHR	93	35.331	107.649	NA	7,041	7,251
141	Kpl	RHR	103	35.311	107.686	08/01/77	7,056	7,169
142	Kpl	Stone	13.08.26.221	35.333	107.648	09/11/62	6,934	7,215
143	Kpl	RHR	123	35.433	107.607	NA	6,913	6,925
144	Kpl	RHR	127	35.456	107.634	NA	6,972	6,986
145	Kpl	Brod	P2	35.333	107.659	NA	6,959	7,240
146	Kg	RHR	32	35.338	107.662	05/28/02	7,016	7,123
147	Kg	USGS	352632107394801	35.442	107.664	07/23/86	6,485	7,184
148	Km	RHR	72	35.339	107.633	05/29/05	6,649	7,349
149	Km	RHR	72	35.339	107.633	NA	6,649	7,368
150	Km	RHR	107	35.360	107.750	02/01/58	6,799	6,942

Table 1-1. Historical groundwater-elevation data in the study area, 1946–2009.—Continued

[NAD 83, North American Datum of 1983; ft, feet; NAVD 88, North American Vertical Datum of 1988; Qa, Quaternary alluvium; NA, a specific date is not available, but the data are associated with documents that place the date within the range of 1946–2009; Kmf, Cretaceous Menefee Formation; Kpl, Cretaceous Point Lookout Formation; Kg, Cretaceous Gallup Formation; Km, Cretaceous Mancos Formation; Kd, Cretaceous Dakota Formation; Jm, Jurassic Morrison Formation; Je, Jurassic Entrada Complex (includes Entrada, Todilto, Summerville, and Bluff Formations); TRc, Triassic Chinle Group; Psa, Permian San Andres Formation (including Glorieta Formation)]

Line no.	Formation	Data source*	Data identifier**	Latitude (NAD 83)	Longitude (NAD 83)	Date	Water elevation (in ft above NAVD 88)	Land-surface elevation (in ft above NAVD 88)
151	Km	Stone	14.09.05.4323	35.466	107.813	12/16/57	6,831	7,245
152	Km	Stone	14.08.15.244	35.442	107.663	04/03/61	6,978	7,478
153	Km	Brod	MN4	35.398	107.848	03/01/75	6,977	7,010
154	Km	Brod	MN1	35.443	107.673	NA	6,710	7,210
155	Km	Brod	MN3	35.398	107.816	02/01/75	6,815	6,923
156	Km	Brod	MN2	35.467	107.815	12/01/57	6,831	7,245
157	Kd	RHR	14	35.358	107.704	04/01/81	5,863	7,178
158	Kd	RHR	17	35.358	107.728	06/14/03	6,417	7,041
159	Kd	RHR	18	35.360	107.719	12/31/74	6,333	7,133
160	Kd	Stone	14.09.34.422	35.396	107.769	12/18/58	6,500	7,008
161	Kd	Stone	15.11.25.334	35.494	107.959	08/02/61	6,615	7,280
162	Kd	Stone	13.09.13.1114	35.361	107.750	02/13/58	6,792	6,935
163	Kd	Stone	13.09.16.3241	35.353	107.796	12/17/57	6,734	6,810
164	Kd	Stone	13.09.16.333	35.349	107.803	12/17/57	6,822	6,910
165	Kd	Stone	14.09.28.233	35.414	107.960	10/10/57	6,569	6,999
166	Kd	Stone	14.09.28.234	35.414	107.791	10/30/57	6,493	7,022
167	Kd	Brod	DK2	35.361	107.735	02/01/58	6,792	6,935
168	Kd	Brod	DK3	35.349	107.803	12/01/57	6,822	6,910
169	Kd	Brod	DK4	35.351	107.799	12/01/57	6,734	6,810
170	Jm	Stone	13.09.14.4143	35.352	107.757	10/04/58	6,625	6,896
171	Jm	Stone	14.10.11.434a	35.450	107.862	10/18/60	6,495	7,065
172	Jm	RHR	1	35.324	107.614	NA	7,709	8,209
173	Jm	RHR	73	35.339	107.637	10/01/76	6,238	7,300
174	Jm	RHR	109	35.348	107.758	04/02/86	6,643	6,890
175	Jm	RHR	110	35.347	107.781	12/01/57	6,614	6,837
176	Jm	RHR	111	35.349	107.780	07/21/86	6,643	6,847
177	Jm	RHR	112	35.346	107.786	NA	6,611	6,831
178	Jm	RHR	113	35.347	107.783	12/01/58	6,632	6,837
179	Jm	RHR	114	35.346	107.785	10/01/62	6,639	6,837
180	Jm	RHR	117	35.346	107.783	01/18/79	6,641	6,831
181	Jm	RHR	134	35.393	107.750	NA	6,511	7,093
182	Jm	RHR	135	35.396	107.768	NA	6,526	7,034
183	Jm	RHR	137	35.393	107.747	NA	7,133	7,133
184	Jm	Stone	15.10.20.124	35.520	107.919	09/19/77	6,554	7,554
185	Jm	Stone	15.11.29.1132	35.505	108.033	07/26/76	6,632	7,075
186	Jm	Stone	14.10.11.434	35.450	107.862	11/07/57	6,600	7,060
187	Jm	Stone	14.10.22.214	35.433	107.880	03/27/57	6,552	7,077
188	Jm	Stone	14.10.23.114	35.432	107.871	05/07/57	6,551	7,053
189	Jm	Stone	14.10.23.132	35.430	107.871	05/07/57	6,549	7,034
190	Jm	Stone	14.10.23.141	35.430	107.869	05/07/57	6,549	7,047

Table 1-1. Historical groundwater-elevation data in the study area, 1946–2009.—Continued

[NAD 83, North American Datum of 1983; ft, feet; NAVD 88, North American Vertical Datum of 1988; Qa, Quaternary alluvium; NA, a specific date is not available, but the data are associated with documents that place the date within the range of 1946–2009; Kmf, Cretaceous Menefee Formation; Kpl, Cretaceous Point Lookout Formation; Kg, Cretaceous Gallup Formation; Km, Cretaceous Mancos Formation; Kd, Cretaceous Dakota Formation; Jm, Jurassic Morrison Formation; Je, Jurassic Entrada Complex (includes Entrada, Todilto, Summerville, and Bluff Formations); TRc, Triassic Chinle Group; Psa, Permian San Andres Formation (including Glorieta Formation)]

Line no.	Formation	Data source*	Data identifier**	Latitude (NAD 83)	Longitude (NAD 83)	Date	Water elevation (in ft above NAVD 88)	Land-surface elevation (in ft above NAVD 88)
191	Jm	Stone	14.10.23.142	35.430	107.867	05/17/57	6,548	7,037
192	Jm	Stone	14.10.23.232	35.430	107.862	05/17/57	6,547	7,022
193	Jm	Stone	14.10.23.232b	35.430	107.862	05/17/57	6,546	7,022
194	Jm	Stone	14.10.23.232a	35.430	107.862	05/17/57	6,543	7,022
195	Jm	Stone	14.10.23.134	35.429	107.871	05/08/57	6,547	7,030
196	Jm	Stone	14.10.22.422	35.427	107.876	03/17/56	6,574	7,023
197	Jm	Stone	14.10.24.423	35.425	107.842	12/18/57	6,531	6,980
198	Jm	Stone	14.09.30.222c	35.420	107.822	10/02/56	6,065	6,990
199	Jm	Stone	14.09.30.2213	35.419	107.825	04/30/57	6,541	6,984
200	Jm	Stone	14.10.22.132a	35.416	107.853	04/11/57	6,550	6,974
201	Jm	Stone	14.10.22.132c	35.416	107.853	04/11/57	6,549	6,974
202	Jm	Stone	14.10.22.132b	35.416	107.853	04/11/57	6,549	6,974
203	Jm	Stone	14.10.22.132d	35.416	107.687	04/11/57	6,549	6,975
204	Jm	Stone	14.10.25.14	35.416	107.850	11/06/56	6,546	6,970
205	Jm	Stone	14.09.28.143	35.414	107.798	09/28/56	6,541	6,981
206	Jm	Stone	14.10.25.321	35.413	107.852	05/24/57	6,541	6,971
207	Jm	Stone	14.10.25.411	35.413	107.847	05/24/57	6,541	6,970
208	Jm	Stone	14.10.25.411a	35.413	107.847	05/24/57	6,539	6,971
209	Jm	Stone	14.09.29.312	35.413	107.818	02/28/58	6,520	6,980
210	Jm	Stone	14.10.35.221	35.405	107.859	12/18/57	6,549	7,010
211	Jm	Stone	14.09.32.122b	35.405	107.813	11/06/57	6,529	6,943
212	Jm	Stone	14.10.25.413	35.397	107.847	05/24/57	6,539	6,971
213	Jm	Stone	14.09.32.314	35.395	107.819	12/20/57	6,513	6,910
214	Jm	Stone	13.10.11.242	35.373	107.858	08/27/62	6,508	7,240
215	Jm	Stone	13.09.15.343	35.349	107.781	12/05/57	6,616	6,840
216	Jm	Stone	13.09.22.121	35.347	107.781	10/12/62	6,637	6,835
217	Jm	Stone	13.08.24.2433	35.344	107.631	05/10/74	6,276	7,364
218	Jm	Stone	14.09.32.122	35.405	107.813	04/30/57	6,530	6,942
219	Jm	Stone	14.09.32.122a	35.405	107.813	04/30/57	6,530	6,942
220	Jm	Stone	14.10.25.132	35.416	107.853	04/25/57	6,545	6,976
221	Jm	USGS	352023107473201	35.340	107.793	03/26/09	6,666	6,789
222	Jm	USGS	352037107465701	35.346	107.784	08/06/09	6,733	6,834
223	Jm	Brod	B1	35.451	107.864	NA	6,600	7,060
224	Jm	Brod	Mw	35.254	107.637	10/01/72	6,302	7,364
225	Jm	Brod	W2	35.349	107.781	12/01/57	6,616	6,840
226	Jm	Brod	W5	35.338	107.792	10/01/57	6,643	6,785
227	Jm	Brod	W6	35.347	107.771	NA	6,605	6,825
228	Jm	Brod	W8	35.347	107.775	10/01/62	6,637	6,835
229	Jm	Brod	W7	35.347	107.775	12/01/58	6,625	6,830
230	Jm	Brod	W9	35.347	107.764	03/01/75	6,602	6,653

Table 1-1. Historical groundwater-elevation data in the study area, 1946–2009.—Continued

[NAD 83, North American Datum of 1983; ft, feet; NAVD 88, North American Vertical Datum of 1988; Qa, Quaternary alluvium; NA, a specific date is not available, but the data are associated with documents that place the date within the range of 1946–2009; Kmf, Cretaceous Menefee Formation; Kpl, Cretaceous Point Lookout Formation; Kg, Cretaceous Gallup Formation; Km, Cretaceous Mancos Formation; Kd, Cretaceous Dakota Formation; Jm, Jurassic Morrison Formation; Je, Jurassic Entrada Complex (includes Entrada, Todilto, Summerville, and Bluff Formations); TRc, Triassic Chinle Group; Psa, Permian San Andres Formation (including Glorieta Formation)]

Line no.	Formation	Data source*	Data identifier**	Latitude (NAD 83)	Longitude (NAD 83)	Date	Water elevation (in ft above NAVD 88)	Land-surface elevation (in ft above NAVD 88)
231	Jm	Brod	W29	35.433	107.859	05/01/57	6,551	7,053
232	Jm	Brod	W30	35.431	107.865	05/02/57	6,549	7,034
233	Jm	Brod	W31	35.429	107.863	05/03/57	6,549	7,030
234	Jm	Brod	W32	35.431	107.859	05/04/57	6,549	7,047
235	Jm	Brod	W33	35.431	107.861	05/05/57	6,548	7,037
236	Jm	Brod	W34	35.431	107.874	05/06/57	6,549	7,022
237	Jm	Brod	W35	35.431	107.874	05/07/57	6,543	7,022
238	Jm	Brod	W36	35.431	107.874	05/08/57	6,545	7,022
239	Jm	Brod	W37	35.425	107.847	02/01/57	6,531	6,980
240	Jm	Brod	W38	35.416	107.848	04/01/57	6,045	6,476
241	Jm	Brod	W39	35.416	107.848	04/01/57	6,550	6,974
242	Jm	Brod	W40	35.416	107.848	04/01/57	6,549	6,974
243	Jm	Brod	W41	35.416	107.848	04/01/57	6,550	6,974
244	Jm	Brod	W42	35.416	107.848	04/01/57	6,549	6,975
245	Jm	Brod	W43	35.412	107.854	05/01/57	6,541	6,971
246	Jm	Brod	W44	35.412	107.841	05/01/57	6,540	6,970
247	Jm	Brod	W45	35.412	107.841	05/01/57	6,539	6,971
248	Jm	Brod	W46	35.411	107.843	05/01/57	6,539	6,971
249	Jm	Brod	W47	35.405	107.872	12/01/57	6,554	7,015
250	Jm	Brod	W10	35.443	107.834	NA	6,456	7,200
251	Jm	Brod	W11	35.415	107.789	09/01/56	6,547	6,987
252	Jm	Brod	W13	35.415	107.801	10/01/57	6,493	7,022
253	Jm	Brod	W15	35.415	107.801	NA	6,577	7,022
254	Jm	Brod	W18	35.412	107.817	02/01/58	6,530	6,980
255	Jm	Brod	W19	35.419	107.837	12/01/57	6,506	6,984
256	Jm	Brod	W21	35.405	107.812	04/01/57	6,529	6,942
257	Jm	Brod	W22	35.405	107.812	04/01/57	6,530	6,942
258	Jm	Brod	W23	35.405	107.812	11/01/57	6,529	6,943
259	Jm	Brod	W25	35.396	107.814	12/01/57	6,513	6,910
260	Jm	Brod	W27	35.397	107.776	05/01/58	6,500	7,008
261	Jm	Brod	W28	35.397	107.745	05/01/58	6,488	7,070
262	Je	Stone	13.10.18.4113	35.357	107.936	11/13/63	6,685	7,050
263	Je	Stone	13.09.30.213	35.331	107.829	10/30/57	6,557	6,910
264	Je	Brod	T1	35.338	107.830	NA	6,630	6,990
265	TRc	Stone	14.11.30.2112	35.420	108.041	08/03/61	6,787	6,848
266	TRc	Stone	13.11.06.424	35.382	108.035	06/23/48	6,745	6,790
267	TRc	Stone	13.11.06.424a	35.382	108.035	09/05/62	6,735	6,785
268	TRc	Stone	13.11.06.313	35.381	108.050	09/05/62	6,751	6,790
269	TRc	Stone	13.11.08.2211	35.376	108.021	06/24/48	6,734	6,770
270	TRc	Stone	13.12.12.1422	35.374	108.061	08/04/61	6,777	6,822

Table 1-1. Historical groundwater-elevation data in the study area, 1946–2009.—Continued

[NAD 83, North American Datum of 1983; ft, feet; NAVD 88, North American Vertical Datum of 1988; Qa, Quaternary alluvium; NA, a specific date is not available, but the data are associated with documents that place the date within the range of 1946–2009; Kmf, Cretaceous Menefee Formation; Kpl, Cretaceous Point Lookout Formation; Kg, Cretaceous Gallup Formation; Km, Cretaceous Mancos Formation; Kd, Cretaceous Dakota Formation; Jm, Jurassic Morrison Formation; Je, Jurassic Entrada Complex (includes Entrada, Todilto, Summerville, and Bluff Formations); TRc, Triassic Chinle Group; Psa, Permian San Andres Formation (including Glorieta Formation)]

Line no.	Formation	Data source*	Data identifier**	Latitude (NAD 83)	Longitude (NAD 83)	Date	Water elevation (in ft above NAVD 88)	Land-surface elevation (in ft above NAVD 88)
271	TRc	Stone	13.12.12.424	35.367	108.053	06/04/59	6,763	6,825
272	TRc	Stone	13.11.07.431	35.366	108.042	08/03/61	6,758	6,810
273	TRc	Stone	13.11.07.344	35.364	108.044	03/12/75	6,770	6,845
274	TRc	Stone	13.11.17.113a	35.360	108.033	08/02/69	6,820	6,900
275	TRc	Stone	13.11.17.123	35.360	108.029	06/23/48	6,656	6,800
276	TRc	Stone	13.11.17.133	35.356	108.033	08/02/61	6,711	6,822
277	TRc	Stone	13.11.17.411a	35.355	108.024	09/18/62	6,720	6,805
278	TRc	Stone	13.11.17.411b	35.355	108.024	06/23/48	6,653	6,800
279	TRc	Stone	13.11.17.3333	35.349	108.034	10/24/62	6,539	6,920
280	TRc	Stone	13.11.23.324	35.338	107.976	08/03/61	6,496	6,800
281	TRc	Stone	13.11.27.3142	35.324	107.995	12/07/55	6,594	6,720
282	TRc	Stone	13.09.29.343	35.320	107.816	06/05/59	6,522	6,750
283	TRc	Stone	13.10.33.4443	35.306	107.894	07/25/56	6,680	6,718
284	TRc	Stone	13.11.34.433	35.306	107.989	09/19/62	6,528	6,710
285	TRc	Stone	12.10.01.222	35.304	107.836	07/24/56	6,629	6,675
286	TRc	Stone	12.10.05.341	35.293	107.918	05/18/49	6,641	6,705
287	TRc	Stone	12.11.03.342	35.293	107.986	08/31/56	6,533	6,660
288	TRc	Stone	12.11.10.411	35.282	107.984	05/10/46	6,532	6,650
289	TRc	Stone	12.11.10.411a	35.279	107.983	10/01/55	6,480	6,640
290	TRc	Stone	12.09.18.311	35.268	107.834	04/01/59	6,567	6,625
291	TRc	Stone	12.10.23.233a	35.256	107.831	07/11/46	6,519	6,594
292	TRc	Stone	12.10.26.322	35.239	107.862	05/26/56	6,503	6,573
293	TRc	Stone	12.10.34.2141	35.231	107.878	NA	6,476	6,558
294	TRc	Stone	13.11.173.114	35.360	108.031	03/28/61	6,728	6,795
295	TRc	Stone	13.10.20.114	35.346	107.925	09/17/69	6,444	6,890
296	TRc	Stone	13.10.18.212	35.362	107.934	06/16/76	6,993	7,040
297	TRc	Stone	13.11.18.122	35.362	108.044	09/05/62	6,753	6,840
298	TRc	Stone	13.11.18.221	35.362	108.038	08/02/61	6,732	6,805
299	TRc	Stone	13.11.18.224	35.360	108.035	06/23/48	6,812	6,900
300	TRc	Stone	13.11.17.114a	35.360	108.031	06/23/48	6,741	6,800
301	TRc	Stone	13.11.17.141	35.358	108.028	08/02/61	6,735	6,810
302	TRc	Stone	13.11.17.442a	35.351	108.018	07/21/61	6,730	6,830
303	TRc	Stone	13.11.17.442	35.351	108.018	12/18/57	6,685	6,830
304	TRc	USGS	351815107501001	35.304	107.837	07/24/56	6,633	6,679
305	TRc	USGS	351918107485601	35.322	107.816	03/29/84	6,676	6,764
306	TRc	USGS	351644107482901	35.279	107.809	07/25/56	6,689	6,774
307	TRc	Brod	C2	35.304	107.853	07/01/56	6,629	6,675
308	TRc	Brod	C5	35.255	107.870	07/01/46	6,519	6,594
309	TRc	Brod	C1	35.278	107.806	07/01/56	6,685	6,770
310	TRc	Stone	14.12.14.143	35.444	108.080	09/05/62	6,845	7,090

Table 1-1. Historical groundwater-elevation data in the study area, 1946–2009.—Continued

[NAD 83, North American Datum of 1983; ft, feet; NAVD 88, North American Vertical Datum of 1988; Qa, Quaternary alluvium; NA, a specific date is not available, but the data are associated with documents that place the date within the range of 1946–2009; Kmf, Cretaceous Menefee Formation; Kpl, Cretaceous Point Lookout Formation; Kg, Cretaceous Gallup Formation; Km, Cretaceous Mancos Formation; Kd, Cretaceous Dakota Formation; Jm, Jurassic Morrison Formation; Je, Jurassic Entrada Complex (includes Entrada, Todilto, Summerville, and Bluff Formations); TRc, Triassic Chinle Group; Psa, Permian San Andres Formation (including Glorieta Formation)]

Line no.	Formation	Data source*	Data identifier**	Latitude (NAD 83)	Longitude (NAD 83)	Date	Water elevation (in ft above NAVD 88)	Land-surface elevation (in ft above NAVD 88)
311	TRc	Stone	14.11.19.124	35.433	108.043	08/04/61	6,821	6,880
312	TRc	Stone	14.11.19.4113	35.427	108.042	08/03/61	6,810	6,870
313	TRc	Stone	13.10.08.211	35.377	107.919	10/02/56	6,669	7,000
314	Psa	Stone	14.10.22.414	35.425	107.880	03/22/57	6,442	7,016
315	Psa	Stone	12.11.03.212	35.304	107.981	03/01/59	6,510	6,690
316	Psa	Stone	12.10.05.341a	35.293	107.919	01/08/58	6,454	6,700
317	Psa	Stone	12.10.07.1433	35.284	107.935	10/15/55	6,458	6,635
318	Psa	Stone	12.11.15.211	35.274	107.984	02/19/57	6,475	6,632
319	Psa	Stone	12.11.15.223	35.273	107.979	NA	6,510	6,630
320	Psa	Stone	12.11.24.424	35.251	107.942	05/10/46	6,480	6,590
321	Psa	Stone	12.11.24.334	35.248	107.956	NA	6,438	6,598
322	Psa	Stone	12.11.24.334a	35.248	107.955	NA	6,435	6,595
323	Psa	Stone	12.11.25.122	35.246	107.951	04/06/48	6,547	6,595
324	Psa	Stone	12.11.25.12	35.245	107.952	03/05/54	6,553	6,600
325	Psa	Stone	15.18.14.133	35.244	107.944	02/01/51	6,473	6,590
326	Psa	Stone	12.10.26.242	35.243	107.854	05/22/58	6,410	6,590
327	Psa	Stone	12.10.28.44	35.234	107.890	09/01/54	6,479	6,560
328	Psa	Stone	12.10.29.434b	35.233	107.911	02/01/51	6,472	6,555
329	Psa	Stone	12.10.31.211	35.232	107.931	11/17/77	6,453	6,575
330	Psa	Stone	12.10.31.12	35.231	107.934	09/01/58	6,440	6,580
331	Psa	Stone	11.10.04.333	35.204	107.905	01/28/58	6,454	6,540
332	Psa	Stone	11.10.04.344	35.204	107.898	07/26/56	6,450	6,534
333	Psa	Stone	11.10.10.111a	35.204	107.888	11/14/47	6,451	6,536
334	Psa	Stone	11.10.16.434	35.176	107.894	07/27/56	6,443	6,515
335	Psa	Stone	11.10.26.321c	35.153	107.865	06/26/58	6,443	6,465
336	Psa	Stone	11.10.27.444	35.147	107.871	10/01/58	6,385	6,490
337	Psa	Stone	12.11.23.111	35.261	107.975	07/20/56	6,521	6,610
338	Psa	Stone	13.11.14.32	35.354	107.974	10/09/69	6,493	6,855
339	Psa	USGS	352433107462101	35.409	107.773	NA	6,455	6,986
340	Psa	Brod	S2	35.255	107.870	02/01/46	6,476	6,592
341	Psa	Brod	S2	35.255	107.870	08/01/57	6,444	6,592
342	Psa	Brod	B2	35.426	107.877	03/01/57	6,442	7,016
343	Psa	Stone	14.9.28.441	35.409	107.788	10/01/57	6,440	6,982

*Data sources:

Brod—Brod, R.C., and Stone, W.J., 1981, Hydrogeology of Ambrosia Lake-San Mateo area, McKinley and Cibola Counties, New Mexico: New Mexico Bureau of Mines and Mineral Resources, HS-2, text and map, 1:62,500.

Stone—Stone, W.J., Lyford, F.P., Frenzel, P.F., Mizell, N.H., and Padgett, E.T., 1983, Hydrogeology and water resources of San Juan Basin, New Mexico: Socorro, New Mexico Bureau of Mines and Mineral Resources, Hydrologic Report 6, 70 p.

RHR—Roca Honda Resources, LLC, 2009a, 11-20-2009 Permit application, Phase II of a new mine application—Baseline data report: Permit application to the Mining and Minerals Division of the New Mexico Energy, Minerals, and Natural Resources Department, http://www.emnrd.state.nm.us/MMD/MARP/permits/MARP_Permits.htm.

USGS—U.S. Geological Survey, 2009, Groundwater levels for New Mexico: U.S. Geological Survey National Water Information System, http://nwis.waterdata.usgs.gov/nm/nwis/gwlevels.

**Data identifiers: these values are data indicators used by the source to identify the data within the report or database.

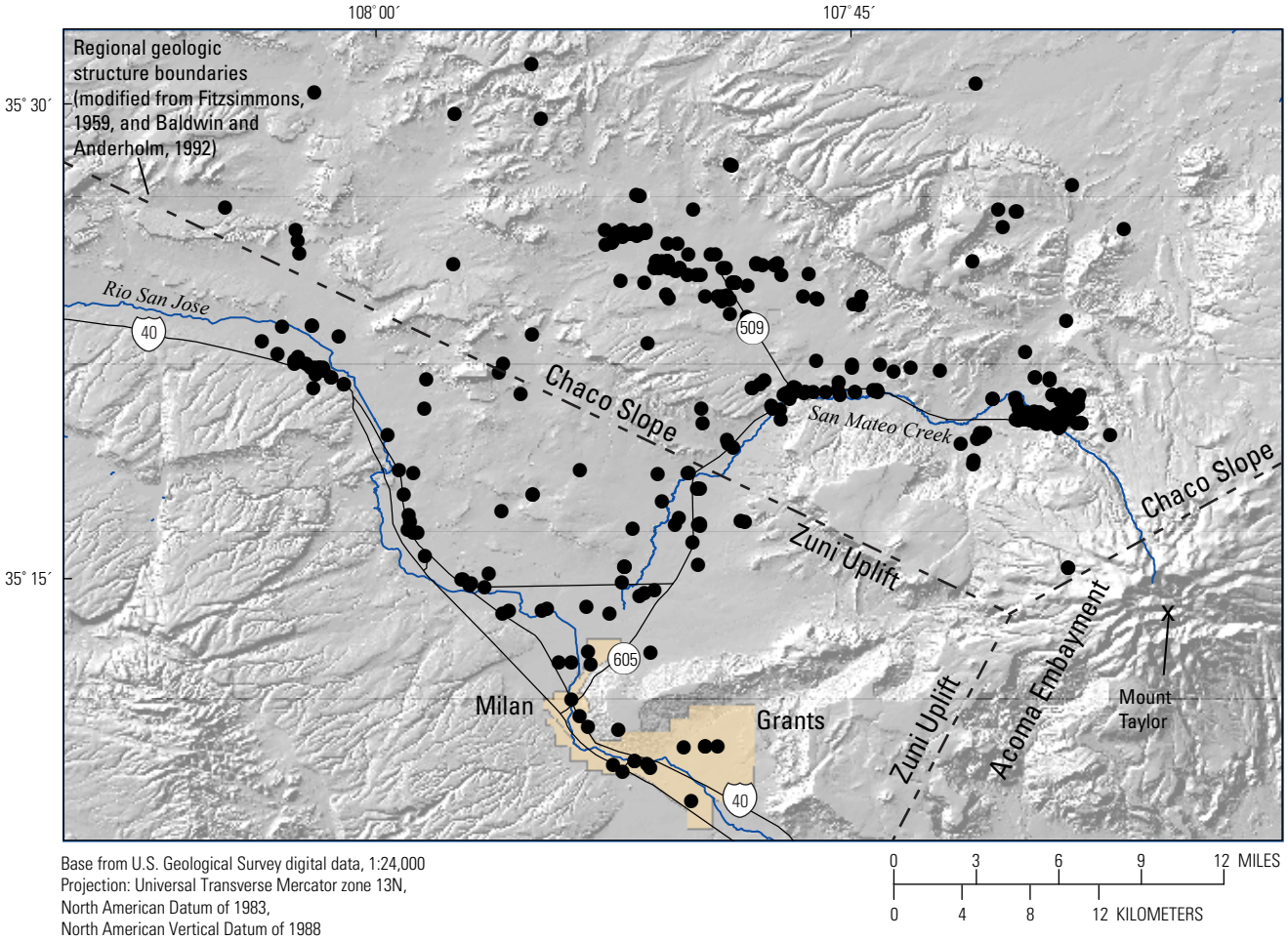

Figure 1-1. Spatial distribution of historical groundwater-elevation data in the study area.

Appendix 2.—Historical Groundwater Major-Element Data

Existing major-element data in the study area are presented in table 2-1. The spatial distribution of the associated wells across the study area is shown in fig. 2-1 (individual well locations can be located through latitude and longitude coordinates presented in table 2-1). The major-element data set is a compilation of multiple sources and is presented in order of increasing geologic age of the associated formation. Initial formation designations were determined by the authors/data collectors of the source references (references listed following the table). Existing major-element data without formation designations were not included for analysis in this study. For this study, formation designations were homogenized to currently (2011) accepted formation nomenclature. This homogenization was necessary because of the long data record (1950s onward) during which formation identification has changed with certain formation names dropped from the lexicon or added as additional studies continued to update the stratigraphic nomenclature of the region (see Methods section).

Table 2-1. Historical groundwater major-element data in the study area, 1958–2009.

[NAD 83, North American Datum of 1983; TDS, total dissolved solids; mg/L, milligrams per liter; Ca, calcium; Mg, magnesium; Na, sodium; K, potassium; HCO_3, bicarbonate; SO_4, sulfate; Cl, chloride; F, fluoride; Qa, Quaternary alluvium; NA, not available; Kmf, Cretaceous Menefee Formation; Kpl, Cretaceous Point Lookout Formation; Kcc, Cretaceous Crevasse Canyon Formation; Kg, Cretaceous Gallup Formation; Km, Cretaceous Mancos Formation; Kd, Cretaceous Dakota Formation; Jm, Jurassic Morrison Formation; Je, Jurassic Entrada Complex (includes Entrada, Todilto, Summerville, and Bluff Formations); TRc, Triassic Chinle Group; Psa, Permian San Andres Formation (including Glorieta Formation)]

Line no.	Form-ation	Data source*	Data identifier**	Latitude (NAD 83)	Longitude (NAD 83)	Date	pH	TDS (mg/L)	Ca (mg/L)	Mg (mg/L)	Na (mg/L)	K (mg/L)	HCO_3 (mg/L)	SO_4 (mg/L)	Cl (mg/L)	F (mg/L)
1	Qa	RHR	120	35.346	107.737	11/18/08	7.7	603	54	20	279	3.0	401	364	24	1.6
2	Qa	Stone	16W.16W.30.3431	35.588	108.574	07/17/70	8.5	1,330	24	43	400	5.0	670	380	42	.8
3	Qa	RHR	33	35.335	107.659	11/17/08	7.5	655	71	17	264	2.0	514	264	34	.7
4	Qa	Stone	15N.17W.14.4224	35.531	108.608	09/17/75	8.2	867	26	11	160	2.0	290	140	23	.7
5	Qa	RHR	21	35.320	107.684	08/21/08	7.0	NA	54	16	78	1.0	382	22	7.0	1.0
6	Qa	Stone	19N.05W.25.4144	35.848	107.317	01/14/76	8.3	703	120	13	110	6.1	427	180	19	.8
7	Qa	RHR	115	35.346	107.774	05/26/09	NA	NA	43	8.0	144	3.0	348	123	13	1.1
8	Qa	RHR	120	35.346	107.737	08/06/08	7.1	NA	69	25	227	3.0	400	356	26	1.3
9	Qa	Stone	19N.05W.09.4112	35.892	107.371	01/14/76	8.0	642	45	3.0	190	5.1	499	100	4.7	.7
10	Qa	Stone	18W.04W.21.220	35.777	107.264	03/19/70	8.3	640	31	5.5	190	3.0	400	140	14	.8
11	Qa	Stone	19N.05W.01.1212	35.906	107.318	03/19/70	8.0	924	94	9.1	200	5.0	350	360	16	.5
12	Qa	Stone	20N.07W.24.222	35.950	107.532	01/05/76	7.6	4,890	440	400	520	7.2	388	3,200	64	5.0
13	Qa	Stone	19N.06W.01.3242	35.907	107.425	01/28/76	7.4	2,740	140	22	800	2.9	867	1,300	35	6.0
14	Qa	Stone	15N.17W.15.1321	35.530	108.625	09/10/69	8.3	760	21	6.1	250	NA	390	200	56	.9
15	Qa	RHR	33	35.335	107.659	09/23/08	NA	NA	71	17	263	2.0	540	300	39	.9
16	Qa	Stone	18N.05W.14.221	35.791	107.335	10/18/71	8.3	6,610	74	47	2,100	NA	1,090	3,800	30	2.2
17	Qa	Stone	20N.02W.19.124	35.949	107.086	04/01/78	6.0	2,800	350	56	450	8.5	320	1,700	33	1.2
18	Qa	Stone	15N.11W.29.1132	35.500	108.026	09/18/62	7.5	3,580	530	330	51	9.5	142	2,550	12	1.6
19	Qa	RHR	120	35.346	107.737	02/18/09	9.3	748	10	4.0	313	4.0	472	273	34	2.8
20	Qa	Stone	13N.08W.26.221	35.326	107.655	10/24/61	8.0	71	10	2.4	10	3.0	68	1	1.6	.3
21	Qa	Stone	13N.07W.20.1232	35.341	107.603	10/23/62	7.9	160	19	7.2	13	3.5	127	1	2.9	.3
22	Qa	Stone	19N.05W.04.214	35.906	107.371	01/14/76	8.3	744	16	2.5	270	2.3	586	150	5.2	1.4
23	Qa	Stone	19N.05W.18.2211	35.878	107.407	01/14/76	8.2	563	27	2.9	180	2.8	443	100	8.5	.8
24	Qa	Stone	19N.05W.23.3431	35.863	107.335	01/13/76	8.1	499	53	4.3	88	5.7	178	190	6.4	.5
25	Qa	Stone	20N.07W.20.1444	35.950	107.603	01/05/76	7.7	482	67	8.4	89	4.2	342	120	5.9	.4
26	Qa	Stone	20N.07W.22.1221	35.950	107.567	01/05/76	8.3	1,300	120	44	230	6.4	318	710	21	.4
27	Kmf	Stone	19N.05W.17.4434	35.877	107.389	01/13/76	7.4	1,880	150	40	410	8.3	501	990	12	.2
28	Kmf	Stone	20.03.15.44	35.964	107.140	06/18/59	8.9	596	2	NA	226	.4	324	164	5.0	1.8
29	Kmf	RHR	62	35.333	107.642	11/11/08	8.0	446	30	9.0	183	1.0	400	67	45	.6
30	Kmf	RHR	87	35.327	107.642	08/12/08	7.8	NA	21	7.0	135	2.0	377	23	4.0	1.8

Table 2-1. Historical groundwater major-element data in the study area, 1958–2009.—Continued

[NAD 83, North American Datum of 1983; TDS, total dissolved solids; mg/L, milligrams per liter; Ca, calcium; Mg, magnesium; Na, sodium; K, potassium; HCO_3, bicarbonate; SO_4, sulfate; Cl, chloride; F, fluoride; Qa, Quaternary alluvium; NA, not available; Kmf, Cretaceous Menefee Formation; Kpl, Cretaceous Point Lookout Formation; Kcc, Cretaceous Crevasse Canyon Formation; Kg, Cretaceous Gallup Formation; Km, Cretaceous Mancos Formation; Kd, Cretaceous Dakota Formation; Jm, Jurassic Morrison Formation; Je, Jurassic Entrada Complex (includes Entrada, Todilto, Summerville, and Bluff Formations); TRc, Triassic Chinle Group; Psa, Permian San Andres Formation (including Glorieta Formation)]

Line no.	Form-ation	Data source*	Data identifier**	Latitude (NAD 83)	Longitude (NAD 83)	Date	pH	TDS (mg/L)	Ca (mg/L)	Mg (mg/L)	Na (mg/L)	K (mg/L)	HCO_3 (mg/L)	SO_4 (mg/L)	Cl (mg/L)	F (mg/L)
31	Kmf	RHR	27	35.335	107.655	08/06/08	6.8	NA	72	11	38	4.0	310	21	6.0	0.4
32	Kmf	Stone	19N.12W.27.14	35.849	108.101	02/20/67	8.7	1,710	3	.6	470	.8	410	540	35	1.2
33	Kmf	Stone	20N.06W.11.4244	35.979	107.443	01/13/76	7.3	173	11	.9	43	.7	65	48	9.2	.4
34	Kmf	Stone	19N.09W.35.13	35.833	107.762	08/27/70	8.7	830	19	7.3	250	2.0	200	390	8.9	.6
35	Kmf	Stone	18.09.15.42	35.790	107.780	12/07/72	9.0	799	6	NA	300	NA	400	270	14	NA
36	Kmf	Stone	18.09.12.1	35.804	107.744	02/20/67	9.0	1,120	2	.6	400	NA	360	430	59	1.5
37	Kmf	Stone	15N.09W.09.2442	35.544	107.796	10/03/62	8.4	223	5	1.1	81	1.5	207	11	1.5	.5
38	Kmf	Stone	18N.09W.12.1A	35.804	107.744	12/04/72	8.9	2,110	2	NA	800	2.0	1,220	520	85	.6
39	Kmf	RHR	62	35.333	107.642	05/26/09	NA	NA	22	7.0	168	1.0	380	60	40	.6
40	Kmf	Stone	15N.06W.22.3123	35.514	107.460	10/03/62	8.4	290	3	.5	109	1.4	270	10	3.9	.4
41	Kmf	RHR	62	35.333	107.642	08/20/08	7.4	NA	48	14	188	2.0	415	74	106	.6
42	Kmf	Stone	16N.08W.20.1312	35.602	107.708	10/15/62	8.7	625	6	1.8	220	2.0	320	200	13	1.0
43	Kmf	Stone	13N.09W.15.343	35.355	107.778	09/18/62	8.1	516	14	3.4	179	1.7	370	102	14	.9
44	Kmf	Stone	18N.11W.29.3111	35.762	108.030	07/27/64	8.7	768	2	.7	270	.8	24	520	15	1.2
45	Kmf	RHR	100	35.320	107.693	11/08/08	7.8	202	29	9.0	39	11	228	6	8.0	.3
46	Kmf	Stone	20N.04W.34.4421	35.920	107.246	05/14/64	8.5	519	3	NA	190	.6	308	146	8.6	.3
47	Kmf	Stone	21N.07W.35.1231	36.008	107.546	01/27/76	8.2	275	60	3.5	21	1.7	119	100	5.1	.4
48	Kmf	Stone	20N.05W.22.4422	35.949	107.353	11/01/63	8.2	168	14	4.1	38	.4	120	24	6.9	.5
49	Kmf	Stone	21N.01W.29.223	36.017	106.972	06/18/59	7.1	1,030	208	20	92	4.4	254	521	38	.5
50	Kmf	RHR	100	35.320	107.693	08/21/08	7.0	NA	18	5.0	39	9.0	158	13	13	.2
51	Kmf	Stone	18N.06W.04.3421	35.820	107.478	02/21/67	8.7	1,720	4	.6	600	1.0	600	760	22	3.1
52	Kmf	RHR	27	35.335	107.655	11/13/08	7.4	249	63	10	34	4.0	304	20	6.0	.4
53	Kmf	Stone	15N.09W.13.144	35.529	107.745	10/16/62	7.5	731	140	57	32	3.0	570	180	4.8	.6
54	Kmf	RHR	7	35.367	107.658	02/16/09	8.7	1,988	18	5.0	986	4.0	947	1,300	77	2.8
55	Kmf	RHR	87	35.327	107.642	02/16/09	8.5	331	27	9.0	113	2.0	398	22	4.0	1.6
56	Kmf	Stone	19N.02W.21.34	35.863	107.051	04/25/78	6.2	5,800	300	570	630	13	470	4,000	19	.6
57	Kmf	RHR	62	35.333	107.642	02/18/09	8.4	417	19	6.0	154	1.0	376	62	35	.6
58	Kmf	RHR	27	35.335	107.655	05/19/09	NA	NA	56	9.0	41	4.0	314	17	5.0	.5
59	Kmf	RHR	100	35.320	107.693	02/11/09	7.6	209	33	10	35	8.0	254	6	4.0	.5
60	Kmf	RHR	27	35.335	107.655	02/16/09	7.7	250	57	9.0	35	4.0	302	18	6.0	.4

Table 2-1. Historical groundwater major-element data in the study area, 1958–2009.—Continued

[NAD 83, North American Datum of 1983; TDS, total dissolved solids; mg/L, milligrams per liter; Ca, calcium; Mg, magnesium; Na, sodium; K, potassium; HCO_3, bicarbonate; SO_4, sulfate; Cl, chloride; F, fluoride; Qa, Quaternary alluvium; NA, not available; Kmf, Cretaceous Menefee Formation; Kpl, Cretaceous Point Lookout Formation; Kcc, Cretaceous Crevasse Canyon Formation; Kg, Cretaceous Gallup Formation; Km, Cretaceous Mancos Formation; Kd, Cretaceous Dakota Formation; Jm, Jurassic Morrison Formation; Je, Jurassic Entrada Complex (includes Entrada, Todilto, Summerville, and Bluff Formations); TRc, Triassic Chinle Group; Psa, Permian San Andres Formation (including Glorieta Formation)]

Line no.	Form-ation	Data source*	Data identifier**	Latitude (NAD 83)	Longitude (NAD 83)	Date	pH	TDS (mg/L)	Ca (mg/L)	Mg (mg/L)	Na (mg/L)	K (mg/L)	HCO_3 (mg/L)	SO_4 (mg/L)	Cl (mg/L)	F (mg/L)
61	Kmf	Stone	17N.11W.15.	35.704	107.994	02/20/67	7.8	1,400	190	24	190	2.0	250	800	12	0.3
62	Kmf	RHR	100	35.320	107.693	05/19/09	NA	NA	34	10	34	6.0	258	4	4.0	.5
63	Kmf	RHR	87	35.327	107.642	05/19/09	NA	NA	23	8.0	111	2.0	401	24	4.0	1.7
64	Kmf	Stone	20N.07W.18.4112	35.965	107.621	12/27/75	8.6	1,750	2	.7	670	2.5	859	490	89	3.0
65	Kmf	Stone	19N.05W.25.424	35.848	107.317	01/15/76	8.9	2,510	9	58	790	.2	543	1,300	44	2.0
66	Kmf	Stone	19N.06W.35.3244	35.834	107.443	12/28/75	8.6	2,000	2	.7	770	3.2	1,250	450	79	8.1
67	Kmf	Stone	16N.13W.11.3413	35.632	108.185	11/24/64	7.1	1,400	380	74	69	5.0	31	1,300	14	.6
68	Kmf	Stone	18N.08W.09.111	35.804	107.691	03/19/70	8.1	3,560	400	150	430	11	510	2,000	39	.8
69	Kmf	Stone	20N.09W.08.343	35.979	107.815	01/28/76	7.3	857	140	85	26	2.3	456	350	14	.2
70	Kmf	Stone	19N.08W.04.2144	35.906	107.691	01/26/76	8.7	2,010	10	3.1	650	2.5	237	1,200	6.0	4.0
71	Kmf	Stone	19N.06W.35.3244	35.834	107.443	12/28/75	8.3	1,320	7	3.1	520	6.4	1,270	100	19	2.6
72	Kmf	Stone	19N.08W.34.2131	35.833	107.673	01/05/76	8.0	1,700	4	2.2	590	2.3	529	810	26	1.2
73	Kmf	Stone	19N.09W.07.3324	35.891	107.833	09/22/75	4.3	2,060	280	170	72	3.6	NA	1,500	11	.4
74	Kmf	Stone	19N.07W.01.4112	35.907	107.532	01/12/76	7.3	953	93	41	160	3.5	344	460	6.3	.1
75	Kmf	Stone	20N.10W.01.22	35.994	107.850	01/28/76	8.0	1,940	150	78	350	4.5	280	1,200	11	.4
76	Kpl	Stone	19N.05W.18.2224	35.878	107.407	01/14/76	7.7	383	62	14	49	1.2	209	77	29	1.2
77	Kpl	Stone	19N.06W.24.2212	35.863	107.425	01/15/76	8.6	2,770	3	1.3	1,000	3.4	1,040	1,100	71	4.9
78	Kpl	Stone	19N.05W.12.3234	35.892	107.318	01/13/76	8.4	1,610	3	1.0	600	2.2	891	480	19	5.5
79	Kpl	Stone	16N.07W.26.2214	35.588	107.549	10/03/62	8.7	875	3	.7	320	2.0	380	330	11	.9
80	Kpl	Stone	19N.13W.13.444	35.878	108.173	11/02/71	8.7	2,060	6	1.2	700	3.0	420	1,000	60	2.4
81	Kpl	Stone	13N.09W.22.2124	35.341	107.778	09/11/62	8.1	510	74	24	76	3.0	360	100	22	1.0
82	Kpl	Stone	16N.09W.22.4444	35.602	107.778	10/02/62	8.5	964	7	1.8	342	2.2	395	387	9.1	.6
83	Kpl	Stone	16N.08W.33.1341	35.573	107.691	10/02/62	8.3	1,470	6	2.3	557	2.3	826	397	74	3.7
84	Kpl	Stone	16N.10W.08.321	35.631	107.918	09/20/62	8.7	1,390	7	NA	482	2.7	393	648	28	1.4
85	Kpl	Stone	19N.12W.34	35.834	108.101	11/02/71	8.6	1,920	4	1.2	670	3.0	470	940	47	3.4
86	Kpl	Stone	16N.11W.17.4322	35.616	108.026	09/19/62	7.4	1,550	96	53	338	6.1	307	876	15	.5
87	Kpl	Stone	15N.17W.12.34	35.545	108.591	10/04/62	7.0	1,940	330	162	54	4.9	546	1,100	7.7	.8
88	Kpl	Stone	16N.07W.32.4141	35.573	107.602	10/02/62	7.6	2,000	62	24	573	4.3	326	1,130	37	.8
89	Kpl	Stone	13N.07W.09.433	35.368	107.585	09/21/62	7.7	174	23	9.4	13	6.0	150	4	3.6	.2
90	Kpl	Stone	17N.11W.35.223	35.660	107.977	02/20/67	8.7	1,710	8	2.4	580	NA	270	1,000	26	.8

Table 2-1. Historical groundwater major-element data in the study area, 1958–2009.—Continued

[NAD 83, North American Datum of 1983; TDS, total dissolved solids; mg/L, milligrams per liter; Ca, calcium; Mg, magnesium; Na, sodium; K, potassium; HCO_3, bicarbonate; SO_4, sulfate; Cl, chloride; F, fluoride; Qa, Quaternary alluvium; NA, not available; Kmf, Cretaceous Menefee Formation; Kpl, Cretaceous Point Lookout Formation; Kcc, Cretaceous Crevasse Canyon Formation; Kg, Cretaceous Gallup Formation; Km, Cretaceous Mancos Formation; Kd, Cretaceous Dakota Formation; Jm, Jurassic Morrison Formation; Je, Jurassic Entrada Complex (includes Entrada, Todilto, Summerville, and Bluff Formations); TRc, Triassic Chinle Group; Psa, Permian San Andres Formation (including Glorieta Formation)]

Line no.	Form-ation	Data source*	Data identifier**	Latitude (NAD 83)	Longitude (NAD 83)	Date	pH	TDS (mg/L)	Ca (mg/L)	Mg (mg/L)	Na (mg/L)	K (mg/L)	HCO_3 (mg/L)	SO_4 (mg/L)	Cl (mg/L)	F (mg/L)
91	Kpl	Stone	13N.07W.11.1313	35.370	107.550	08/27/62	7.7	216	31	13	20	4.0	190	15	6.4	0.2
92	Kpl	Stone	14N.08W.04.3343	35.472	107.690	08/29/62	7.8	149	20	8.5	10	3.0	120	6	5.4	.3
93	Kcc	Stone	18N.13W.23.3212	35.776	108.190	11/02/71	8.5	2,000	6	1.2	720	2.0	510	650	300	6.0
94	Kcc	Stone	17N.02W.07.422	35.719	107.086	11/04/68	8.3	242	33	9.1	38	7.0	190	41	3.9	.3
95	Kcc	Stone	16N.14W.21.3334	35.603	108.326	07/11/61	7.0	3,410	620	230	110	11	710	2,000	23	.3
96	Kcc	Stone	15N.11W.17.1111	35.529	108.026	01/15/70	7.9	2,320	120	170	280	7.0	180	1,300	75	.7
97	Kcc	Stone	15N.10W.04.1311	35.558	107.901	09/12/62	7.5	3,440	88	23	990	8.0	170	2,200	40	2.0
98	Kcc	Stone	15N.10W.32.214	35.486	107.919	08/01/61	7.5	1,450	110	44	290	7.0	270	840	10	.4
99	Kg	Stone	16N.05W.19.414	35.602	107.407	04/13/78	9.2	312	1	.3	120	.8	269	18	3.5	.7
100	Kg	RHR	16	35.356	107.704	05/19/09	NA	NA	14	20	158	4.0	226	229	5.0	.4
101	Kg	Stone	14N.09W.18.243	35.442	107.831	10/01/62	9.6	3,340	3	1.8	1,120	5.1	194	1,940	76	2.5
102	Kg	RHR	16	35.356	107.704	08/25/08	7.9	NA	32	32	169	5.0	293	285	7.0	.5
103	Kg	Stone	15N.11W.17.1111	35.529	108.026	09/18/62	8.8	1,130	3	.9	401	1.8	348	444	73	1.2
104	Kg	Stone	16N.11W.33.332	35.573	108.008	02/12/73	7.9	882	78	34	160	1.0	190	490	5.3	.5
105	Kg	Stone	16N.08W.14.1114	35.617	107.655	10/02/62	7.9	1,110	9	5.0	365	3.2	276	563	12	.8
106	Kg	Stone	15N.10W.32.214	35.486	107.919	07/18/73	8.1	1,110	100	36	180	3.1	210	580	7.1	.6
107	Kg	Stone	17N.13W.10.44	35.718	108.208	03/10/70	7.8	654	80	26	87	5.0	270	260	8.9	.4
108	Kg	Stone	16N.07W.13.2244	35.617	107.531	09/19/62	8.2	2,190	10	2.1	718	3.2	308	1,250	42	.8
109	Kg	RHR	16	35.356	107.704	02/12/09	8.9	466	17	22	152	6.0	245	258	5.0	.4
110	Kg	Stone	16N.18W.35.14	35.574	108.716	01/24/69	7.9	879	46	9.5	240	6.0	280	330	86	1.1
111	Km	Stone	16N.15W.21.	35.603	108.432	11/18/71	8.7	799	7	2.4	300	.8	510	160	22	2.2
112	Km	Stone	16N.04W.36.2321	35.573	107.210	06/05/73	8.5	7,760	120	9.0	2,400	6.6	241	4,500	580	2.9
113	Kd	Stone	16N.14W.33.22	35.574	108.326	03/20/74	9.0	977	9	NA	340	NA	310	400	14	1.3
114	Kd	Stone	16N.15W.20.	35.603	108.450	02/23/70	9.3	592	2	NA	220	.7	370	140	7.0	.2
115	Kd	Stone	16N.17W.25.1132	35.588	108.591	03/26/74	8.8	982	14	2.4	340	NA	500	220	83	2.6
116	Kd	Stone	14N.09W.28.143	35.414	107.795	04/30/63	7.7	1,520	140	56	280	8.0	320	850	17	.3
117	Kd	Stone	15N.06W.22.3123	35.514	107.460	10/30/68	8.4	820	65	21	180	2.0	310	340	15	.4
118	Kd	Stone	14N.09W.28.143	35.414	107.795	08/30/63	7.7	1,525	140	56	276	7.6	319	850	17	.3
119	Kd	Stone	16N.15W.17.1431	35.618	108.450	02/13/74	8.3	324	38	8.5	73	3.0	280	48	5.3	.4
120	Kd	Stone	14N.09W.18.400	35.442	107.831	08/08/62	7.6	742	38	11	200	8.0	280	320	8.8	.7

Table 2-1. Historical groundwater major-element data in the study area, 1958–2009.—Continued

[NAD 83, North American Datum of 1983; TDS, total dissolved solids; mg/L, milligrams per liter; Ca, calcium; Mg, magnesium; Na, sodium; K, potassium; HCO_3, bicarbonate; SO_4, sulfate; Cl, chloride; F, fluoride; Qa, Quaternary alluvium; NA, not available; Kmf, Cretaceous Menefee Formation; Kpl, Cretaceous Point Lookout Formation; Kcc, Cretaceous Crevasse Canyon Formation; Kg, Cretaceous Gallup Formation; Km, Cretaceous Mancos Formation; Kd, Cretaceous Dakota Formation; Jm, Jurassic Morrison Formation; Je, Jurassic Entrada Complex (includes Entrada, Todilto, Summerville, and Bluff Formations); TRc, Triassic Chinle Group; Psa, Permian San Andres Formation (including Glorieta Formation)]

Line no.	Form-ation	Data source*	Data identifier**	Latitude (NAD 83)	Longitude (NAD 83)	Date	pH	TDS (mg/L)	Ca (mg/L)	Mg (mg/L)	Na (mg/L)	K (mg/L)	HCO_3 (mg/L)	SO_4 (mg/L)	Cl (mg/L)	F (mg/L)
121	Kd	Stone	14N.09W.18.400	35.442	107.831	08/08/62	7.5	1,410	71	27	360	6.0	300	770	14	0.5
122	Kd	Stone	17N.13W.10.42	35.718	108.208	10/29/74	8.3	379	12	4.1	120	2.3	252	93	3.4	.4
123	Kd	Stone	14N.09W.17.300	35.442	107.814	10/16/62	8.1	4,470	420	200	691	13	383	2,880	50	1.2
124	Kd	Stone	15N.12W.17.111	35.531	108.131	07/31/61	8.4	431	6	1.7	147	2.8	247	124	9.6	.6
125	Kd	Stone	14N.10W.11.434A	35.457	107.867	04/24/64	7.8	945	53	13	252	5.2	209	536	8.7	.9
126	Kd	Stone	14N.10W.11.434A	35.457	107.867	05/06/63	7.6	1,050	100	33	200	4.0	340	500	25	.4
127	Kd	Stone	14N.09W.18.400	35.442	107.831	08/08/62	7.7	606	29	6.2	170	6.0	280	230	8.8	.7
128	Kd	Stone	16N.10W.22.212	35.602	107.883	05/23/75	NA	915	31	17	250	4.3	271	450	12	.4
129	Jm	RHR	116	35.345	107.780	02/10/09	7.3	1,727	538	142	240	6.0	210	1,940	48	.7
130	Jm	RHR	114	35.346	107.781	02/18/09	7.8	1,688	524	135	215	11	229	1,880	48	.5
131	Jm	RHR	116	35.345	107.780	11/13/08	6.9	1,687	518	144	240	6.0	213	1,970	52	.7
132	Jm	Stone	16N.12W.16.23	35.617	108.114	09/08/72	8.5	790	30	4.9	210	3.0	160	370	11	.3
133	Jm	Stone	14N.09W.32.314	35.399	107.813	05/03/63	8.1	478	20	7.3	140	8.0	250	160	5.2	.2
134	Jm	RHR	113	35.346	107.781	11/10/08	7.4	1,833	539	148	224	6.0	212	2,030	50	.5
135	Jm	RHR	116	35.345	107.780	05/21/09	NA	NA	496	136	242	6.0	222	1,920	48	.7
136	Jm	Stone	14N.09W.34.422	35.399	107.777	02/14/58	8.3	420	6	5.0	140	2.0	240	120	6.0	.4
137	Jm	RHR	113	35.346	107.781	09/22/08	6.6	NA	548	147	236	7.0	205	2,090	52	.5
138	Jm	Stone	14N.10W.22.414	35.428	107.884	08/08/62	7.6	478	32	9.7	120	6.0	240	160	9.8	.8
139	Jm	RHR	116	35.345	107.780	08/19/08	6.5	NA	544	146	236	6.0	214	2,080	57	.6
140	Jm	Stone	14N.10W.22.414	35.428	107.884	08/08/62	7.6	477	30	10	120	6.0	240	160	8.0	.8
141	Jm	Stone	15N.12W.17.123	35.531	108.131	09/30/76	NA	801	44	16	210	7.0	220	420	8.9	.5
142	Jm	RHR	113	35.346	107.781	05/26/09	NA	NA	501	142	237	7.0	219	2,000	48	.5
143	Jm	Stone	14N.09W.28.233	35.414	107.795	08/30/63	8.0	611	25	9.2	178	6.2	300	222	7.9	.6
144	Jm	Stone	15N.12W.19.223	35.516	108.149	05/04/63	8.3	247	29	5.8	52	3.0	220	22	4.6	.4
145	Jm	Stone	14N.09W.32.122	35.399	107.813	08/13/59	7.8	1,370	211	62	127	4.2	256	794	10	.6
146	Jm	RHR	113	35.346	107.781	02/12/09	7.6	1,715	507	138	231	6.0	205	2,010	48	.6
147	Jm	Stone	14N.09W.36.313	35.398	107.742	08/11/59	7.3	524	46	12	114	7.6	220	218	8.0	.4
148	Jm	Stone	14N.10W.25.132	35.414	107.849	04/29/63	7.8	437	32	17	90	7.4	247	136	5.6	1.0
149	Jm	Stone	14N.10W.11.434	35.457	107.867	04/24/63	8.2	718	15	4.9	226	3.7	252	322	7.7	.3
150	Jm	RHR	114	35.346	107.781	09/18/08	6.6	NA	504	125	208	10	213	1,910	51	.5

Table 2-1. Historical groundwater major-element data in the study area, 1958–2009.—Continued

[NAD 83, North American Datum of 1983; TDS, total dissolved solids; mg/L, milligrams per liter; Ca, calcium; Mg, magnesium; Na, sodium; K, potassium; HCO_3, bicarbonate; SO_4, sulfate; Cl, chloride; F, fluoride; Qa, Quaternary alluvium; NA, not available; Kmf, Cretaceous Menefee Formation; Kpl, Cretaceous Point Lookout Formation; Kcc, Cretaceous Crevasse Canyon Formation; Kg, Cretaceous Gallup Formation; Km, Cretaceous Mancos Formation; Kd, Cretaceous Dakota Formation; Jm, Jurassic Morrison Formation; Je, Jurassic Entrada Complex (includes Entrada, Todilto, Summerville, and Bluff Formations); TRc, Triassic Chinle Group; Psa, Permian San Andres Formation (including Glorieta Formation)]

Line no.	Form-ation	Data source*	Data identifier**	Latitude (NAD 83)	Longitude (NAD 83)	Date	pH	TDS (mg/L)	Ca (mg/L)	Mg (mg/L)	Na (mg/L)	K (mg/L)	HCO_3 (mg/L)	SO_4 (mg/L)	Cl (mg/L)	F (mg/L)
151	Jm	Stone	14N.09W.28.143	35.414	107.795	10/17/62	7.9	1,880	90	26	485	5.6	253	1,110	22	1.1
152	Jm	Stone	16N.17W.33.4223	35.574	108.645	03/26/74	8.3	736	34	11	200	.1	300	290	20	.3
153	Jm	Stone	14N.10W.22.414	35.428	107.884	08/08/62	8.0	386	11	2.3	120	4.0	240	98	8.4	.8
154	Jm	Stone	14N.10W.22.214	35.428	107.884	10/18/60	8.3	2,260	26	3.9	700	4.0	170	1,400	60	2.4
155	Jm	RHR	114	35.346	107.781	05/26/09	NA	NA	433	114	201	11	210	1,802	45	.5
156	Je	Stone	14N.12W.17.3333	35.444	108.131	09/05/62	9.0	656	3	.6	254	2.2	395	115	34	7.0
157	Je	Stone	16N.17W.15.2324	35.617	108.626	02/13/74	8.5	303	20	1.6	100	2.0	250	29	14	.5
158	Je	Stone	13N.10W.18.4113	35.356	107.938	02/02/67	NA	242	12	2.4	140	3.0	210	130	11	.9
159	Je	Stone	14N.12W.14.143	35.443	108.078	08/04/61	7.7	1,150	115	43	206	2.6	332	579	22	.3
160	Je	Stone	15N.13W.22.1111	35.517	108.202	07/11/61	7.9	528	36	5.8	141	4.8	228	164	47	.5
161	Je	Stone	16N.15W.16.300	35.618	108.432	11/05/73	8.2	361	26	2.4	69	1.6	200	47	9.0	.5
162	Je	Stone	20N.07W.08.321	35.980	107.603	04/24/75	NA	2,740	67	5.8	850	8.9	615	1,400	62	7.7
163	Je	Stone	19N.05W.01.3323	35.906	107.318	12/27/75	7.5	8,240	100	8.4	2,600	22	343	4,600	700	4.6
164	Je	Stone	13N.10W.18.212	35.356	107.938	02/28/58	7.6	1,890	260	9.7	320	3.0	190	1,100	22.0	1.2
165	TRc	Stone	14N.13W.33.141	35.401	108.221	07/18/61	7.2	567	124	25	39	2.2	265	230	14.0	.2
166	TRc	Stone	14N.15W.28.1434	35.415	108.432	05/14/69	7.9	796	160	33	35	3.0	250	380	10.0	.4
167	TRc	Stone	13N.10W.20.114	35.341	107.920	06/18/76	7.9	15,200	660	67	4,600	16	100	2,100	6,900	.5
168	TRc	Stone	15N.16W.06.2	35.559	108.574	06/15/66	NA	624	180	39	29	.8	240	450	12	.2
169	TRc	Stone	13N.11W.08.2211	35.370	108.026	03/12/75	NA	337	18	6.3	100	3.0	301	42	8.2	.5
170	TRc	Stone	13N.10W.20.114	35.341	107.920	12/22/76	7.9	23,000	1,100	91	7,100	27	52	1,000	13,000	.4
171	Psa	Stone	16N.04W.18.4444	35.617	107.300	06/05/73	6.8	11,100	350	61	3,500	88	1,410	3,300	3,100	3.4
172	Psa	Stone	15N.16W.06.2	35.559	108.574	07/01/70	7.2	893	190	38	27	NA	230	410	7.0	.2
173	Psa	Stone	14N.13W.20.4322	35.430	108.238	07/14/70	8.5	467	31	14	170	NA	220	72	150	.3
174	Psa	Stone	15N.16W.30.3443	35.502	108.574	03/23/72	8.4	1,070	170	82	27	5.0	190	590	6.4	.3
175	Psa	Stone	15N.12W.17.123A	35.531	108.131	01/26/75	7.7	628	54	18	130	NA	180	300	1.8	.5
176	Psa	Stone	15N.12W.19.22	35.516	108.149	02/08/77	9.3	775	6	NA	270	3.0	220	220	130	2.7
177	Psa	Stone	15N.17W.12.34	35.545	108.591	10/02/68	7.3	4,560	260	59	1,100	21	110	3,000	63	.4
178	Psa	Stone	14N.13W.33.124	35.401	108.221	03/13/75	7.3	652	150	28	11	1.8	177	350	4.8	.4
179	Psa	Stone	14N.15W.04.1134	35.473	108.432	07/19/61	7.4	344	90	15	10	1.2	280	72	4.8	.2
180	Psa	Stone	15N.16W.06.2	35.559	108.574	11/06/69	7.7	936	190	38	22	2.0	240	460	9.9	.3

Table 2-1. Historical groundwater major-element data in the study area, 1958–2009.—Continued

[NAD 83, North American Datum of 1983; TDS, total dissolved solids; mg/L, milligrams per liter; Ca, calcium; Mg, magnesium; Na, sodium; K, potassium; HCO_3, bicarbonate; SO_4, sulfate; Cl, chloride; F, fluoride; Qa, Quaternary alluvium; NA, not available; Kmf, Cretaceous Menefee Formation; Kpl, Cretaceous Point Lookout Formation; Kcc, Cretaceous Crevasse Canyon Formation; Kg, Cretaceous Gallup Formation; Km, Cretaceous Mancos Formation; Kd, Cretaceous Dakota Formation; Jm, Jurassic Morrison Formation; Je, Jurassic Entrada Complex (includes Entrada, Todilto, Summerville, and Bluff Formations); TRc, Triassic Chinle Group; Psa, Permian San Andres Formation (including Glorieta Formation)]

Line no.	Form-ation	Data source*	Data identifier**	Latitude (NAD 83)	Longitude (NAD 83)	Date	pH	TDS (mg/L)	Ca (mg/L)	Mg (mg/L)	Na (mg/L)	K (mg/L)	HCO_3 (mg/L)	SO_4 (mg/L)	Cl (mg/L)	F (mg/L)
181	Psa	Stone	15N.16W.06.2	35.559	108.574	03/16/72	7.9	906	190	37	25	NA	240	460	9.9	0.4
182	Psa	Stone	15N.17W.13.3141	35.531	108.590	08/18/64	NA	883	120	59	110	4.0	23	730	14	.4
183	Psa	Stone	15N.16W.06.2	35.559	108.574	12/08/70	7.7	895	190	38	27	.1	42	450	140	.2
184	Psa	Stone	14N.15W.04.1134	35.473	108.432	03/13/75	NA	356	91	16	10	1.4	279	85	4.7	.1
185	Psa	Stone	14N.13W.33.124	35.401	108.221	12/06/67	7.4	770	180	29	10	NA	250	360	17	.3
186	Psa	Stone	14N.13W.33.124	35.401	108.221	04/07/72	7.5	724	180	28	7	NA	250	360	10	.3
187	Psa	Stone	15N.17W.13.3141	35.531	108.590	01/01/67	8.0	1,050	120	60	110	4.0	230	570	22	.3
188	Psa	Stone	15N.17W.13.1142	35.531	108.590	01/01/67	8.2	1,060	120	15	200	3.0	200	610	23	.5
189	Psa	Stone	14N.13W.20.4323	35.430	108.238	03/13/75	NA	399	2	.1	150	2.0	326	58	15	.2

*Data sources:

Stone—Stone, W.J., Lyford, F.P., Frenzel, P.F., Mizell, N.H., and Padgett, E.T., 1983, Hydrogeology and water resources of San Juan Basin, New Mexico: Socorro, New Mexico Bureau of Mines and Mineral Resources, Hydrologic Report 6, 70 p.

RHR—Roca Honda Resources, LLC, 2009a, 11-20-2009 Permit application, Phase II of a new mine application—Baseline data report: Permit application to the Mining and Minerals Division of the New Mexico Energy, Minerals, and Natural Resources Department, http://www.emnrd.state.nm.us/MMD/MARP/permits/MARP_Permits.htm.

**Data identifiers: these values are data indicators used by the source to identify the data within the report or database.

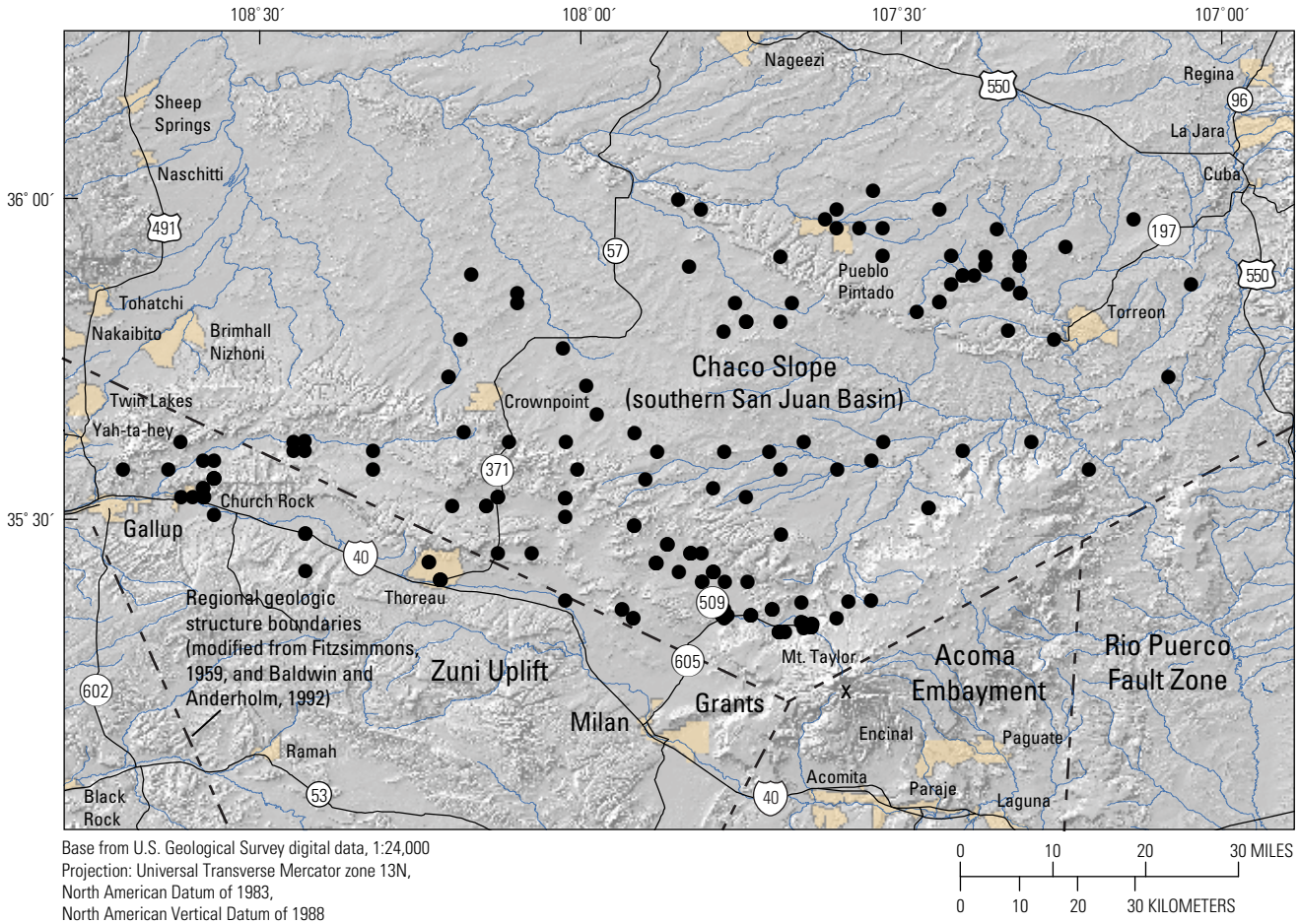

Figure 2-1. Spatial distribution of historical groundwater major-element data in the study area.

Appendix 3.—Historical Groundwater Trace-Element Data

Existing trace-element data in the study area are presented in table 3-1. The spatial distribution of the associated wells across the study area is shown in fig. 3-1 (individual well locations can be located through latitude and longitude coordinates presented in table 3-1). The trace-element data set is a compilation of multiple sources and is presented in order of increasing geologic age of the associated formation. Initial formation designations were determined by the authors/data collectors of the source references (references listed following the table). Existing trace-element data without formation designations were not included for analysis in this study. For this study, formation designations were homogenized to currently (2011) accepted formation nomenclature. This homogenization was necessary because of the long data record (1940s onward) during which formation identification has changed with certain formation names dropped from the lexicon or added as additional studies continued to update the stratigraphic nomenclature of the region (see Methods section).

Table 3-1. Historical groundwater trace-element data in the study area, 1942–2009.

[NAD 83, North American Datum of 1983; Ba, barium; µg/L, micrograms per liter; B, boron; Fe, iron; Li, lithium; Mn, manganese; V, vanadium; Zn, zinc; Qa, Quaternary alluvium; NA, not available; Kmf, Cretaceous Menefee Formation; Kpl, Cretaceous Point Lookout Formation; Kcc, Cretaceous Crevasse Canyon Formation; Kg, Cretaceous Gallup Formation; Km, Cretaceous Mancos Formation; Kd, Cretaceous Dakota Formation; Jm, Jurassic Morrison Formation; Je, Jurassic Entrada Complex (includes Entrada, Todilto, Summerville, and Bluff Formations); TRc, Triassic Chinle Group; Psa, Permian San Andres Formation (including Glorieta Formation)]

Line no.	Form-ation	Data source*	Data identifier**	Latitude (NAD 83)	Longitude (NAD 83)	Date	Ba (µg/L)	B (µg/L)	Fe (µg/L)	Li (µg/L)	Mn (µg/L)	V (µg/L)	Zn (µg/L)
1	Qa	RHR	120	35.346	107.737	08/06/08	NA	200	NA	NA	70	NA	NA
2	Qa	RHR	120	35.346	107.737	02/18/09	NA	500	80	NA	10	NA	NA
3	Qa	RHR	120	35.346	107.737	05/26/09	NA	200	NA	NA	100	NA	NA
4	Qa	RHR	121	35.346	107.737	08/18/08	NA	300	NA	NA	NA	NA	NA
5	Qa	RHR	21	35.320	107.684	08/21/08	100	NA	NA	NA	NA	NA	NA
6	Qa	RHR	21	35.320	107.684	11/08/08	100	100	NA	NA	NA	NA	NA
7	Qa	RHR	115	35.346	107.774	11/13/08	NA	200	NA	NA	NA	NA	NA
8	Qa	RHR	33	35.335	107.659	09/23/08	NA	300	50	NA	260	NA	NA
9	Qa	RHR	33	35.335	107.659	11/17/08	NA	300	NA	NA	140	NA	NA
10	Qa	Stone	20N.07W.20.1444	35.950	107.603	01/05/76	NA	270	10	NA	NA	NA	NA
11	Qa	Stone	20N.07W.20.1423	35.950	107.603	01/05/76	NA	70	10	NA	NA	NA	NA
12	Qa	Stone	20N.07W.18.4112	35.965	107.621	01/05/76	NA	50	NA	NA	NA	NA	NA
13	Qa	Stone	19N.05W.25.424	35.848	107.317	01/28/76	NA	80	140	NA	NA	NA	NA
14	Qa	Stone	19N.05W.25.4144	35.848	107.317	01/29/76	NA	150	20	NA	NA	NA	NA
15	Qa	Stone	19N.05W.18.2224	35.878	107.407	01/14/76	NA	110	NA	NA	NA	NA	NA
16	Qa	Stone	19N.05W.18.2211	35.878	107.407	01/13/76	NA	700	100	NA	NA	NA	NA
17	Qa	Stone	19N.05W.12.3234	35.892	107.318	01/14/76	NA	30	NA	NA	NA	NA	NA
18	Qa	Stone	19N.05W.01.3323	35.906	107.318	01/14/76	NA	70	NA	NA	NA	NA	NA
19	Qa	Stone	19N.05W.01.1212	35.906	107.318	01/14/76	NA	40	70	NA	NA	NA	NA
20	Qa	Stone	19N.04W.09	35.892	107.264	03/19/70	NA	NA	70	NA	NA	NA	NA
21	Qa	Stone	18N.04W.23.13	35.777	107.229	10/18/71	NA	380	NA	NA	NA	NA	NA
22	Qa	Stone	18N.04W.06	35.820	107.300	03/19/70	NA	50	70	NA	NA	NA	NA
23	Qa	Stone	16N.17W.33.4223	35.574	108.645	03/26/74	NA	670	NA	NA	NA	NA	NA
24	Qa	Stone	16N.17W.25.1132	35.588	108.591	10/06/76	NA	180	20	NA	NA	NA	NA
25	Qa	Stone	16N.16W.19.1	35.603	108.574	07/17/70	NA	50	70	NA	NA	NA	NA
26	Qa	Stone	15N.17W.14.2322B	35.531	108.608	09/17/75	NA	300	NA	NA	NA	NA	NA
27	Qa	Stone	15N.17W.14.1A	35.531	108.608	08/07/75	NA	540	NA	NA	NA	NA	NA
28	Qa	Stone	15N.17W.14.1	35.531	108.608	08/07/75	NA	260	NA	NA	NA	NA	NA
29	Qa	Stone	15N.17W.13.3414	35.531	108.590	10/15/65	NA	NA	20	NA	NA	NA	NA
30	Qa	Stone	15N.10W.32.214	35.486	107.919	09/18/62	NA	80	NA	NA	NA	NA	NA

Table 3-1. Historical groundwater trace-element data in the study area, 1942–2009.—Continued

[NAD 83, North American Datum of 1983; Ba, barium; µg/L, micrograms per liter; B, boron; Fe, iron; Li, lithium; Mn, manganese; V, vanadium; Zn, zinc; Qa, Quaternary alluvium; NA, not available; Kmf, Cretaceous Menefee Formation; Kpl, Cretaceous Point Lookout Formation; Kcc, Cretaceous Crevasse Canyon Formation; Kg, Cretaceous Gallup Formation; Km, Cretaceous Mancos Formation; Kd, Cretaceous Dakota Formation; Jm, Jurassic Morrison Formation; Je, Jurassic Entrada Complex (includes Entrada, Todilto, Summerville, and Bluff Formations); TRc, Triassic Chinle Group; Psa, Permian San Andres Formation (including Glorieta Formation)]

Line no.	Form-ation	Data source*	Data identifier**	Latitude (NAD 83)	Longitude (NAD 83)	Date	Ba (µg/L)	B (µg/L)	Fe (µg/L)	Li (µg/L)	Mn (µg/L)	V (µg/L)	Zn (µg/L)
31	Qa	Stone	12N.11W.14.311A	35.269	107.968	07/12/46	NA	37	NA	NA	NA	NA	NA
32	Qa	Stone	12N.11W.14.311	35.269	107.968	07/12/46	NA	NA	NA	NA	NA	NA	NA
33	Qa	Stone	12N.10W.29.434	35.240	107.916	07/12/46	NA	36	NA	NA	NA	NA	NA
34	Qa	Stone	11N.10W.21.221	35.168	107.898	06/07/57	NA	30	NA	NA	NA	NA	NA
35	Qa	Stone	11N.010W.26.321	35.154	107.863	05/07/57	NA	70	NA	NA	NA	NA	NA
36	Qa	Stone	13N.07W.31.414	35.311	107.620	10/24/62	NA	40	NA	NA	NA	NA	NA
37	Qa	Stone	13N.07W.20.1232	35.341	107.603	08/29/62	NA	30	10	NA	NA	NA	NA
38	Qa	Stone	13N.07W.09.433	35.368	107.585	10/23/62	NA	50	10	NA	NA	NA	NA
39	Qa	Stone	15N.17W.13.3243	35.531	108.590	10/13/65	NA	NA	10	NA	NA	NA	NA
40	Qa	Stone	15N.17W.14.4224	35.531	108.608	10/05/65	NA	NA	20	NA	NA	NA	NA
41	Qa	Stone	15N.17W.13.3141	35.531	108.590	10/15/65	NA	NA	30	NA	NA	NA	NA
42	Qa	Stone	15N.17W.13.3141	35.531	108.590	10/15/65	NA	NA	30	NA	NA	NA	NA
43	Qa	Stone	15N.17W.13.3141	35.531	108.590	10/05/65	NA	NA	30	NA	NA	NA	NA
44	Qa	Stone	15N.17W.14.2324A	35.531	108.608	09/10/69	NA	580	190	NA	NA	NA	NA
45	Qa	Stone	20N.07W.22.1221	35.950	107.567	12/27/75	NA	190	20	20	50	1	10
46	Qa	RHR	21	35.320	107.684	05/19/09	100	NA	NA	NA	NA	NA	30
47	Qa	RHR	115	35.346	107.774	05/26/09	NA	200	NA	NA	NA	NA	30
48	Qa	RHR	115	35.346	107.774	09/16/08	NA	200	NA	NA	NA	NA	20
49	Qa	RHR	33	35.335	107.659	05/19/09	400	NA	NA	NA	NA	NA	20
50	Qa	RHR	120	35.346	107.737	11/18/08	NA	300	NA	NA	70	NA	10
51	Kmf	Stone	20N.07W.08.321	35.980	107.603	02/21/67	NA	30	190	NA	NA	NA	NA
52	Kmf	Stone	19N.05W.17.4434	35.877	107.389	01/14/76	NA	20	NA	NA	NA	NA	NA
53	Kmf	Stone	19N.05W.04.214	35.906	107.371	01/13/76	NA	400	30	NA	NA	NA	NA
54	Kmf	Stone	20N.07W.24.222	35.950	107.532	12/28/75	NA	470	10	110	20	9.7	330
55	Kmf	Stone	19N.06W.01.3242	35.907	107.425	01/15/76	NA	360	170	80	40	.5	20
56	Kmf	Stone	19N.05W.09.4112	35.892	107.371	01/13/76	NA	1,500	10	NA	NA	NA	NA
57	Kmf	RHR	87	35.327	107.642	02/16/09	NA	300	NA	NA	NA	NA	NA
58	Kmf	RHR	100	35.320	107.693	08/21/08	NA	NA	NA	NA	100	NA	NA
59	Kmf	RHR	100	35.320	107.693	11/08/08	NA	NA	NA	NA	300	NA	NA
60	Kmf	RHR	100	35.320	107.693	02/11/09	100	NA	NA	NA	260	NA	NA

Table 3-1. Historical groundwater trace-element data in the study area, 1942–2009.—Continued

[NAD 83, North American Datum of 1983; Ba, barium; µg/L, micrograms per liter; B, boron; Fe, iron; Li, lithium; Mn, manganese; V, vanadium; Zn, zinc; Qa, Quaternary alluvium; NA, not available; Kmf, Cretaceous Menefee Formation; Kpl, Cretaceous Point Lookout Formation; Kcc, Cretaceous Crevasse Canyon Formation; Kg, Cretaceous Gallup Formation; Km, Cretaceous Mancos Formation; Kd, Cretaceous Dakota Formation; Jm, Jurassic Morrison Formation; Je, Jurassic Entrada Complex (includes Entrada, Todilto, Summerville, and Bluff Formations); TRc, Triassic Chinle Group; Psa, Permian San Andres Formation (including Glorieta Formation)]

Line no.	Form-ation	Data source*	Data identifier**	Latitude (NAD 83)	Longitude (NAD 83)	Date	Ba (µg/L)	B (µg/L)	Fe (µg/L)	Li (µg/L)	Mn (µg/L)	V (µg/L)	Zn (µg/L)
61	Kmf	RHR	100	35.320	107.693	05/19/09	100	NA	NA	NA	210	NA	NA
62	Kmf	Stone	20N.05W.22.4422	35.949	107.353	01/13/76	NA	10	NA	NA	NA	NA	NA
63	Kmf	Stone	20N.04W.34.4421	35.920	107.246	11/01/63	NA	NA	40	NA	NA	NA	NA
64	Kmf	Stone	20N.03W.15.44	35.964	107.140	05/14/64	NA	70	10	NA	NA	NA	NA
65	Kmf	Stone	20N.02W.31.2	35.920	107.086	09/29/52	NA	NA	580	NA	NA	NA	NA
66	Kmf	Stone	20N.02W.19.124	35.949	107.086	06/18/59	NA	270	700	NA	NA	NA	NA
67	Kmf	Stone	21N.12W.33.1222	36.010	108.120	04/02/74	NA	350	NA	NA	NA	NA	NA
68	Kmf	Stone	20N.12W.26.444	35.936	108.083	05/02/67	NA	20	190	NA	NA	NA	NA
69	Kmf	Stone	20N.05W.07.33C	35.978	107.407	01/29/76	NA	920	30	NA	NA	NA	NA
70	Kmf	Stone	19N.09W.35.13	35.833	107.762	02/20/67	NA	20	260	NA	NA	NA	NA
71	Kmf	Stone	19N.09W.07.3324	35.891	107.833	08/27/70	NA	80	110	NA	NA	NA	NA
72	Kmf	Stone	19N.01W.08.223	35.892	106.962	04/25/78	NA	650	3,700	570	NA	NA	NA
73	Kmf	Stone	18N.09W.12.1A	35.804	107.744	11/30/66	NA	10	70	NA	NA	NA	NA
74	Kmf	Stone	18N.09W.12.121	35.804	107.744	07/27/64	NA	NA	80	NA	NA	NA	NA
75	Kmf	Stone	18N.09W.12.1131	35.804	107.744	12/07/72	NA	580	150	NA	NA	NA	NA
76	Kmf	Stone	18N.08W.09.111	35.804	107.691	02/20/67	NA	10	260	NA	NA	NA	NA
77	Kmf	Stone	18N.05W.01.134	35.820	107.318	02/21/67	NA	20	110	NA	NA	NA	NA
78	Kmf	Stone	17N.08W.30.4143	35.674	107.726	11/30/77	NA	10	110	NA	NA	NA	NA
79	Kmf	Stone	17N.08W.19.434	35.689	107.726	02/20/67	NA	NA	110	NA	NA	NA	NA
80	Kmf	Stone	16N.08W.33.1341	35.573	107.691	10/02/62	NA	260	30	NA	NA	NA	NA
81	Kmf	Stone	16N.07W.32.4141	35.573	107.602	10/15/62	NA	130	NA	NA	NA	NA	NA
82	Kmf	Stone	15N.08W.21.4414	35.515	107.692	10/16/62	NA	90	20	NA	NA	NA	NA
83	Kmf	Stone	15N.06W.22.3123	35.514	107.460	10/22/62	NA	300	230	NA	NA	NA	NA
84	Kmf	Stone	15N.06W.20.121	35.515	107.495	10/03/62	NA	100	20	NA	NA	NA	NA
85	Kmf	Stone	13N.08W.24.3348	35.341	107.637	09/10/62	NA	130	20	NA	NA	NA	NA
86	Kmf	Stone	18N.06W.04.3421	35.820	107.478	02/26/71	NA	NA	220	NA	NA	NA	NA
87	Kmf	Stone	18N.06W.04.3421	35.820	107.478	12/04/72	NA	NA	250	NA	NA	NA	NA
88	Kmf	RHR	27	35.335	107.655	11/13/08	200	NA	NA	NA	NA	NA	260
89	Kmf	RHR	27	35.335	107.655	05/19/09	200	NA	NA	NA	NA	NA	220
90	Kmf	RHR	27	35.335	107.655	08/06/08	200	NA	NA	NA	NA	NA	150

Table 3-1. Historical groundwater trace-element data in the study area, 1942–2009.—Continued

[NAD 83, North American Datum of 1983; Ba, barium; µg/L, micrograms per liter; B, boron; Fe, iron; Li, lithium; Mn, manganese; V, vanadium; Zn, zinc; Qa, Quaternary alluvium; NA, not available; Kmf, Cretaceous Menefee Formation; Kpl, Cretaceous Point Lookout Formation; Kcc, Cretaceous Crevasse Canyon Formation; Kg, Cretaceous Gallup Formation; Km, Cretaceous Mancos Formation; Kd, Cretaceous Dakota Formation; Jm, Jurassic Morrison Formation; Je, Jurassic Entrada Complex (includes Entrada, Todilto, Summerville, and Bluff Formations); TRc, Triassic Chinle Group; Psa, Permian San Andres Formation (including Glorieta Formation)]

Line no.	Form-ation	Data source*	Data identifier**	Latitude (NAD 83)	Longitude (NAD 83)	Date	Ba (µg/L)	B (µg/L)	Fe (µg/L)	Li (µg/L)	Mn (µg/L)	V (µg/L)	Zn (µg/L)
91	Kmf	RHR	27	35.335	107.655	02/16/09	200	NA	NA	NA	NA	NA	110
92	Kmf	RHR	7	35.367	107.658	09/17/08	NA	400	120	NA	10	NA	80
93	Kmf	RHR	7	35.367	107.658	11/16/08	NA	500	510	NA	10	NA	80
94	Kmf	RHR	83	35.331	107.640	08/20/08	NA	700	NA	NA	NA	NA	70
95	Kmf	RHR	7	35.367	107.658	02/16/09	NA	500	570	NA	60	NA	50
96	Kmf	RHR	83	35.331	107.640	11/10/08	NA	700	NA	NA	NA	NA	40
97	Kmf	RHR	62	35.333	107.642	08/20/08	NA	NA	NA	NA	10	NA	30
98	Kmf	RHR	62	35.333	107.642	05/26/09	NA	100	NA	NA	NA	NA	30
99	Kmf	RHR	62	35.333	107.642	11/11/08	NA	100	NA	NA	NA	NA	30
100	Kmf	RHR	87	35.327	107.642	11/12/08	100	400	NA	NA	NA	NA	20
101	Kmf	RHR	87	35.327	107.642	05/19/09	NA	300	NA	NA	NA	NA	20
102	Kmf	RHR	62	35.333	107.642	02/18/09	NA	100	NA	NA	NA	NA	20
103	Kmf	RHR	7	35.367	107.658	05/18/09	NA	500	540	NA	60	NA	20
104	Kmf	RHR	87	35.327	107.642	08/12/08	200	400	NA	NA	NA	NA	10
105	Kmf	Stone	16N.11W.33.411	35.573	108.008	11/24/64	NA	NA	100	NA	NA	NA	NA
106	Kmf	Stone	16N.11W.33.313	35.573	108.008	06/06/62	NA	NA	140	NA	NA	NA	NA
107	Kmf	Stone	21N.05W.32.424	36.006	107.386	01/23/78	NA	80	20	200	NA	NA	NA
108	Kmf	Stone	19N.08W.04.2144	35.906	107.691	09/22/75	NA	150	NA	NA	NA	NA	NA
109	Kmf	Stone	19N.06W.35.3244	35.834	107.443	01/26/76	NA	200	NA	NA	NA	NA	NA
110	Kmf	Stone	19N.06W.31.2242	35.835	107.514	01/12/76	NA	150	20	NA	NA	NA	NA
111	Kmf	Stone	19N.06W.24.2212	35.863	107.425	12/28/75	NA	290	NA	NA	NA	NA	NA
112	Kmf	Stone	19N.06W.10.2111	35.892	107.460	12/28/75	NA	400	10	NA	NA	NA	NA
113	Kmf	Stone	18N.05W.14.221	35.791	107.335	03/19/70	NA	50	70	NA	NA	NA	NA
114	Kmf	Stone	19N.05W.23.3431	35.863	107.335	01/15/76	NA	240	NA	NA	NA	NA	NA
115	Kmf	Stone	20N.062.29.4143	35.936	107.496	12/28/75	NA	450	NA	80	10	1.1	240
116	Kmf	Stone	19N.07W.01.4112	35.907	107.532	01/05/76	NA	340	10	50	NA	.1	10
117	Kmf	Stone	20N.06W.34.1143	35.921	107.460	12/27/75	NA	300	1,100	60	50	.5	NA
118	Kpl	RHR	90	35.331	107.649	11/10/08	400	100	NA	NA	NA	NA	NA
119	Kpl	RHR	122	35.398	107.559	03/06/79	NA	130	180,000	NA	6,000	NA	NA
120	Kpl	RHR	132	35.418	107.635	10/18/79	450	250	NA	NA	20,000	NA	NA

Table 3-1. Historical groundwater trace-element data in the study area, 1942–2009.—Continued

[NAD 83, North American Datum of 1983; Ba, barium; µg/L, micrograms per liter; B, boron; Fe, iron; Li, lithium; Mn, manganese; V, vanadium; Zn, zinc; Qa, Quaternary alluvium; NA, not available; Kmf, Cretaceous Menefee Formation; Kpl, Cretaceous Point Lookout Formation; Kcc, Cretaceous Crevasse Canyon Formation; Kg, Cretaceous Gallup Formation; Km, Cretaceous Mancos Formation; Kd, Cretaceous Dakota Formation; Jm, Jurassic Morrison Formation; Je, Jurassic Entrada Complex (includes Entrada, Todilto, Summerville, and Bluff Formations); TRc, Triassic Chinle Group; Psa, Permian San Andres Formation (including Glorieta Formation)]

Line no.	Form-ation	Data source*	Data identifier**	Latitude (NAD 83)	Longitude (NAD 83)	Date	Ba (µg/L)	B (µg/L)	Fe (µg/L)	Li (µg/L)	Mn (µg/L)	V (µg/L)	Zn (µg/L)
121	Kpl	Stone	19N.13W.13.444	35.878	108.173	11/02/71	NA	750	270	NA	NA	NA	NA
122	Kpl	Stone	19N.12W.27.14	35.849	108.101	11/02/71	NA	750	50	NA	NA	NA	NA
123	Kpl	Stone	19N.12W.05.	35.907	108.137	11/02/71	NA	750	30	NA	NA	NA	NA
124	Kpl	Stone	17N.11W.24.413	35.689	107.959	02/20/67	NA	NA	150	NA	NA	NA	NA
125	Kpl	Stone	14N.05W.14.422	35.438	107.334	08/29/62	NA	50	NA	NA	NA	NA	NA
126	Kpl	Stone	13N.08W.26.221	35.326	107.655	09/11/62	NA	140	20	NA	NA	NA	NA
127	Kpl	Stone	16N.10W.22.212	35.602	107.883	09/19/62	NA	140	NA	NA	NA	NA	NA
128	Kpl	Stone	16N.09W.22.4444	35.602	107.778	09/20/62	NA	330	NA	NA	NA	NA	NA
129	Kpl	Stone	16N.08W.20.1312	35.602	107.708	10/02/62	NA	140	100	NA	NA	NA	NA
130	Kpl	Stone	16N.08W.14.1114	35.617	107.655	10/02/62	NA	220	310	NA	NA	NA	NA
131	Kpl	Stone	16N.07W.13.2244	35.617	107.531	10/02/62	NA	190	NA	NA	NA	NA	NA
132	Kpl	Stone	16N.06W.29.231	35.588	107.495	10/03/62	NA	210	40	NA	NA	NA	NA
133	Kpl	Stone	15N.09W.13.144	35.529	107.745	10/04/62	NA	120	NA	NA	NA	NA	NA
134	Kpl	Stone	16N.04W.18.444	35.617	107.300	07/27/78	90	110	50	NA	9	2	10
135	Kpl	RHR	90	35.331	107.649	08/11/08	400	100	30	NA	NA	NA	90
136	Kpl	RHR	102	35.311	107.687	09/24/08	200	500	40	NA	20	NA	90
137	Kpl	RHR	102	35.311	107.687	02/11/09	100	400	90	NA	NA	NA	60
138	Kpl	RHR	102	35.311	107.687	11/08/08	NA	500	250	NA	NA	NA	50
139	Kpl	RHR	90	35.331	107.649	02/16/09	200	400	NA	NA	NA	NA	40
140	Kpl	RHR	22	35.342	107.664	05/19/09	300	NA	NA	NA	NA	NA	40
141	Kpl	RHR	22	35.342	107.664	11/13/08	300	NA	30	NA	NA	NA	30
142	Kpl	RHR	90	35.331	107.649	05/19/09	400	NA	NA	NA	NA	NA	20
143	Kpl	RHR	22	35.342	107.664	08/21/08	300	NA	NA	NA	NA	NA	20
144	Kpl	RHR	22	35.342	107.664	02/11/09	300	NA	40	NA	NA	NA	20
145	Kcc	Stone	15N.09W.09.2442	35.544	107.796	09/12/62	NA	360	20	NA	NA	NA	NA
146	Kcc	Stone	18N.13W.23.3212	35.776	108.190	11/02/71	NA	750	40	NA	NA	NA	NA
147	Kcc	Stone	18N.13W.01.4	35.820	108.173	11/02/71	NA	1300	80	NA	NA	NA	NA
148	Kcc	Stone	16N.13W.11.3413	35.632	108.185	07/11/61	NA	350	10	NA	NA	NA	NA
149	Kcc	Stone	15N.10W.06.2421	35.558	107.936	08/01/61	NA	220	20	NA	NA	NA	NA
150	Kcc	Stone	15N.10W.13.1314	35.529	107.848	07/18/73	NA	260	20	NA	NA	NA	NA

Table 3-1. Historical groundwater trace-element data in the study area, 1942–2009.—Continued

[NAD 83, North American Datum of 1983; Ba, barium; µg/L, micrograms per liter; B, boron; Fe, iron; Li, lithium; Mn, manganese; V, vanadium; Zn, zinc; Qa, Quaternary alluvium; NA, not available; Kmf, Cretaceous Menefee Formation; Kpl, Cretaceous Point Lookout Formation; Kcc, Cretaceous Crevasse Canyon Formation; Kg, Cretaceous Gallup Formation; Km, Cretaceous Mancos Formation; Kd, Cretaceous Dakota Formation; Jm, Jurassic Morrison Formation; Je, Jurassic Entrada Complex (includes Entrada, Todilto, Summerville, and Bluff Formations); TRc, Triassic Chinle Group; Psa, Permian San Andres Formation (including Glorieta Formation)]

Line no.	Form-ation	Data source*	Data identifier**	Latitude (NAD 83)	Longitude (NAD 83)	Date	Ba (µg/L)	B (µg/L)	Fe (µg/L)	Li (µg/L)	Mn (µg/L)	V (µg/L)	Zn (µg/L)
151	Kcc	Stone	15N.10W.06.2421	35.558	107.936	01/15/70	NA	150	70	NA	NA	NA	NA
152	Kg	RHR	32	35.336	107.662	08/21/08	NA	400	60	NA	10	NA	NA
153	Kg	RHR	16	35.356	107.704	11/11/08	NA	500	NA	NA	NA	NA	NA
154	Kg	RHR	16	35.356	107.704	05/19/09	NA	400	NA	NA	NA	NA	NA
155	Kg	Stone	17N.13W.21.111	35.689	108.226	09/17/76	NA	120	10	NA	NA	NA	NA
156	Kg	Stone	17N.12W.33.244	35.660	108.119	03/10/70	NA	NA	320	NA	NA	NA	NA
157	Kg	Stone	16N.18W.35.14	35.574	108.716	05/25/56	NA	NA	10	NA	NA	NA	NA
158	Kg	Stone	16N.11W.17.4322	35.616	108.026	02/12/73	NA	120	10	NA	NA	NA	NA
159	Kg	Stone	16N.07W.26.2214	35.588	107.549	10/02/62	NA	120	20	NA	NA	NA	NA
160	Kg	Stone	16N.05W.19.414	35.602	107.407	09/19/62	NA	130	200	NA	NA	NA	NA
161	Kg	Stone	16N.04W.36.2321	35.573	107.210	04/13/78	NA	80	10	30	NA	NA	NA
162	Kg	Stone	15N.10W.04.1311	35.558	107.901	07/18/73	NA	180	NA	NA	NA	NA	NA
163	Kg	Stone	14N.08W.15.244	35.442	107.672	10/01/62	NA	800	NA	NA	NA	NA	NA
164	Kg	Stone	15N.18W.14.2223	35.531	108.716	11/28/55	NA	NA	10	NA	NA	NA	NA
165	Kg	Stone	15N.18W.13.1134A	35.531	108.698	11/22/48	NA	NA	20	NA	NA	NA	NA
166	Kg	Stone	15N.18W.14.2223	35.531	108.716	12/06/48	NA	NA	30	NA	NA	NA	NA
167	Kg	Stone	15N.10W.13.1314	35.529	107.848	09/18/62	NA	240	570	NA	NA	NA	NA
168	Kg	RHR	16	35.356	107.704	02/12/09	NA	400	13,800	NA	80	NA	50
169	Kg	RHR	16	35.356	107.704	08/25/08	NA	300	NA	NA	20	NA	20
170	Km	Stone	16N.01W.29.2322	35.588	106.961	06/05/73	NA	1,800	30	1,200	20	NA	NA
171	Km	Stone	16N.15W.20.1314	35.603	108.450	11/18/71	NA	600	20	NA	NA	NA	NA
172	Kd	Stone	16N.10W.02.23	35.646	107.864	05/23/75	NA	NA	1,300	NA	60	NA	NA
173	Kd	Stone	14N.08W.04.3343	35.472	107.690	10/16/62	NA	380	20	NA	NA	NA	NA
174	Kd	Stone	17N.12W.30.3243	35.675	108.154	10/29/74	NA	NA	10	NA	NA	NA	NA
175	Kd	Stone	17N.12W.30.142	35.675	108.154	10/13/64	NA	NA	30	NA	NA	NA	NA
176	Kd	Stone	16N.16W.15.4322	35.617	108.521	02/07/74	NA	20	NA	NA	NA	NA	NA
177	Kd	Stone	16N.15W.11.3323	35.632	108.397	02/13/74	NA	120	NA	NA	NA	NA	NA
178	Kd	Stone	16N.14W.21.3334	35.603	108.326	03/20/74	NA	40	500	NA	NA	NA	NA
179	Kd	Stone	16N.14W.15.1342	35.617	108.309	03/20/74	NA	320	2,000	NA	NA	NA	NA
180	Kd	Stone	15N.11W.17.1111	35.529	108.026	07/31/61	NA	100	20	NA	NA	NA	NA

Table 3-1. Historical groundwater trace-element data in the study area, 1942–2009.—Continued

[NAD 83, North American Datum of 1983; Ba, barium; µg/L, micrograms per liter; B, boron; Fe, iron; Li, lithium; Mn, manganese; V, vanadium; Zn, zinc; Qa, Quaternary alluvium; NA, not available; Kmf, Cretaceous Menefee Formation; Kpl, Cretaceous Point Lookout Formation; Kcc, Cretaceous Crevasse Canyon Formation; Kg, Cretaceous Gallup Formation; Km, Cretaceous Mancos Formation; Kd, Cretaceous Dakota Formation; Jm, Jurassic Morrison Formation; Je, Jurassic Entrada Complex (includes Entrada, Todilto, Summerville, and Bluff Formations); TRc, Triassic Chinle Group; Psa, Permian San Andres Formation (including Glorieta Formation)]

Line no.	Form-ation	Data source*	Data identifier**	Latitude (NAD 83)	Longitude (NAD 83)	Date	Ba (µg/L)	B (µg/L)	Fe (µg/L)	Li (µg/L)	Mn (µg/L)	V (µg/L)	Zn (µg/L)
181	Kd	Stone	14N.09W.36.313	35.398	107.742	04/24/63	NA	NA	80	NA	NA	NA	NA
182	Kd	Stone	14N.09W.36.313	35.398	107.742	05/06/63	NA	NA	20	50	NA	NA	NA
183	Kd	Brod	16N.15W.20.1314	35.603	108.450	11/23/70	NA	120	40	NA	NA	NA	NA
184	Kd	Brod	16N.15W.17.1431	35.618	108.450	07/29/70	NA	50	110	NA	NA	NA	NA
185	Kd	Brod	16N.15W.17.1431	35.618	108.450	02/23/70	NA	20	390	NA	NA	NA	NA
186	Kd	Stone	14N.09W.17.300	35.442	107.814	08/08/62	NA	170	NA	NA	NA	NA	NA
187	Kd	Stone	16N.15W.20.1314	35.603	108.450	02/13/74	NA	60	100	NA	NA	NA	30
188	Kd	Stone	16N.17W.15.2324	35.617	108.626	03/26/74	10	740	10	NA	8	NA	6
189	Jm	Stone	17N.16W.35.413	35.660	108.510	03/23/71	NA	NA	500	NA	NA	NA	NA
190	Jm	Stone	16N.17W.21.3442	35.603	108.644	03/26/74	NA	200	NA	NA	NA	NA	NA
191	Jm	Stone	16N.16W.17.2114	35.617	108.556	02/07/74	NA	60	30	NA	NA	NA	NA
192	Jm	Stone	16N.14W.33.22	35.574	108.326	03/06/73	NA	1,700	NA	NA	NA	NA	NA
193	Jm	Stone	16N.11W.33.332	35.573	108.008	09/08/72	NA	NA	20	NA	NA	NA	NA
194	Jm	Stone	15N.12W.17.123A	35.531	108.131	05/04/63	NA	NA	260	10	NA	NA	NA
195	Jm	Stone	14N.10W.25.100	35.414	107.849	08/18/59	NA	210	NA	NA	NA	NA	NA
196	Jm	Stone	14N.09W.32.314	35.399	107.813	08/11/59	NA	100	NA	NA	NA	NA	NA
197	Jm	Stone	14N.09W.32.122	35.399	107.813	02/14/58	NA	NA	2,100	NA	NA	NA	NA
198	Jm	Stone	14N.09W.30.2213	35.414	107.831	05/03/63	NA	NA	NA	120	NA	NA	NA
199	Jm	Stone	14N.09W.29.312	35.413	107.813	08/13/59	NA	170	430	NA	NA	NA	NA
200	Jm	Stone	14N.09W.18.400	35.442	107.831	08/30/63	NA	NA	60	50	NA	NA	NA
201	Jm	Stone	14N.09W.18.243	35.442	107.831	10/17/62	NA	230	10	NA	NA	NA	NA
202	Jm	Stone	14N.10W.11.434A	35.457	107.867	10/18/60	NA	330	NA	NA	NA	NA	NA
203	Jm	Stone	16N.16W.30.3431	35.588	108.574	05/02/72	NA	80	10	NA	NA	NA	NA
204	Jm	Stone	15N.11W.29.1132	35.500	108.026	09/30/76	30	50	NA	NA	NA	NA	NA
205	Jm	Stone	14N.09W.34.422	35.399	107.777	04/24/63	NA	NA	NA	70	NA	NA	NA
206	Jm	Stone	14N.10W.24.400	35.428	107.849	04/29/63	NA	NA	20	50	NA	NA	NA
207	Jm	Stone	14N.10W.22.2	35.428	107.884	08/08/62	NA	160	10	NA	NA	NA	NA
208	Jm	Stone	14N.10W.22.2	35.428	107.884	08/08/62	NA	140	NA	NA	NA	NA	NA
209	Jm	RHR	113	35.346	107.781	02/12/09	NA	NA	NA	NA	170	NA	460
210	Jm	RHR	116	35.345	107.780	08/19/08	NA	300	NA	NA	NA	NA	210

Table 3-1. Historical groundwater trace-element data in the study area, 1942–2009.—Continued

[NAD 83, North American Datum of 1983; Ba, barium; µg/L, micrograms per liter; B, boron; Fe, iron; Li, lithium; Mn, manganese; V, vanadium; Zn, zinc; Qa, Quaternary alluvium; NA, not available; Kmf, Cretaceous Menefee Formation; Kpl, Cretaceous Point Lookout Formation; Kcc, Cretaceous Crevasse Canyon Formation; Kg, Cretaceous Gallup Formation; Km, Cretaceous Mancos Formation; Kd, Cretaceous Dakota Formation; Jm, Jurassic Morrison Formation; Je, Jurassic Entrada Complex (includes Entrada, Todilto, Summerville, and Bluff Formations); TRc, Triassic Chinle Group; Psa, Permian San Andres Formation (including Glorieta Formation)]

Line no.	Form-ation	Data source*	Data identifier**	Latitude (NAD 83)	Longitude (NAD 83)	Date	Ba (µg/L)	B (µg/L)	Fe (µg/L)	Li (µg/L)	Mn (µg/L)	V (µg/L)	Zn (µg/L)
211	Jm	RHR	113	35.346	107.781	09/22/08	NA	300	NA	NA	110	NA	200
212	Jm	RHR	116	35.345	107.780	05/21/09	NA	300	NA	NA	NA	NA	110
213	Jm	RHR	116	35.345	107.780	02/10/09	NA	200	NA	NA	NA	NA	80
214	Jm	RHR	116	35.345	107.780	11/13/08	NA	200	NA	NA	NA	NA	70
215	Jm	RHR	114	35.346	107.781	02/18/09	100	300	NA	NA	70	NA	40
216	Jm	RHR	114	35.346	107.781	09/18/08	200	200	NA	NA	70	NA	20
217	Jm	RHR	113	35.346	107.781	11/10/08	NA	200	NA	NA	NA	NA	20
218	Jm	RHR	114	35.346	107.781	05/26/09	200	300	NA	NA	60	NA	10
219	Jm	RHR	113	35.346	107.781	05/26/09	NA	300	NA	NA	NA	NA	10
220	Je	Stone	14N.12W.14.143	35.443	108.078	09/05/62	NA	310	100	NA	NA	NA	NA
221	Je	Stone	14N.12W.09.221	35.458	108.114	09/05/62	NA	1,600	30	NA	NA	NA	NA
222	Je	Stone	14N.11W.19.124	35.428	108.043	08/04/61	NA	180	10	NA	NA	NA	NA
223	Je	Stone	13N.10W.08.211	35.370	107.920	02/02/67	NA	60	70	NA	NA	NA	NA
224	Je	Stone	13N.10W.20.114	35.341	107.920	07/23/76	NA	1,000	280	NA	NA	NA	NA
225	Je	Stone	20N.06W.32.23	35.921	107.496	04/24/75	NA	NA	170	450	90	NA	NA
226	Je	Stone	16N.16W.25.2344	35.588	108.486	02/13/74	NA	500	220	NA	NA	NA	NA
227	Je	Stone	15N.14W.13.413	35.531	108.273	06/10/70	NA	NA	260	NA	NA	NA	NA
228	Je	Stone	13N.10W.18.4113	35.356	107.938	04/26/72	NA	1,200	630	NA	NA	NA	NA
229	Je	Stone	15N.13W.12.144	35.546	108.167	07/11/61	NA	150	210	NA	NA	NA	NA
230	Je	Stone	15N.17W.14.4224	35.531	108.608	10/15/65	NA	NA	40	NA	NA	NA	NA
231	Je	Stone	15N.13W.22.1111	35.517	108.202	09/24/70	NA	890	150	NA	NA	NA	NA
232	Je	Stone	15N.17W.14.4224	35.531	108.608	09/30/66	NA	NA	520	NA	NA	NA	NA
233	Je	Stone	15N.13W.22.1111	35.517	108.202	03/20/74	NA	1,030	340	NA	NA	NA	170
234	Je	Stone	19N.04W.13.111C	35.877	107.211	12/27/75	NA	1,900	800	1,200	90	6.7	NA
235	TRc	Stone	13N.12W.10.2444	35.370	108.096	08/23/67	NA	500	400	NA	NA	NA	NA
236	TRc	Brod	14N.13W.20.4323	35.430	108.238	07/12/61	NA	210	80	NA	NA	NA	NA
237	TRc	Stone	13N.11W.07.344	35.370	108.043	03/12/75	NA	NA	10	NA	30	NA	NA
238	TRc	Brod	12N.10W.23.233	35.254	107.862	07/12/46	NA	550	NA	NA	NA	NA	NA
239	TRc	Brod	14N.13W.33.124	35.401	108.221	07/18/61	NA	120	10	NA	NA	NA	NA
240	TRc	Stone	15N.15W.20.313	35.517	108.449	06/15/66	NA	NA	40	NA	NA	NA	NA

Table 3-1. Historical groundwater trace-element data in the study area, 1942–2009.—Continued

[NAD 83, North American Datum of 1983; Ba, barium; µg/L, micrograms per liter; B, boron; Fe, iron; Li, lithium; Mn, manganese; V, vanadium; Zn, zinc; Qa, Quaternary alluvium; NA, not available; Kmf, Cretaceous Menefee Formation; Kpl, Cretaceous Point Lookout Formation; Kcc, Cretaceous Crevasse Canyon Formation; Kg, Cretaceous Gallup Formation; Km, Cretaceous Mancos Formation; Kd, Cretaceous Dakota Formation; Jm, Jurassic Morrison Formation; Je, Jurassic Entrada Complex (includes Entrada, Todilto, Summerville, and Bluff Formations); TRc, Triassic Chinle Group; Psa, Permian San Andres Formation (including Glorieta Formation)]

Line no.	Form-ation	Data source*	Data identifier**	Latitude (NAD 83)	Longitude (NAD 83)	Date	Ba (µg/L)	B (µg/L)	Fe (µg/L)	Li (µg/L)	Mn (µg/L)	V (µg/L)	Zn (µg/L)
241	TRc	Stone	15N.15W.20.313	35.517	108.449	10/24/67	NA	200	70	NA	NA	NA	NA
242	TRc	Stone	13N.10W.18.212	35.356	107.938	06/18/76	NA	NA	90	NA	NA	NA	NA
243	TRc	Stone	13N.10W.18.212	35.356	107.938	12/22/76	660	2,600	100	NA	NA	NA	NA
244	TRc	Stone	14N.13W.25.1334	35.415	108.167	09/30/71	NA	450	150	NA	NA	NA	NA
245	TRc	Brod	14N.15W.04.1134	35.473	108.432	05/14/69	NA	NA	220	NA	NA	NA	NA
246	TRc	Stone	14N.13W.25.1334	35.415	108.167	03/01/66	NA	30	230	NA	NA	NA	NA
247	TRc	Stone	15N.16W.06.2	35.559	108.574	03/28/72	NA	80	NA	NA	NA	NA	NA
248	Psa	Stone	15N.16W.30.3443	35.502	108.574	10/02/68	NA	1,100	110	NA	NA	NA	NA
249	Psa	Stone	14N.13W.33.3341	35.401	108.221	07/19/61	NA	110	10	NA	NA	NA	NA
250	Psa	Stone	13N.12W.34.332	35.313	108.097	09/04/62	NA	140	NA	NA	NA	NA	NA
251	Psa	Stone	12N.10W.32.111	35.225	107.915	07/12/46	NA	70	NA	NA	NA	NA	NA
252	Psa	Stone	12N.10W.30.421	35.240	107.933	05/07/57	NA	70	NA	NA	NA	NA	NA
253	Psa	Stone	12N.10W.27.333	35.240	107.880	05/07/57	NA	330	NA	NA	NA	NA	NA
254	Psa	Stone	12N.10W.23.233	35.254	107.862	07/12/46	NA	276	NA	NA	NA	NA	NA
255	Psa	Stone	11N.10W.16.121	35.182	107.898	07/12/46	NA	70	NA	NA	NA	NA	NA
256	Psa	Stone	11N.10W.09.221	35.197	107.898	07/11/46	NA	70	NA	NA	NA	NA	NA
257	Psa	Stone	11N.10W.04.333	35.211	107.898	08/23/66	NA	160	NA	NA	NA	NA	NA
258	Psa	Stone	11N.10W.04.211	35.211	107.898	06/07/57	NA	40	NA	NA	NA	NA	NA
259	Psa	Stone	15N.17W.13.222	35.531	108.590	10/01/64	NA	NA	60	NA	NA	NA	NA
260	Psa	Stone	15N.16W.23.3132	35.517	108.503	03/23/72	NA	80	NA	NA	NA	NA	NA
261	Psa	Stone	14N.13W.20.4322	35.430	108.238	03/13/75	NA	NA	10	NA	20	NA	NA
262	Psa	Stone	14N.13W.20.4321	35.430	108.238	03/13/75	NA	NA	50	NA	NA	NA	NA
263	Psa	Stone	14N.13W.19.1	35.430	108.256	07/14/70	NA	300	NA	NA	NA	NA	NA
264	Psa	Stone	14N.15W.04.1134	35.473	108.432	03/03/75	NA	NA	20	NA	NA	NA	NA
265	Psa	Stone	14N.13W.33.124	35.401	108.221	03/13/75	NA	NA	10	NA	30	NA	NA
266	Psa	Stone	11N.10W.16.121A	35.182	107.898	08/15/62	NA	150	NA	NA	NA	NA	NA
267	Psa	Stone	15N.17W.24.4121	35.517	108.591	07/22/65	NA	NA	10	NA	NA	NA	NA
268	Psa	Stone	15N.17W.24.4121	35.517	108.591	07/22/65	NA	NA	10	NA	NA	NA	NA
269	Psa	Stone	15N.18W.13.1134A	35.531	108.698	07/25/67	NA	NA	10	NA	NA	NA	NA
270	Psa	Stone	15N.17W.24.4121	35.517	108.591	06/05/64	NA	NA	20	NA	NA	NA	NA

Table 3-1. Historical groundwater trace-element data in the study area, 1942–2009.—Continued

[NAD 83, North American Datum of 1983; Ba, barium; µg/L, micrograms per liter; B, boron; Fe, iron; Li, lithium; Mn, manganese; V, vanadium; Zn, zinc; Qa, Quaternary alluvium; NA, not available; Kmf, Cretaceous Menefee Formation; Kpl, Cretaceous Point Lookout Formation; Kcc, Cretaceous Crevasse Canyon Formation; Kg, Cretaceous Gallup Formation; Km, Cretaceous Mancos Formation; Kd, Cretaceous Dakota Formation; Jm, Jurassic Morrison Formation; Je, Jurassic Entrada Complex (includes Entrada, Todilto, Summerville, and Bluff Formations); TRc, Triassic Chinle Group; Psa, Permian San Andres Formation (including Glorieta Formation)]

Line no.	Form-ation	Data source*	Data identifier**	Latitude (NAD 83)	Longitude (NAD 83)	Date	Ba (µg/L)	B (µg/L)	Fe (µg/L)	Li (µg/L)	Mn (µg/L)	V (µg/L)	Zn (µg/L)
271	Psa	Stone	15N.17W.24.4121	35.517	108.591	10/06/60	NA	NA	40	NA	NA	NA	NA
272	Psa	Brod	15N.15W.18.3344	35.531	108.467	11/06/69	NA	220	70	NA	NA	NA	NA
273	Psa	Brod	15N.17W.12.34	35.545	108.591	04/01/69	NA	NA	70	NA	NA	NA	NA
274	Psa	Brod	15N.15W.18.3344	35.531	108.467	06/15/66	NA	NA	70	NA	NA	NA	NA
275	Psa	Stone	15N.15W.18.3344	35.531	108.467	08/12/70	NA	NA	70	NA	NA	NA	NA
276	Psa	Stone	15N.15W.18.3344	35.531	108.467	08/01/68	NA	50	80	NA	NA	NA	NA
277	Psa	Stone	15N.15W.18.3344	35.531	108.467	11/06/69	NA	50	110	NA	NA	NA	NA
278	Psa	Stone	15N.17W.13.1142	35.531	108.590	08/18/64	NA	NA	120	NA	NA	NA	NA
279	Psa	Stone	14N.13W.127.342A	35.458	108.167	12/06/67	NA	NA	140	NA	NA	NA	NA
280	Psa	Stone	15N.18W.13.1134A	35.531	108.698	08/31/66	NA	NA	170	NA	NA	NA	NA
281	Psa	Brod	15N.17W.12.34	35.545	108.591	11/30/66	NA	50	190	NA	NA	NA	NA
282	Psa	Brod	15N.17W.13.1142	35.531	108.590	11/30/66	NA	20	260	NA	NA	NA	NA
283	Psa	Brod	15N.17W.24.4121	35.517	108.591	08/25/58	NA	NA	270	NA	NA	NA	NA
284	Psa	Brod	15N.12W.17.111	35.531	108.131	02/08/76	NA	1,400	360	NA	NA	NA	NA
285	Psa	Stone	15N.17W.24.4121	35.517	108.591	02/05/42	NA	NA	600	NA	NA	NA	NA
286	Psa	Stone	12N.11W.25.213	35.240	107.950	07/11/46	NA	147	NA	NA	NA	NA	NA
287	Psa	Stone	11N.10W.16.121A	35.182	107.898	08/22/66	NA	260	NA	NA	NA	NA	NA
288	Psa	Brod	12N.11W.25.213	35.240	107.950	05/07/57	NA	330	NA	NA	NA	NA	NA
289	Psa	Stone	14N.13W.127.342A	35.458	108.167	04/07/72	NA	120	NA	NA	NA	NA	NA
290	Psa	Stone	15N.15W.20.313	35.517	108.449	03/16/72	NA	160	NA	NA	NA	NA	NA
291	Psa	Stone	12N.11W.15.211	35.269	107.985	05/06/57	NA	1,200	NA	NA	NA	NA	NA
292	Psa	Stone	15N.12W.17.111	35.531	108.131	01/26/75	NA	NA	1,900	NA	180	NA	220

*Data sources:

Brod—Brod, R.C., and Stone, W.J., 1981, Hydrogeology of Ambrosia Lake-San Mateo area, McKinley and Cibola Counties, New Mexico: New Mexico Bureau of Mines and Mineral Resources, HS-2, text and map, 1:62,500.

Stone—Stone, W.J., Lyford, F.P., Frenzel, P.F., Mizell, N.H., and Padgett, E.T., 1983, Hydrogeology and water resources of San Juan Basin, New Mexico: Socorro, New Mexico Bureau of Mines and Mineral Resources, Hydrologic Report 6, 70 p.

RHR—Roca Honda Resources, LLC, 2009a, 11-20-2009 Permit application, Phase II of a new mine application—Baseline data report: Permit application to the Mining and Minerals Division of the New Mexico Energy, Minerals, and Natural Resources Department, http://www.emnrd.state.nm.us/MMD/MARP/permits/MARP_Permits.htm.

**Data identifiers: these values are data indicators used by the source to identify the data within the report or database.

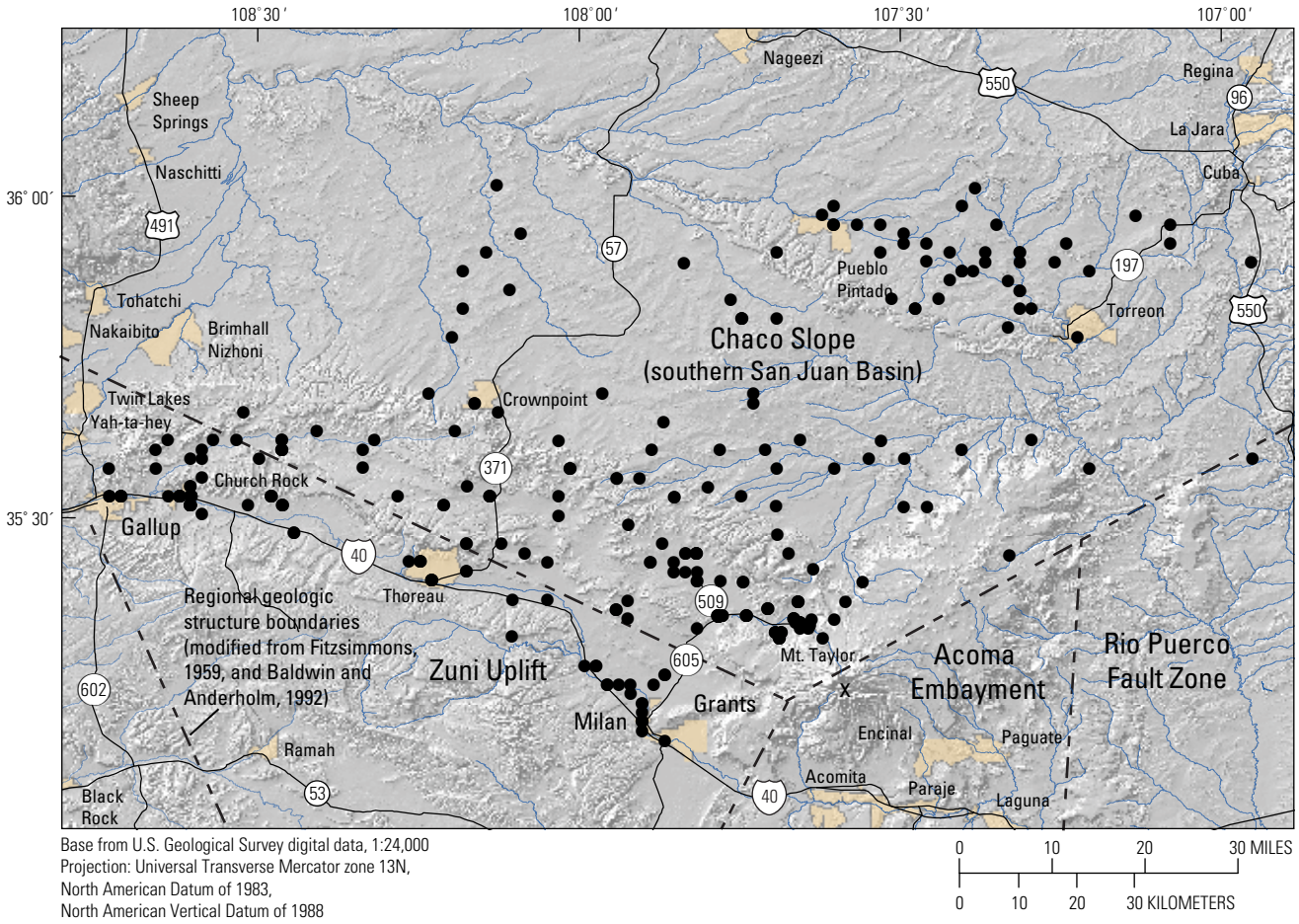

Figure 3-1. Spatial distribution of historical groundwater trace-element data in the study area.

Appendix 4.—Historical Groundwater Contaminants-of-Concern Data

Data for the contaminants of concern in the study area (NO_3, U, Ra, and gross alpha) are presented in table 4-1. The spatial distribution of the associated wells across the study area is shown in fig. 4-1 (individual well locations can be located through latitude and longitude coordinates presented in table 4-1). The contaminants-of-concern data set is a compilation of multiple sources and is presented in order of increasing geologic age of the associated formation. Initial formation designations were determined by the authors/data collectors of the source references (references listed following the table). Contaminant data without formation designations were not included for analysis in this study. For this study, formation designations were homogenized to currently (2011) accepted formation nomenclature. This homogenization was necessary because of the long data record (1940s onward) during which formation identification has changed, with certain formation names dropped from the lexicon or added as additional studies continued to update the stratigraphic nomenclature of the region (see Methods section).

Table 4-1. Historical groundwater contaminants-of-concern data in the study area, 1942–2009.

[NAD 83, North American Datum of 1983; NO_3, nitrate or nitrate plus nitrite; N, nitrogen; mg/L, milligrams per liter; U, uranium; µg/L, micrograms per liter; Ra, radium; pCi/L, picocuries per liter; Qa, Quaternary alluvium; NA, not available; Kmf, Cretaceous Menefee Formation; Kpl, Cretaceous Point Lookout Formation; Kcc, Cretaceous Crevasse Canyon Formation; Kg, Cretaceous Gallup Formation; Km, Cretaceous Mancos Formation; Kd, Cretaceous Dakota Formation; Jm, Jurassic Morrison Formation; Je, Jurassic Entrada Complex (includes Entrada, Todilto, Summerville, and Bluff Formations); TRc, Triassic Chinle Group; Psa, Permian San Andres Formation (including Glorieta Formation)]

Line no.	Form-ation	Data source*	Data identifier**	Latitude (NAD 83)	Longitude (NAD 83)	Date	NO_3 (as N, mg/L)	U (µg/L)	Ra 226 (pCi/L)	Ra 228 (pCi/L)	Ra 228 +226 (pCi/L)	Gross alpha (pCi/L)
1	Qa	RHR	120	35.348	107.738	08/06/08	NA	3.3	0.41	0.42	0.83	6.7
2	Qa	RHR	120	35.348	107.738	11/18/08	NA	2.7	.41	.25	.66	11.8
3	Qa	RHR	120	35.348	107.738	02/18/09	NA	NA	NA	.71	.71	2.1
4	Qa	RHR	120	35.348	107.738	05/26/09	NA	3.6	.51	2.60	3.11	5.3
5	Qa	RHR	121	35.348	107.739	08/18/08	1.7	NA	NA	.27	.27	1.8
6	Qa	RHR	21	35.323	107.684	08/21/08	NA	4.9	.03	.31	.34	8.8
7	Qa	RHR	21	35.323	107.684	11/08/08	NA	5.3	.09	2.40	2.49	7.4
8	Qa	RHR	21	35.323	107.684	02/11/09	NA	5.5	NA	.46	.46	5.6
9	Qa	RHR	21	35.323	107.684	05/19/09	NA	5.1	NA	1.00	1.00	8.6
10	Qa	RHR	115	35.347	107.776	09/16/08	5.7	180	NA	.32	.32	205
11	Qa	RHR	115	35.347	107.776	11/13/08	5.6	166	NA	.01	.01	228
12	Qa	RHR	115	35.347	107.776	05/26/09	5.7	192	NA	.03	.03	166
13	Qa	RHR	33	35.334	107.657	09/23/08	2.0	8.5	NA	NA	NA	26.8
14	Qa	RHR	33	35.334	107.657	11/17/08	2.8	8.0	NA	.01	.01	13.7
15	Qa	RHR	33	35.334	107.657	05/19/09	NA	NA	.3	.05	.35	3.5
16	Qa	Stone	11N.10W.21.221	35.168	107.898	06/07/57	8.2	NA	NA	NA	NA	NA
17	Qa	Stone	11N.10W.26.321	35.154	107.863	05/07/57	3.1	NA	NA	NA	NA	NA
18	Qa	Stone	11N.10W.26.321A	35.154	107.863	10/21/44	5.7	NA	NA	NA	NA	NA
19	Qa	Stone	11N.10W.26.321A	35.154	107.863	06/15/55	3.8	NA	NA	NA	NA	NA
20	Qa	Stone	12N.10W.27.244	35.240	107.880	07/25/56	10	NA	NA	NA	NA	NA
21	Qa	Stone	12N.10W.29.434	35.240	107.916	07/12/46	14	NA	NA	NA	NA	NA
22	Qa	Stone	12N.11W.14.213	35.269	107.968	07/23/56	.9	NA	NA	NA	NA	NA
23	Qa	Stone	12N.11W.14.311A	35.269	107.968	07/18/56	16	NA	NA	NA	NA	NA
24	Qa	Stone	13N.07W.09.433	35.368	107.585	10/23/62	.1	NA	NA	NA	NA	NA
25	Qa	Stone	13N.07W.20.1232	35.341	107.603	08/29/62	.2	NA	NA	NA	NA	NA
26	Qa	Stone	13N.07W.31.414	35.311	107.620	10/24/61	.5	NA	NA	NA	NA	NA
27	Qa	Stone	13N.09W.22.2124	35.341	107.778	12/06/57	12	NA	NA	NA	NA	NA
28	Qa	Stone	15N.10W.32.214	35.486	107.919	09/18/62	10	NA	NA	NA	NA	NA
29	Qa	Stone	15N.15W.07.23	35.545	108.468	04/07/53	20	NA	NA	NA	NA	NA
30	Qa	Stone	15N.17W.13.3243	35.531	108.590	10/13/65	2.7	NA	NA	NA	NA	NA

Table 4-1. Historical groundwater contaminants-of-concern data in the study area, 1942–2009.—Continued

[NAD 83, North American Datum of 1983; NO_3, nitrate or nitrate plus nitrite; N, nitrogen; mg/L, milligrams per liter; U, uranium; µg/L, micrograms per liter; Ra, radium; pCi/L, picocuries per liter; Qa, Quaternary alluvium; NA, not available; Kmf, Cretaceous Menefee Formation; Kpl, Cretaceous Point Lookout Formation; Kcc, Cretaceous Crevasse Canyon Formation; Kg, Cretaceous Gallup Formation; Km, Cretaceous Mancos Formation; Kd, Cretaceous Dakota Formation; Jm, Jurassic Morrison Formation; Je, Jurassic Entrada Complex (includes Entrada, Todilto, Summerville, and Bluff Formations); TRc, Triassic Chinle Group; Psa, Permian San Andres Formation (including Glorieta Formation)]

Line no.	Form-ation	Data source*	Data identifier**	Latitude (NAD 83)	Longitude (NAD 83)	Date	NO_3 (as N, mg/L)	U (µg/L)	Ra 226 (pCi/L)	Ra 228 (pCi/L)	Ra 228 +226 (pCi/L)	Gross alpha (pCi/L)
31	Qa	Stone	15N.17W.13.3243	35.531	108.590	10/12/66	0.2	NA	NA	NA	NA	NA
32	Qa	Stone	15N.17W.13.3414	35.531	108.590	10/15/65	.4	NA	NA	NA	NA	NA
33	Qa	Stone	15N.17W.14.1	35.531	108.608	08/07/75	.6	NA	NA	NA	NA	NA
34	Qa	Stone	15N.17W.14.1A	35.531	108.608	08/07/75	.6	NA	NA	NA	NA	NA
35	Qa	Stone	15N.17W.14.2322B	35.531	108.608	09/17/75	.5	NA	NA	NA	NA	NA
36	Qa	Stone	15N.17W.15.1321	35.530	108.625	03/07/65	.2	NA	NA	NA	NA	NA
37	Qa	Stone	15N.17W.15.24142	35.530	108.625	03/19/65	29	NA	NA	NA	NA	NA
38	Qa	Stone	16N.15W.19.42	35.603	108.468	05/11/50	.1	NA	NA	NA	NA	NA
39	Qa	Stone	16N.15W.20.1134	35.603	108.450	08/30/49	2.2	NA	NA	NA	NA	NA
40	Qa	Stone	16N.16W.19.1	35.603	108.574	07/17/70	1.2	NA	NA	NA	NA	NA
41	Qa	Stone	18N.04W.06.	35.820	107.300	03/19/70	8.7	NA	NA	NA	NA	NA
42	Qa	Stone	18N.04W.22.21	35.777	107.247	12/14/50	.9	NA	NA	NA	NA	NA
43	Qa	Stone	18N.04W.22.231	35.777	107.247	01/04/64	.4	NA	NA	NA	NA	NA
44	Qa	Stone	19N.04W.09.	35.892	107.264	03/19/70	5.0	NA	NA	NA	NA	NA
45	Qa	Stone	20N.05W.23.3	35.949	107.335	07/26/54	.8	NA	NA	NA	NA	NA
46	Qa	Stone	16N.17W.25.1132	35.588	108.591	10/06/76	NA	2.1	NA	NA	NA	NA
47	Qa	Stone	11N.10W.26.321B	35.154	107.863	06/12/58	.1	NA	NA	NA	NA	NA
48	Qa	Stone	12N.10W.30.242	35.240	107.933	06/08/56	26	NA	NA	NA	NA	NA
49	Qa	Stone	12N.10W.30.242	35.240	107.933	05/07/57	20	NA	NA	NA	NA	NA
50	Qa	Stone	12N.11W.11.334	35.284	107.968	06/27/56	16	NA	NA	NA	NA	NA
51	Qa	Stone	12N.11W.11.334	35.284	107.968	05/09/57	14	NA	NA	NA	NA	NA
52	Qa	Stone	12N.11W.14.311	35.269	107.968	06/07/57	6.6	NA	NA	NA	NA	NA
53	Qa	Stone	12N.11W.14.311	35.269	107.968	10/21/44	36	NA	NA	NA	NA	NA
54	Qa	Stone	12N.11W.14.311	35.269	107.968	07/12/46	30	NA	NA	NA	NA	NA
55	Qa	Stone	12N.11W.15.211	35.269	107.985	05/08/57	16	NA	NA	NA	NA	NA
56	Qa	Stone	15N.17W.13.3141	35.531	108.590	10/15/65	.2	NA	NA	NA	NA	NA
57	Qa	Stone	15N.17W.13.3141	35.531	108.590	10/05/66	.2	NA	NA	NA	NA	NA
58	Qa	Stone	15N.17W.14.2324A	35.531	108.608	10/01/64	9.2	NA	NA	NA	NA	NA
59	Qa	Stone	15N.17W.14.2324A	35.531	108.608	09/10/69	6.2	NA	NA	NA	NA	NA
60	Qa	Stone	16N.17W.25.1132	35.588	108.591	06/22/54	13	NA	NA	NA	NA	NA

Table 4-1. Historical groundwater contaminants-of-concern data in the study area, 1942–2009.—Continued

[NAD 83, North American Datum of 1983; NO_3, nitrate or nitrate plus nitrite; N, nitrogen; mg/L, milligrams per liter; U, uranium; µg/L, micrograms per liter; Ra, radium; pCi/L, picocuries per liter; Qa, Quaternary alluvium; NA, not available; Kmf, Cretaceous Menefee Formation; Kpl, Cretaceous Point Lookout Formation; Kcc, Cretaceous Crevasse Canyon Formation; Kg, Cretaceous Gallup Formation; Km, Cretaceous Mancos Formation; Kd, Cretaceous Dakota Formation; Jm, Jurassic Morrison Formation; Je, Jurassic Entrada Complex (includes Entrada, Todilto, Summerville, and Bluff Formations); TRc, Triassic Chinle Group; Psa, Permian San Andres Formation (including Glorieta Formation)]

Line no.	Form-ation	Data source*	Data identifier**	Latitude (NAD 83)	Longitude (NAD 83)	Date	NO_3 (as N, mg/L)	U (µg/L)	Ra 226 (pCi/L)	Ra 228 (pCi/L)	Ra 228 +226 (pCi/L)	Gross alpha (pCi/L)
61	Qa	Stone	16N.17W.33.4223	35.574	108.645	09/24/53	0.3	NA	NA	NA	NA	NA
62	Qa	Stone	16N.17W.33.4223	35.574	108.645	03/26/74	13	NA	NA	NA	NA	NA
63	Qa	Stone	18N.09W.12.1	35.804	107.744	08/20/48	14	NA	NA	NA	NA	NA
64	Qa	Stone	18N.09W.12.1	35.804	107.744	07/27/64	1.1	NA	NA	NA	NA	NA
65	Qa	Stone	21N.10W.29.2	36.024	107.922	03/05/63	8.1	NA	NA	NA	NA	NA
66	Qa	Stone	21N.10W.29.2	36.024	107.922	04/18/64	7.5	NA	NA	NA	NA	NA
67	Qa	Stone	21N.10W.29.2	36.024	107.922	05/28/65	6.6	NA	NA	NA	NA	NA
68	Qa	Stone	21N.10W.29.2	36.024	107.922	01/23/66	8.1	NA	NA	NA	NA	NA
69	Qa	Stone	21N.10W.29.2	36.024	107.922	04/15/67	5.8	NA	NA	NA	NA	NA
70	Qa	Stone	21N.10W.29.2114	36.024	107.922	02/05/68	3.3	NA	NA	NA	NA	NA
71	Qa	Stone	21N.10W.29.2114	36.024	107.922	09/14/56	5.1	NA	NA	NA	NA	NA
72	Kmf	RHR	27	35.335	107.657	08/06/08	NA	4.9	NA	.03	.03	5.5
73	Kmf	RHR	27	35.335	107.657	11/13/08	NA	4.9	NA	NA	NA	5.8
74	Kmf	RHR	27	35.335	107.657	02/16/09	NA	5.1	NA	1.30	1.30	5.3
75	Kmf	RHR	27	35.335	107.657	05/19/09	NA	414	NA	NA	NA	11.1
76	Kmf	RHR	87	35.330	107.643	08/12/08	NA	2.5	.12	.39	.51	8.0
77	Kmf	RHR	87	35.330	107.643	11/12/08	.5	1.8	NA	NA	NA	8.4
78	Kmf	RHR	87	35.330	107.643	02/16/09	.8	1.6	NA	2.10	2.10	2.0
79	Kmf	RHR	87	35.330	107.643	05/19/09	NA	1.6	NA	NA	NA	7.3
80	Kmf	RHR	62	35.334	107.643	08/20/08	NA	4.8	NA	.77	.77	4.2
81	Kmf	RHR	62	35.334	107.643	11/11/08	NA	2.9	NA	NA	NA	5.5
82	Kmf	RHR	62	35.334	107.643	02/18/09	NA	1.6	.16	.85	1.01	3.1
83	Kmf	RHR	62	35.334	107.643	05/26/09	NA	1.7	.14	.70	.84	3.8
84	Kmf	RHR	100	35.320	107.693	08/21/08	NA	.4	.13	.79	.92	1.9
85	Kmf	RHR	100	35.320	107.693	11/08/08	.8	.9	.01	1.50	1.51	6.6
86	Kmf	RHR	100	35.320	107.693	02/11/09	NA	5.3	.12	.60	.72	6.3
87	Kmf	RHR	100	35.320	107.693	05/19/09	NA	2.4	.01	.58	.59	8.2
88	Kmf	RHR	7	35.368	107.659	09/17/08	1.0	.7	NA	.10	.10	6.9
89	Kmf	RHR	7	35.368	107.659	11/16/08	.9	.4	.89	.14	1.03	48.9
90	Kmf	RHR	7	35.368	107.659	02/16/09	1.0	NA	1.3	2.60	3.90	15.8

Table 4-1. Historical groundwater contaminants-of-concern data in the study area, 1942–2009.—Continued

[NAD 83, North American Datum of 1983; NO_3, nitrate or nitrate plus nitrite; N, nitrogen; mg/L, milligrams per liter; U, uranium; µg/L, micrograms per liter; Ra, radium; pCi/L, picocuries per liter; Qa, Quaternary alluvium; NA, not available; Kmf, Cretaceous Menefee Formation; Kpl, Cretaceous Point Lookout Formation; Kcc, Cretaceous Crevasse Canyon Formation; Kg, Cretaceous Gallup Formation; Km, Cretaceous Mancos Formation; Kd, Cretaceous Dakota Formation; Jm, Jurassic Morrison Formation; Je, Jurassic Entrada Complex (includes Entrada, Todilto, Summerville, and Bluff Formations); TRc, Triassic Chinle Group; Psa, Permian San Andres Formation (including Glorieta Formation)]

Line no.	Form-ation	Data source*	Data identifier**	Latitude (NAD 83)	Longitude (NAD 83)	Date	NO_3 (as N, mg/L)	U (µg/L)	Ra 226 (pCi/L)	Ra 228 (pCi/L)	Ra 228 +226 (pCi/L)	Gross alpha (pCi/L)
91	Kmf	RHR	7	35.368	107.659	05/18/09	0.7	NA	0.37	0.45	0.82	35.9
92	Kmf	Stone	13N.08W.24.334B	35.341	107.637	09/10/62	8.3	NA	NA	NA	NA	NA
93	Kmf	Stone	13N.08W.26.221	35.326	107.655	09/11/62	14	NA	NA	NA	NA	NA
94	Kmf	Stone	14N.05W.14.422	35.438	107.334	08/29/62	1.4	NA	NA	NA	NA	NA
95	Kmf	Stone	15N.06W.22.3123	35.514	107.460	10/22/62	1.0	NA	NA	NA	NA	NA
96	Kmf	Stone	15N.08W.21.4414	35.515	107.692	10/16/62	.7	NA	NA	NA	NA	NA
97	Kmf	Stone	15N.13W.08.	35.546	108.238	11/15/48	.4	NA	NA	NA	NA	NA
98	Kmf	Stone	15N.18W.19.244	35.515	108.786	06/10/55	.6	NA	NA	NA	NA	NA
99	Kmf	Stone	16N.05W.15.233	35.617	107.353	09/19/62	1.1	NA	NA	NA	NA	NA
100	Kmf	Stone	16N.07W.32.4141	35.573	107.602	10/15/62	.6	NA	NA	NA	NA	NA
101	Kmf	Stone	16N.08W.33.1341	35.573	107.691	10/02/62	.4	NA	NA	NA	NA	NA
102	Kmf	Stone	16N.11W.33.411	35.573	108.008	11/24/64	9.2	NA	NA	NA	NA	NA
103	Kmf	Stone	17N.08W.19.434	35.689	107.726	02/20/67	1.9	NA	NA	NA	NA	NA
104	Kmf	Stone	17N.11W.24.413	35.689	107.959	02/20/67	1.1	NA	NA	NA	NA	NA
105	Kmf	Stone	17N.11W.30.431	35.674	108.048	07/18/73	.6	NA	NA	NA	NA	NA
106	Kmf	Stone	18N.03W.01.23	35.820	107.104	12/14/50	.4	NA	NA	NA	NA	NA
107	Kmf	Stone	18N.04W.16.4	35.791	107.264	01/20/57	2.1	NA	NA	NA	NA	NA
108	Kmf	Stone	18N.05W.01.134	35.820	107.318	02/21/67	1.5	NA	NA	NA	NA	NA
109	Kmf	Stone	18N.05W.14.221	35.791	107.335	03/19/70	1.9	NA	NA	NA	NA	NA
110	Kmf	Stone	18N.06W.04.3421	35.820	107.478	02/26/71	.6	NA	NA	NA	NA	NA
111	Kmf	Stone	18N.09W.12.121	35.804	107.744	07/27/64	1.1	NA	NA	NA	NA	NA
112	Kmf	Stone	19N.02W.21.34	35.863	107.051	05/20/65	.2	NA	NA	NA	NA	NA
113	Kmf	Stone	19N.03W.34.34	35.834	107.140	12/12/50	143	NA	NA	NA	NA	NA
114	Kmf	Stone	19N.05W.36.1132	35.834	107.318	04/16/56	2.6	NA	NA	NA	NA	NA
115	Kmf	Stone	19N.06W.10.2111	35.892	107.460	04/16/56	2.2	NA	NA	NA	NA	NA
116	Kmf	Stone	19N.08W.34.2131	35.833	107.673	08/20/48	1.3	NA	NA	NA	NA	NA
117	Kmf	Stone	19N.09W.07.3324	35.891	107.833	08/27/70	.1	NA	NA	NA	NA	NA
118	Kmf	Stone	19N.09W.11.4433	35.891	107.762	08/20/48	1.3	NA	NA	NA	NA	NA
119	Kmf	Stone	19N.09W.35.13	35.833	107.762	02/20/67	2.4	NA	NA	NA	NA	NA
120	Kmf	Stone	19N.12W.05.	35.907	108.137	11/02/71	1.9	NA	NA	NA	NA	NA

Table 4-1. Historical groundwater contaminants-of-concern data in the study area, 1942–2009.—Continued

[NAD 83, North American Datum of 1983; NO_3, nitrate or nitrate plus nitrite; N, nitrogen; mg/L, milligrams per liter; U, uranium; µg/L, micrograms per liter; Ra, radium; pCi/L, picocuries per liter; Qa, Quaternary alluvium; NA, not available; Kmf, Cretaceous Menefee Formation; Kpl, Cretaceous Point Lookout Formation; Kcc, Cretaceous Crevasse Canyon Formation; Kg, Cretaceous Gallup Formation; Km, Cretaceous Mancos Formation; Kd, Cretaceous Dakota Formation; Jm, Jurassic Morrison Formation; Je, Jurassic Entrada Complex (includes Entrada, Todilto, Summerville, and Bluff Formations); TRc, Triassic Chinle Group; Psa, Permian San Andres Formation (including Glorieta Formation)]

Line no.	Form-ation	Data source*	Data identifier**	Latitude (NAD 83)	Longitude (NAD 83)	Date	NO_3 (as N, mg/L)	U (µg/L)	Ra 226 (pCi/L)	Ra 228 (pCi/L)	Ra 228 +226 (pCi/L)	Gross alpha (pCi/L)
121	Kmf	Stone	19N.12W.27.14	35.849	108.101	11/02/71	0.1	NA	NA	NA	NA	NA
122	Kmf	Stone	19N.13W.28.1	35.849	108.227	01/05/50	1.2	NA	NA	NA	NA	NA
123	Kmf	Stone	20N.07W.08.321	35.980	107.603	02/21/67	1.1	NA	NA	NA	NA	NA
124	Kmf	Stone	20N.09W.08.343	35.979	107.815	12/20/63	.1	NA	NA	NA	NA	NA
125	Kmf	Stone	20N.10W.01.22	35.994	107.850	01/24/64	.1	NA	NA	NA	NA	NA
126	Kmf	Stone	20N.12W.26.444	35.936	108.083	05/02/67	.9	NA	NA	NA	NA	NA
127	Kmf	Stone	20N.13W.07.31	35.980	108.263	09/13/49	1.3	NA	NA	NA	NA	NA
128	Kmf	Stone	21N.08W.25.3223	36.022	107.635	02/21/67	2.7	NA	NA	NA	NA	NA
129	Kmf	Stone	21N.12W.33.1222	36.010	108.120	04/02/74	4.3	NA	NA	NA	NA	NA
130	Kmf	Stone	16N.04W.18.444	35.617	107.300	07/27/78	NA	1.1	NA	NA	NA	NA
131	Kmf	Stone	15N.06W.20.121	35.515	107.495	10/03/62	1.2	NA	NA	NA	NA	NA
132	Kmf	Stone	18N.08W.09.111	35.804	107.691	12/04/72	2.5	NA	NA	NA	NA	NA
133	Kmf	Stone	18N.08W.09.111	35.804	107.691	02/20/67	2.4	NA	NA	NA	NA	NA
134	Kmf	Stone	18N.09W.12.1131	35.804	107.744	08/01/58	1.4	NA	NA	NA	NA	NA
135	Kmf	Stone	18N.09W.12.1131	35.804	107.744	12/07/72	1.2	NA	NA	NA	NA	NA
136	Kmf	Stone	19N.13W.13.444	35.878	108.173	01/04/52	2.7	NA	NA	NA	NA	NA
137	Kmf	Stone	19N.13W.13.444	35.878	108.173	11/02/71	.3	NA	NA	NA	NA	NA
138	Kpl	RHR	90	35.332	107.651	08/11/08	NA	NA	.24	2.10	2.34	.3
139	Kpl	RHR	90	35.332	107.651	11/10/08	NA	NA	.01	.32	.33	6.0
140	Kpl	RHR	90	35.332	107.651	02/16/09	NA	NA	NA	1.10	1.10	.4
141	Kpl	RHR	90	35.332	107.651	05/19/09	NA	NA	.36	.76	1.12	1.3
142	Kpl	RHR	22	35.343	107.664	08/21/08	NA	NA	.31	1.10	1.41	.9
143	Kpl	RHR	22	35.343	107.664	11/13/08	NA	NA	.24	.57	.81	.8
144	Kpl	RHR	22	35.343	107.664	02/11/09	NA	NA	.28	.22	.50	1.5
145	Kpl	RHR	22	35.343	107.664	05/19/09	NA	NA	.21	.60	.81	.6
146	Kpl	RHR	102	35.311	107.687	09/24/08	NA	NA	.08	NA	.08	1.5
147	Kpl	RHR	102	35.311	107.687	11/08/08	NA	NA	NA	1.60	1.60	.4
148	Kpl	RHR	102	35.311	107.687	02/11/09	NA	NA	.06	1.30	1.36	.5
149	Kpl	Stone	16N.06W.29.231	35.588	107.495	10/03/62	.9	NA	NA	NA	NA	NA
150	Kpl	Stone	16N.07W.13.2244	35.617	107.531	10/02/62	1.5	NA	NA	NA	NA	NA

Table 4-1. Historical groundwater contaminants-of-concern data in the study area, 1942–2009.—Continued

[NAD 83, North American Datum of 1983; NO_3, nitrate or nitrate plus nitrite; N, nitrogen; mg/L, milligrams per liter; U, uranium; µg/L, micrograms per liter; Ra, radium; pCi/L, picocuries per liter; Qa, Quaternary alluvium; NA, not available; Kmf, Cretaceous Menefee Formation; Kpl, Cretaceous Point Lookout Formation; Kcc, Cretaceous Crevasse Canyon Formation; Kg, Cretaceous Gallup Formation; Km, Cretaceous Mancos Formation; Kd, Cretaceous Dakota Formation; Jm, Jurassic Morrison Formation; Je, Jurassic Entrada Complex (includes Entrada, Todilto, Summerville, and Bluff Formations); TRc, Triassic Chinle Group; Psa, Permian San Andres Formation (including Glorieta Formation)]

Line no.	Form-ation	Data source*	Data identifier**	Latitude (NAD 83)	Longitude (NAD 83)	Date	NO_3 (as N, mg/L)	U (µg/L)	Ra 226 (pCi/L)	Ra 228 (pCi/L)	Ra 228 +226 (pCi/L)	Gross alpha (pCi/L)
151	Kpl	Stone	16N.08W.14.1114	35.617	107.655	10/02/62	0.5	NA	NA	NA	NA	NA
152	Kpl	Stone	16N.08W.20.1312	35.602	107.708	10/02/62	.8	NA	NA	NA	NA	NA
153	Kpl	Stone	16N.09W.22.4444	35.602	107.778	09/20/62	.8	NA	NA	NA	NA	NA
154	Kpl	Stone	16N.10W.22.212	35.602	107.883	09/19/62	.6	NA	NA	NA	NA	NA
155	Kpl	Stone	18N.11W.29.3111	35.762	108.030	04/06/53	.2	NA	NA	NA	NA	NA
156	Kpl	Stone	20N.02W.17.132	35.964	107.069	04/30/58	.4	NA	NA	NA	NA	NA
157	Kpl	Stone	20N.04W.34.4421	35.920	107.246	11/01/63	4.3	NA	NA	NA	NA	NA
158	Kpl	Stone	21N.01W.28.213	36.021	106.945	10/19/57	.2	NA	NA	NA	NA	NA
159	Kpl	Stone	21N.01W.29.24	36.017	106.972	10/24/55	.1	NA	NA	NA	NA	NA
160	Kpl	Stone	15N.09W.13.144	35.529	107.745	08/01/51	.1	NA	NA	NA	NA	NA
161	Kpl	Stone	15N.09W.13.144	35.529	107.745	10/04/62	.1	NA	NA	NA	NA	NA
162	Kpl	Stone	20N.02W.21.22	35.949	107.051	06/18/59	.4	NA	NA	NA	NA	NA
163	Kcc	Stone	14N.08W.04.3343	35.472	107.690	10/16/62	14	NA	NA	NA	NA	NA
164	Kcc	Stone	15N.09W.09.2442	35.544	107.796	09/12/62	2.7	NA	NA	NA	NA	NA
165	Kcc	Stone	16N.12W.16.23	35.617	108.114	05/19/55	.2	NA	NA	NA	NA	NA
166	Kcc	Stone	17N.11W.35.223	35.660	107.977	06/18/59	.2	NA	NA	NA	NA	NA
167	Kcc	Stone	17N.12W.03.41	35.733	108.101	08/03/49	1.8	NA	NA	NA	NA	NA
168	Kcc	Stone	17N.13W.11.33	35.718	108.190	12/03/51	1.4	NA	NA	NA	NA	NA
169	Kcc	Stone	18N.13W.23.3212	35.776	108.190	11/02/71	.3	NA	NA	NA	NA	NA
170	Kcc	Stone	18N.13W.01.4	35.820	108.173	08/03/49	2.8	NA	NA	NA	NA	NA
171	Kcc	Stone	18N.13W.01.4	35.820	108.173	11/02/71	.1	NA	NA	NA	NA	NA
172	Kcc	Stone	15N.06W.20.331	35.515	107.495	10/16/62	.2	NA	NA	NA	NA	NA
173	Kcc	Stone	15N.10W.06.2421	35.558	107.936	02/05/54	.1	NA	NA	NA	NA	NA
174	Kcc	Stone	15N.10W.06.2421	35.558	107.936	02/17/54	.1	NA	NA	NA	NA	NA
175	Kcc	Stone	15N.10W.06.2421	35.558	107.936	08/01/61	.2	NA	NA	NA	NA	NA
176	Kcc	Stone	15N.10W.13.1314	35.529	107.848	01/15/70	.6	NA	NA	NA	NA	NA
177	Kcc	Stone	15N.10W.13.1314	35.529	107.848	07/18/73	3.1	NA	NA	NA	NA	NA
178	Kcc	Stone	16N.13W.11.3413	35.632	108.185	03/18/54	.2	NA	NA	NA	NA	NA
179	Kcc	Stone	16N.13W.11.3413	35.632	108.185	07/11/61	1.1	NA	NA	NA	NA	NA
180	Kg	RHR	32	35.338	107.662	08/21/08	NA	NA	.13	1.20	1.33	2.2

Table 4-1. Historical groundwater contaminants-of-concern data in the study area, 1942–2009.—Continued

[NAD 83, North American Datum of 1983; NO_3, nitrate or nitrate plus nitrite; N, nitrogen; mg/L, milligrams per liter; U, uranium; µg/L, micrograms per liter; Ra, radium; pCi/L, picocuries per liter; Qa, Quaternary alluvium; NA, not available; Kmf, Cretaceous Menefee Formation; Kpl, Cretaceous Point Lookout Formation; Kcc, Cretaceous Crevasse Canyon Formation; Kg, Cretaceous Gallup Formation; Km, Cretaceous Mancos Formation; Kd, Cretaceous Dakota Formation; Jm, Jurassic Morrison Formation; Je, Jurassic Entrada Complex (includes Entrada, Todilto, Summerville, and Bluff Formations); TRc, Triassic Chinle Group; Psa, Permian San Andres Formation (including Glorieta Formation)]

Line no.	Form-ation	Data source*	Data identifier**	Latitude (NAD 83)	Longitude (NAD 83)	Date	NO_3 (as N, mg/L)	U (µg/L)	Ra 226 (pCi/L)	Ra 228 (pCi/L)	Ra 228 +226 (pCi/L)	Gross alpha (pCi/L)
181	Kg	RHR	16	35.359	107.703	08/25/08	0.6	NA	0.85	1.10	1.95	3.9
182	Kg	RHR	16	35.359	107.703	11/11/08	NA	NA	.32	NA	.32	5.7
183	Kg	RHR	16	35.359	107.703	02/12/09	1.1	NA	.71	.13	.84	6.0
184	Kg	RHR	16	35.359	107.703	05/19/09	.6	NA	.48	.53	1.01	8.8
185	Kg	Stone	14N.08W.15.244	35.442	107.672	10/01/62	5.8	NA	NA	NA	NA	NA
186	Kg	Stone	15N.10W.04.1311	35.558	107.901	10/22/64	.1	NA	NA	NA	NA	NA
187	Kg	Stone	15N.18W.08.320	35.545	108.769	02/24/56	.2	NA	NA	NA	NA	NA
188	Kg	Stone	15N.18W.13.324	35.531	108.698	12/10/53	11	NA	NA	NA	NA	NA
189	Kg	Stone	15N.18W.14.2223	35.531	108.716	11/28/55	.8	NA	NA	NA	NA	NA
190	Kg	Stone	15N.18W.14.2244	35.531	108.716	02/06/56	1.9	NA	NA	NA	NA	NA
191	Kg	Stone	15N.18W.16.341	35.530	108.751	12/13/55	.1	NA	NA	NA	NA	NA
192	Kg	Stone	15N.18W.18.3444	35.530	108.786	06/22/55	.6	NA	NA	NA	NA	NA
193	Kg	Stone	15N.18W.24.23	35.516	108.698	01/02/56	40	NA	NA	NA	NA	NA
194	Kg	Stone	15N.18W.30.3232	35.501	108.786	06/10/55	.1	NA	NA	NA	NA	NA
195	Kg	Stone	16N.05W.19.414	35.602	107.407	09/19/62	.1	NA	NA	NA	NA	NA
196	Kg	Stone	16N.07W.26.2214	35.588	107.549	10/02/62	1.8	NA	NA	NA	NA	NA
197	Kg	Stone	16N.18W.07.423	35.630	108.785	01/31/68	.1	NA	NA	NA	NA	NA
198	Kg	Stone	16N.18W.17.122A	35.616	108.767	01/12/69	.2	NA	NA	NA	NA	NA
199	Kg	Stone	16N.18W.32.44	35.574	108.768	12/06/55	.1	NA	NA	NA	NA	NA
200	Kg	Stone	17N.12W.33.244	35.660	108.119	03/10/70	.3	NA	NA	NA	NA	NA
201	Kg	Stone	15N.10W.06.2421	35.558	107.936	07/18/73	.1	NA	NA	NA	NA	NA
202	Kg	Stone	15N.10W.13.1314	35.529	107.848	09/18/62	.4	NA	NA	NA	NA	NA
203	Kg	Stone	15N.18W.13.1134A	35.531	108.698	12/06/48	.4	NA	NA	NA	NA	NA
204	Kg	Stone	15N.18W.13.1134A	35.531	108.698	11/28/55	.4	NA	NA	NA	NA	NA
205	Kg	Stone	15N.18W.14.144	35.531	108.716	02/06/56	1.9	NA	NA	NA	NA	NA
206	Kg	Stone	15N.18W.20.211	35.515	108.769	09/15/57	.1	NA	NA	NA	NA	NA
207	Kg	Stone	15N.18W.20.211	35.515	108.769	09/24/57	.1	NA	NA	NA	NA	NA
208	Kg	Stone	15N.18W.20.2211	35.515	108.769	05/19/57	.1	NA	NA	NA	NA	NA
209	Kg	Stone	16N.11W.17.4322	35.616	108.026	02/12/73	.6	NA	NA	NA	NA	NA
210	Kg	Stone	16N.18W.17.122	35.616	108.767	03/04/68	.3	NA	NA	NA	NA	NA

Table 4-1. Historical groundwater contaminants-of-concern data in the study area, 1942–2009.—Continued

[NAD 83, North American Datum of 1983; NO_3, nitrate or nitrate plus nitrite; N, nitrogen; mg/L, milligrams per liter; U, uranium; µg/L, micrograms per liter; Ra, radium; pCi/L, picocuries per liter; Qa, Quaternary alluvium; NA, not available; Kmf, Cretaceous Menefee Formation; Kpl, Cretaceous Point Lookout Formation; Kcc, Cretaceous Crevasse Canyon Formation; Kg, Cretaceous Gallup Formation; Km, Cretaceous Mancos Formation; Kd, Cretaceous Dakota Formation; Jm, Jurassic Morrison Formation; Je, Jurassic Entrada Complex (includes Entrada, Todilto, Summerville, and Bluff Formations); TRc, Triassic Chinle Group; Psa, Permian San Andres Formation (including Glorieta Formation)]

Line no.	Form-ation	Data source*	Data identifier**	Latitude (NAD 83)	Longitude (NAD 83)	Date	NO_3 (as N, mg/L)	U (µg/L)	Ra 226 (pCi/L)	Ra 228 (pCi/L)	Ra 228 +226 (pCi/L)	Gross alpha (pCi/L)
211	Kg	Stone	16N.18W.17.122	35.616	108.767	03/09/68	0.8	NA	NA	NA	NA	NA
212	Kg	Stone	16N.18W.17.122	35.616	108.767	03/09/68	.2	NA	NA	NA	NA	NA
213	Kg	Stone	16N.18W.17.122	35.616	108.767	03/10/68	.3	NA	NA	NA	NA	NA
214	Kg	Stone	16N.18W.17.122	35.616	108.767	03/12/68	.4	NA	NA	NA	NA	NA
215	Kg	Stone	16N.18W.17.122	35.616	108.767	03/13/68	.6	NA	NA	NA	NA	NA
216	Kg	Stone	16N.18W.17.122	35.616	108.767	03/13/68	1.4	NA	NA	NA	NA	NA
217	Kg	Stone	16N.18W.32.211	35.574	108.768	01/24/69	.2	NA	NA	NA	NA	NA
218	Kg	Stone	17N.12W.30.4111	35.675	108.154	08/02/51	.2	NA	NA	NA	NA	NA
219	Km	Stone	16N.15W.20.1314	35.603	108.450	11/18/71	.1	NA	NA	NA	NA	NA
220	Km	Stone	16N.15W.20.32	35.603	108.450	08/31/49	24	NA	NA	NA	NA	NA
221	Kd	Stone	15N.12W.19.22	35.516	108.149	05/21/56	.4	NA	NA	NA	NA	NA
222	Kd	Stone	15N.12W.19.223	35.516	108.149	09/02/49	2.3	NA	NA	NA	NA	NA
223	Kd	Stone	15N.13W.07.33	35.546	108.255	11/19/48	.3	NA	NA	NA	NA	NA
224	Kd	Stone	16N.14W.21.3334	35.603	108.326	03/20/74	4.9	NA	NA	NA	NA	NA
225	Kd	Stone	16N.15W.11.3323	35.632	108.397	02/13/74	.2	NA	NA	NA	NA	NA
226	Kd	Stone	16N.16W.01.2344	35.646	108.485	06/09/55	1.5	NA	NA	NA	NA	NA
227	Kd	Stone	16N.16W.15.4322	35.617	108.521	02/07/74	52	NA	NA	NA	NA	NA
228	Kd	Stone	16N.17W.15.2324	35.617	108.626	03/26/74	5.6	NA	NA	NA	NA	NA
229	Kd	Stone	14N.09W.17.300	35.442	107.814	08/08/62	.2	NA	NA	NA	NA	NA
230	Kd	Stone	14N.09W.17.300	35.442	107.814	08/08/62	.2	NA	NA	NA	NA	NA
231	Kd	Stone	14N.09W.17.300	35.442	107.814	08/08/62	.1	NA	NA	NA	NA	NA
232	Kd	Stone	14N.09W.18.243	35.442	107.831	04/30/63	1.0	NA	NA	NA	NA	NA
233	Kd	Stone	14N.09W.18.243	35.442	107.831	08/30/63	1.0	NA	NA	NA	NA	NA
234	Kd	Stone	14N.09W.28.233	35.414	107.795	10/10/57	.3	NA	NA	NA	NA	NA
235	Kd	Stone	14N.09W.28.233	35.414	107.795	10/10/57	.5	NA	NA	NA	NA	NA
236	Kd	Stone	14N.09W.36.313	35.398	107.742	04/24/63	.3	NA	NA	NA	NA	NA
237	Kd	Stone	14N.09W.36.313	35.398	107.742	05/06/63	.7	NA	NA	NA	NA	NA
238	Kd	Stone	15N.06W.20.121	35.515	107.495	02/10/54	.5	NA	NA	NA	NA	NA
239	Kd	Stone	15N.06W.20.121	35.515	107.495	05/15/54	.2	NA	NA	NA	NA	NA
240	Kd	Stone	15N.06W.20.121	35.515	107.495	10/30/68	.5	NA	NA	NA	NA	NA

Table 4-1. Historical groundwater contaminants-of-concern data in the study area, 1942–2009.—Continued

[NAD 83, North American Datum of 1983; NO_3, nitrate or nitrate plus nitrite; N, nitrogen; mg/L, milligrams per liter; U, uranium; µg/L, micrograms per liter; Ra, radium; pCi/L, picocuries per liter; Qa, Quaternary alluvium; NA, not available; Kmf, Cretaceous Menefee Formation; Kpl, Cretaceous Point Lookout Formation; Kcc, Cretaceous Crevasse Canyon Formation; Kg, Cretaceous Gallup Formation; Km, Cretaceous Mancos Formation; Kd, Cretaceous Dakota Formation; Jm, Jurassic Morrison Formation; Je, Jurassic Entrada Complex (includes Entrada, Todilto, Summerville, and Bluff Formations); TRc, Triassic Chinle Group; Psa, Permian San Andres Formation (including Glorieta Formation)]

Line no.	Form-ation	Data source*	Data identifier**	Latitude (NAD 83)	Longitude (NAD 83)	Date	NO_3 (as N, mg/L)	U (µg/L)	Ra 226 (pCi/L)	Ra 228 (pCi/L)	Ra 228 +226 (pCi/L)	Gross alpha (pCi/L)
241	Kd	Stone	15N.11W.17.1111	35.529	108.026	10/23/52	0.2	NA	NA	NA	NA	NA
242	Kd	Stone	15N.11W.17.1111	35.529	108.026	07/31/61	.4	NA	NA	NA	NA	NA
243	Kd	Stone	15N.12W.17.123	35.531	108.131	04/08/53	.2	NA	NA	NA	NA	NA
244	Kd	Stone	15N.12W.17.123A	35.531	108.131	05/21/56	.4	NA	NA	NA	NA	NA
245	Kd	Stone	16N.14W.15.1342	35.617	108.309	11/02/51	.6	NA	NA	NA	NA	NA
246	Kd	Stone	16N.14W.15.1342	35.617	108.309	03/20/74	4.3	NA	NA	NA	NA	NA
247	Kd	Stone	16N.15W.17.1431	35.618	108.450	02/23/70	.6	NA	NA	NA	NA	NA
248	Kd	Stone	16N.15W.17.1431	35.618	108.450	07/29/70	.6	NA	NA	NA	NA	NA
249	Kd	Stone	16N.15W.17.1431	35.618	108.450	11/23/70	.6	NA	NA	NA	NA	NA
250	Kd	Stone	16N.15W.17.1431	35.618	108.450	05/01/72	.6	NA	NA	NA	NA	NA
251	Kd	Stone	16N.15W.17.1431	35.618	108.450	02/13/74	.2	NA	NA	NA	NA	NA
252	Kd	Stone	17N.12W.30.142	35.675	108.154	12/12/48	.5	NA	NA	NA	NA	NA
253	Kd	Stone	17N.12W.30.142	35.675	108.154	10/13/64	.1	NA	NA	NA	NA	NA
254	Kd	Stone	14N.09W.17.300	35.442	107.814	08/30/63	NA	3.4	NA	NA	NA	NA
255	Jm	Stone	14N.09W.34.422	35.399	107.777	04/24/63	.2	NA	NA	NA	NA	NA
256	Jm	Stone	14N.10W.11.434A	35.457	107.867	10/18/60	1.1	NA	NA	NA	NA	NA
257	Jm	Stone	15N.11W.29.1132	35.500	108.026	09/30/76	.1	NA	NA	NA	NA	NA
258	Jm	Stone	16W.16W.30.3431	35.588	108.574	05/02/72	20	NA	NA	NA	NA	NA
259	Jm	Stone	16N.14W.33.2223	35.574	108.326	02/22/52	.5	NA	NA	NA	NA	NA
260	Jm	Stone	16N.14W.33.2223	35.574	108.326	05/14/53	.1	NA	NA	NA	NA	NA
261	Jm	Stone	16N.14W.33.2223	35.574	108.326	03/06/73	.6	NA	NA	NA	NA	NA
262	Jm	RHR	116	35.345	107.786	08/19/08	19.7	10.9	.35	.77	1.12	22.6
263	Jm	RHR	116	35.345	107.786	11/13/08	21.3	10.6	.37	.50	.87	17.9
264	Jm	RHR	116	35.345	107.786	02/10/09	20.1	12.1	.27	.58	.85	23.7
265	Jm	RHR	116	35.345	107.786	05/21/09	18.2	10.3	.47	1.30	1.77	20.6
266	Jm	RHR	114	35.346	107.785	09/18/08	24.3	19.9	.96	.79	1.75	50.4
267	Jm	RHR	114	35.346	107.785	02/18/09	19.2	21.7	.45	.90	1.35	50.3
268	Jm	RHR	114	35.346	107.785	05/26/09	23.3	20.8	.47	.50	.97	36.0
269	Jm	RHR	113	35.347	107.783	09/22/08	24.6	15.8	.26	NA	.26	25.4
270	Jm	RHR	113	35.347	107.783	11/10/08	19.8	15.5	.27	.35	.62	28.2

Table 4-1. Historical groundwater contaminants-of-concern data in the study area, 1942–2009.—Continued

[NAD 83, North American Datum of 1983; NO_3, nitrate or nitrate plus nitrite; N, nitrogen; mg/L, milligrams per liter; U, uranium; µg/L, micrograms per liter; Ra, radium; pCi/L, picocuries per liter; Qa, Quaternary alluvium; NA, not available; Kmf, Cretaceous Menefee Formation; Kpl, Cretaceous Point Lookout Formation; Kcc, Cretaceous Crevasse Canyon Formation; Kg, Cretaceous Gallup Formation; Km, Cretaceous Mancos Formation; Kd, Cretaceous Dakota Formation; Jm, Jurassic Morrison Formation; Je, Jurassic Entrada Complex (includes Entrada, Todilto, Summerville, and Bluff Formations); TRc, Triassic Chinle Group; Psa, Permian San Andres Formation (including Glorieta Formation)]

Line no.	Form-ation	Data source*	Data identifier**	Latitude (NAD 83)	Longitude (NAD 83)	Date	NO_3 (as N, mg/L)	U (µg/L)	Ra 226 (pCi/L)	Ra 228 (pCi/L)	Ra 228 +226 (pCi/L)	Gross alpha (pCi/L)
271	Jm	RHR	113	35.347	107.783	02/12/09	22.3	16.9	0.31	0.32	0.63	21.0
272	Jm	RHR	113	35.347	107.783	05/26/09	23.9	16.1	NA	.53	.53	25.4
273	Jm	Stone	13N.09W.15.343	35.355	107.778	02/13/58	7.7	NA	NA	NA	NA	NA
274	Jm	Stone	14N.09W.18.400	35.442	107.831	08/30/63	.2	NA	NA	NA	NA	NA
275	Jm	Stone	14N.09W.29.312	35.413	107.813	08/13/59	15	NA	NA	NA	NA	NA
276	Jm	Stone	14N.09W.30.2213	35.414	107.831	05/03/63	.2	NA	NA	NA	NA	NA
277	Jm	Stone	14N.10W.22.214	35.428	107.884	03/19/57	4.6	NA	NA	NA	NA	NA
278	Jm	Stone	14N.11W.03.3334	35.471	107.991	03/13/57	4.0	NA	NA	NA	NA	NA
279	Jm	Stone	16N.11W.33.332	35.573	108.008	09/08/72	.1	NA	NA	NA	NA	NA
280	Jm	Stone	16N.14W.33.22	35.574	108.326	03/06/73	.6	NA	NA	NA	NA	NA
281	Jm	Stone	16N.16W.17.2114	35.617	108.556	02/07/74	2.4	NA	NA	NA	NA	NA
282	Jm	Stone	16N.17W.21.3442	35.603	108.644	03/26/74	3.7	NA	NA	NA	NA	NA
283	Jm	Stone	14N.09W.18.400	35.442	107.831	08/30/63	NA	55	NA	NA	NA	NA
284	Jm	Stone	14N.09W.29.312	35.413	107.813	08/13/59	NA	12	NA	NA	NA	NA
285	Jm	Stone	14N.09W.18.243	35.442	107.831	10/17/62	1.2	NA	NA	NA	NA	NA
286	Jm	Stone	14N.10W.22.2	35.428	107.884	08/08/62	.2	NA	NA	NA	NA	NA
287	Jm	Stone	14N.10W.22.2	35.428	107.884	08/08/62	4.9	NA	NA	NA	NA	NA
288	Jm	Stone	14N.10W.22.2	35.428	107.884	08/08/62	3.9	NA	NA	NA	NA	NA
289	Jm	Stone	14N.10W.24.400	35.428	107.849	08/18/59	.1	NA	NA	NA	NA	NA
290	Jm	Stone	15N.12W.17.123A	35.531	108.131	05/04/63	.7	NA	NA	NA	NA	NA
291	Je	Stone	13N.09W.29.143	35.327	107.813	02/28/58	25	NA	NA	NA	NA	NA
292	Je	Stone	13N.10W.08.211	35.370	107.920	02/02/67	17	NA	NA	NA	NA	NA
293	Je	Stone	14N.11W.19.124	35.428	108.043	08/04/61	4.8	NA	NA	NA	NA	NA
294	Je	Stone	14N.12W.09.221	35.458	108.114	09/05/62	5.7	NA	NA	NA	NA	NA
295	Je	Stone	14N.12W.14.143	35.443	108.078	09/05/62	20	NA	NA	NA	NA	NA
296	Je	Stone	14N.12W.17.3333	35.444	108.131	11/15/48	8.6	NA	NA	NA	NA	NA
297	Je	Stone	15N.13W.12.144	35.546	108.167	07/11/61	1.0	NA	NA	NA	NA	NA
298	Je	Stone	15N.13W.22.1111	35.517	108.202	03/20/74	5.0	NA	NA	NA	NA	NA
299	Je	Stone	15N.14W.13.413	35.531	108.273	06/10/70	5.0	NA	NA	NA	NA	NA
300	Je	Stone	16N.14W.33.234	35.574	108.326	11/05/73	1.2	NA	NA	NA	NA	NA

Table 4-1. Historical groundwater contaminants-of-concern data in the study area, 1942–2009.—Continued

[NAD 83, North American Datum of 1983; NO_3, nitrate or nitrate plus nitrite; N, nitrogen; mg/L, milligrams per liter; U, uranium; µg/L, micrograms per liter; Ra, radium; pCi/L, picocuries per liter; Qa, Quaternary alluvium; NA, not available; Kmf, Cretaceous Menefee Formation; Kpl, Cretaceous Point Lookout Formation; Kcc, Cretaceous Crevasse Canyon Formation; Kg, Cretaceous Gallup Formation; Km, Cretaceous Mancos Formation; Kd, Cretaceous Dakota Formation; Jm, Jurassic Morrison Formation; Je, Jurassic Entrada Complex (includes Entrada, Todilto, Summerville, and Bluff Formations); TRc, Triassic Chinle Group; Psa, Permian San Andres Formation (including Glorieta Formation)]

Line no.	Form-ation	Data source*	Data identifier**	Latitude (NAD 83)	Longitude (NAD 83)	Date	NO_3 (as N, mg/L)	U (µg/L)	Ra 226 (pCi/L)	Ra 228 (pCi/L)	Ra 228 +226 (pCi/L)	Gross alpha (pCi/L)
301	Je	Stone	16W.16W.25.2344	35.588	108.486	02/13/74	5.5	NA	NA	NA	NA	NA
302	Je	Stone	13N.10W.18.4113	35.356	107.938	11/15/63	.7	NA	NA	NA	NA	NA
303	Je	Stone	13N.10W.18.4113	35.356	107.938	04/26/72	13	NA	NA	NA	NA	NA
304	Je	Stone	15N.13W.22.1111	35.517	108.202	05/08/64	1.2	NA	NA	NA	NA	NA
305	Je	Stone	15N.13W.22.1111	35.517	108.202	09/24/70	.6	NA	NA	NA	NA	NA
306	Je	Stone	15N.17W.14.4224	35.531	108.608	10/15/65	.3	NA	NA	NA	NA	NA
307	Je	Stone	15N.17W.14.4224	35.531	108.608	09/30/66	.6	NA	NA	NA	NA	NA
308	TRc	Stone	12N.10W.23.233A	35.254	107.862	07/12/46	4.4	NA	NA	NA	NA	NA
309	TRc	Stone	12N.10W.33.444	35.225	107.898	06/28/56	2.4	NA	NA	NA	NA	NA
310	TRc	Stone	12N.10W.34.412	35.225	107.880	08/28/56	.6	NA	NA	NA	NA	NA
311	TRc	Stone	13N.10W.20.114	35.341	107.920	07/23/76	.3	NA	NA	NA	NA	NA
312	TRc	Stone	13N.11W.07.433	35.370	108.043	06/24/48	5.6	NA	NA	NA	NA	NA
313	TRc	Stone	13N.11W.08.2211	35.370	108.026	06/23/48	5.5	NA	NA	NA	NA	NA
314	TRc	Stone	13N.12W.10.2444	35.370	108.096	08/23/67	77	NA	NA	NA	NA	NA
315	TRc	Stone	13N.12W.11.32	35.370	108.079	06/23/48	.5	NA	NA	NA	NA	NA
316	TRc	Stone	14N.12W.20.111	35.429	108.131	05/11/50	1.1	NA	NA	NA	NA	NA
317	TRc	Stone	14N.13W.20.4323	35.430	108.238	07/12/61	1.1	NA	NA	NA	NA	NA
318	TRc	Stone	14N.13W.33.141	35.401	108.221	12/06/48	10	NA	NA	NA	NA	NA
319	TRc	Stone	14N.13W.33.314	35.401	108.221	12/06/48	9.3	NA	NA	NA	NA	NA
320	TRc	Stone	14N.15W.04.1134	35.473	108.432	05/14/69	.6	NA	NA	NA	NA	NA
321	TRc	Stone	15N.15W.31.1242	35.488	108.468	06/04/68	.5	NA	NA	NA	NA	NA
322	TRc	Stone	15N.16W.27.2312	35.502	108.521	04/03/52	.5	NA	NA	NA	NA	NA
323	TRc	Stone	12N.10W.34.2141	35.225	107.880	05/07/57	.2	NA	NA	NA	NA	NA
324	TRc	Stone	12N.10W.34.2141	35.225	107.880	07/17/56	14	NA	NA	NA	NA	NA
325	TRc	Stone	12N.10W.34.2141	35.225	107.880	04/20/65	2.0	NA	NA	NA	NA	NA
326	TRc	Stone	13N.10W.18.212	35.356	107.938	06/18/76	.1	NA	NA	NA	NA	NA
327	TRc	Stone	14N.13W.25.1334	35.415	108.167	03/01/66	1.9	NA	NA	NA	NA	NA
328	TRc	Stone	14N.13W.25.1334	35.415	108.167	09/03/71	.1	NA	NA	NA	NA	NA
329	TRc	Stone	14N.13W.28.1234	35.415	108.221	12/03/48	.9	NA	NA	NA	NA	NA
330	TRc	Stone	14N.13W.33.124	35.401	108.221	08/18/48	4.5	NA	NA	NA	NA	NA

Table 4-1. Historical groundwater contaminants-of-concern data in the study area, 1942–2009.—Continued

[NAD 83, North American Datum of 1983; NO_3, nitrate or nitrate plus nitrite; N, nitrogen; mg/L, milligrams per liter; U, uranium; µg/L, micrograms per liter; Ra, radium; pCi/L, picocuries per liter; Qa, Quaternary alluvium; NA, not available; Kmf, Cretaceous Menefee Formation; Kpl, Cretaceous Point Lookout Formation; Kcc, Cretaceous Crevasse Canyon Formation; Kg, Cretaceous Gallup Formation; Km, Cretaceous Mancos Formation; Kd, Cretaceous Dakota Formation; Jm, Jurassic Morrison Formation; Je, Jurassic Entrada Complex (includes Entrada, Todilto, Summerville, and Bluff Formations); TRc, Triassic Chinle Group; Psa, Permian San Andres Formation (including Glorieta Formation)]

Line no.	Form-ation	Data source*	Data identifier**	Latitude (NAD 83)	Longitude (NAD 83)	Date	NO_3 (as N, mg/L)	U (µg/L)	Ra 226 (pCi/L)	Ra 228 (pCi/L)	Ra 228 +226 (pCi/L)	Gross alpha (pCi/L)
331	TRc	Stone	14N.13W.33.124	35.401	108.221	04/03/53	1.4	NA	NA	NA	NA	NA
332	TRc	Stone	14N.13W.33.124	35.401	108.221	09/30/64	.1	NA	NA	NA	NA	NA
333	TRc	Stone	15N.15W.20.313	35.517	108.449	03/01/58	.6	NA	NA	NA	NA	NA
334	TRc	Stone	15N.15W.20.313	35.517	108.449	06/15/66	.5	NA	NA	NA	NA	NA
335	TRc	Stone	15N.15W.20.313	35.517	108.449	10/24/67	.6	NA	NA	NA	NA	NA
336	Psa	Stone	11N.10W.04.333	35.211	107.898	08/23/66	33	NA	NA	NA	NA	NA
337	Psa	Stone	12N.10W.07.1433	35.284	107.933	06/27/56	.3	NA	NA	NA	NA	NA
338	Psa	Stone	12N.10W.26.242	35.240	107.862	05/22/58	1.2	NA	NA	NA	NA	NA
339	Psa	Stone	12N.10W.26.3222	35.240	107.862	10/15/56	3.2	NA	NA	NA	NA	NA
340	Psa	Stone	12N.10W.27.4311	35.240	107.880	07/25/56	6.9	NA	NA	NA	NA	NA
341	Psa	Stone	12N.10W.30.421	35.240	107.933	05/07/57	26	NA	NA	NA	NA	NA
342	Psa	Stone	12N.10W.30.433	35.240	107.933	10/21/44	32	NA	NA	NA	NA	NA
343	Psa	Stone	12N.11W.24.411	35.255	107.950	04/23/52	15	NA	NA	NA	NA	NA
344	Psa	Stone	13N.12W.34.332	35.313	108.097	09/04/62	.1	NA	NA	NA	NA	NA
345	Psa	Stone	14N.10W.22.414	35.428	107.884	11/21/56	.6	NA	NA	NA	NA	NA
346	Psa	Stone	14N.15W.01.3134	35.473	108.379	01/20/50	.5	NA	NA	NA	NA	NA
347	Psa	Stone	14N.15W.14.3423	35.444	108.397	01/20/50	.3	NA	NA	NA	NA	NA
348	Psa	Stone	14N.15W.28.1434	35.415	108.432	01/20/50	.5	NA	NA	NA	NA	NA
349	Psa	Stone	15N.17W.13.1124	35.531	108.590	05/09/50	.1	NA	NA	NA	NA	NA
350	Psa	Stone	15N.17W.13.222	35.531	108.590	10/01/64	.1	NA	NA	NA	NA	NA
351	Psa	Stone	15N.17W.16.21	35.530	108.644	08/06/53	.2	NA	NA	NA	NA	NA
352	Psa	Stone	15N.17W.16.2222A	35.530	108.644	08/06/53	.4	NA	NA	NA	NA	NA
353	Psa	Stone	15N.17W.16.3131	35.530	108.644	06/12/52	.2	NA	NA	NA	NA	NA
354	Psa	Stone	15N.17W.16.3131A	35.530	108.644	12/31/57	.2	NA	NA	NA	NA	NA
355	Psa	Stone	11N.10W.04.311	35.211	107.898	07/17/56	14	NA	NA	NA	NA	NA
356	Psa	Stone	11N.10W.04.311	35.211	107.898	06/07/57	17	NA	NA	NA	NA	NA
357	Psa	Stone	11N.10W.04.311	35.211	107.898	07/29/68	18	NA	NA	NA	NA	NA
358	Psa	Stone	11N.10W.04.311	35.211	107.898	07/24/56	19	NA	NA	NA	NA	NA
359	Psa	Stone	11N.10W.16.121	35.182	107.898	07/12/46	27	NA	NA	NA	NA	NA
360	Psa	Stone	11N.10W.16.121A	35.182	107.898	07/17/56	13	NA	NA	NA	NA	NA

Table 4-1. Historical groundwater contaminants-of-concern data in the study area, 1942–2009.—Continued

[NAD 83, North American Datum of 1983; NO_3, nitrate or nitrate plus nitrite; N, nitrogen; mg/L, milligrams per liter; U, uranium; µg/L, micrograms per liter; Ra, radium; pCi/L, picocuries per liter; Qa, Quaternary alluvium; NA, not available; Kmf, Cretaceous Menefee Formation; Kpl, Cretaceous Point Lookout Formation; Kcc, Cretaceous Crevasse Canyon Formation; Kg, Cretaceous Gallup Formation; Km, Cretaceous Mancos Formation; Kd, Cretaceous Dakota Formation; Jm, Jurassic Morrison Formation; Je, Jurassic Entrada Complex (includes Entrada, Todilto, Summerville, and Bluff Formations); TRc, Triassic Chinle Group; Psa, Permian San Andres Formation (including Glorieta Formation)]

Line no.	Form-ation	Data source*	Data identifier**	Latitude (NAD 83)	Longitude (NAD 83)	Date	NO_3 (as N, mg/L)	U (µg/L)	Ra 226 (pCi/L)	Ra 228 (pCi/L)	Ra 228 +226 (pCi/L)	Gross alpha (pCi/L)
361	Psa	Stone	11N.10W.16.121A	35.182	107.898	08/15/62	15	NA	NA	NA	NA	NA
362	Psa	Stone	11N.10W.16.121A	35.182	107.898	08/19/63	14	NA	NA	NA	NA	NA
363	Psa	Stone	11N.10W.16.121A	35.182	107.898	08/22/66	14	NA	NA	NA	NA	NA
364	Psa	Stone	11N.10W.16.121A	35.182	107.898	07/29/68	16	NA	NA	NA	NA	NA
365	Psa	Stone	11N.10W.26.321C	35.154	107.863	12/15/58	1.0	NA	NA	NA	NA	NA
366	Psa	Stone	12N.10W.23.233	35.254	107.862	07/12/46	.6	NA	NA	NA	NA	NA
367	Psa	Stone	12N.10W.27.333	35.240	107.880	10/06/54	11	NA	NA	NA	NA	NA
368	Psa	Stone	12N.10W.27.333	35.240	107.880	07/17/56	9.5	NA	NA	NA	NA	NA
369	Psa	Stone	12N.10W.27.333	35.240	107.880	05/07/57	9.1	NA	NA	NA	NA	NA
370	Psa	Stone	12N.10W.27.333	35.240	107.880	04/20/65	13	NA	NA	NA	NA	NA
371	Psa	Stone	12N.10W.29.434A	35.240	107.916	06/28/56	31	NA	NA	NA	NA	NA
372	Psa	Stone	12N.10W.30.1121	35.240	107.933	07/18/56	32	NA	NA	NA	NA	NA
373	Psa	Stone	12N.10W.30.1121	35.240	107.933	05/08/57	58	NA	NA	NA	NA	NA
374	Psa	Stone	12N.10W.30.412	35.240	107.933	05/10/46	32	NA	NA	NA	NA	NA
375	Psa	Stone	12N.10W.30.421	35.240	107.933	07/18/56	27	NA	NA	NA	NA	NA
376	Psa	Stone	12N.10W.32.111	35.225	107.915	07/12/46	21	NA	NA	NA	NA	NA
377	Psa	Stone	12N.10W.32.111	35.225	107.915	06/15/55	22	NA	NA	NA	NA	NA
378	Psa	Stone	12N.10W.32.111	35.225	107.915	07/18/56	14	NA	NA	NA	NA	NA
379	Psa	Stone	12N.11W.10.4312	35.283	107.985	05/10/46	3.6	NA	NA	NA	NA	NA
380	Psa	Stone	12N.11W.15.211	35.269	107.985	06/27/56	7.0	NA	NA	NA	NA	NA
381	Psa	Stone	12N.11W.15.211	35.269	107.985	05/06/57	6.6	NA	NA	NA	NA	NA
382	Psa	Stone	12N.11W.23.231	35.255	107.968	06/04/47	18	NA	NA	NA	NA	NA
383	Psa	Stone	12N.11W.23.231	35.255	107.968	10/28/52	47	NA	NA	NA	NA	NA
384	Psa	Stone	12N.11W.23.231	35.255	107.968	06/27/56	76	NA	NA	NA	NA	NA
385	Psa	Stone	12N.11W.23.231	35.255	107.968	07/18/56	75	NA	NA	NA	NA	NA
386	Psa	Stone	12N.11W.24.233	35.255	107.950	07/18/56	19	NA	NA	NA	NA	NA
387	Psa	Stone	12N.11W.24.334	35.255	107.950	05/07/57	56	NA	NA	NA	NA	NA
388	Psa	Stone	12N.11W.24.334	35.255	107.950	06/28/56	13	NA	NA	NA	NA	NA
389	Psa	Stone	12N.11W.24.334	35.255	107.950	06/07/57	15	NA	NA	NA	NA	NA
390	Psa	Stone	12N.11W.25.122	35.240	107.950	07/18/56	18	NA	NA	NA	NA	NA

Table 4-1. Historical groundwater contaminants-of-concern data in the study area, 1942–2009.—Continued

[NAD 83, North American Datum of 1983; NO_3, nitrate or nitrate plus nitrite; N, nitrogen; mg/L, milligrams per liter; U, uranium; µg/L, micrograms per liter; Ra, radium; pCi/L, picocuries per liter; Qa, Quaternary alluvium; NA, not available; Kmf, Cretaceous Menefee Formation; Kpl, Cretaceous Point Lookout Formation; Kcc, Cretaceous Crevasse Canyon Formation; Kg, Cretaceous Gallup Formation; Km, Cretaceous Mancos Formation; Kd, Cretaceous Dakota Formation; Jm, Jurassic Morrison Formation; Je, Jurassic Entrada Complex (includes Entrada, Todilto, Summerville, and Bluff Formations); TRc, Triassic Chinle Group; Psa, Permian San Andres Formation (including Glorieta Formation)]

Line no.	Form-ation	Data source*	Data identifier**	Latitude (NAD 83)	Longitude (NAD 83)	Date	NO_3 (as N, mg/L)	U (µg/L)	Ra 226 (pCi/L)	Ra 228 (pCi/L)	Ra 228 +226 (pCi/L)	Gross alpha (pCi/L)
391	Psa	Stone	12N.11W.25.122	35.240	107.950	05/07/57	65	NA	NA	NA	NA	NA
392	Psa	Stone	12N.11W.25.122	35.240	107.950	06/27/56	35	NA	NA	NA	NA	NA
393	Psa	Stone	12N.11W.25.213	35.240	107.950	07/11/46	27	NA	NA	NA	NA	NA
394	Psa	Stone	12N.11W.25.213	35.240	107.950	07/18/56	62	NA	NA	NA	NA	NA
395	Psa	Stone	14N.13W.19.1	35.430	108.256	07/14/70	1.2	NA	NA	NA	NA	NA
396	Psa	Stone	14N.13W.27.342A	35.415	108.203	04/07/72	.1	NA	NA	NA	NA	NA
397	Psa	Stone	15N.12W.17.123	35.531	108.131	02/08/77	.1	NA	NA	NA	NA	NA
398	Psa	Stone	15N.15W.18.3344	35.531	108.467	06/15/66	.9	NA	NA	NA	NA	NA
399	Psa	Stone	15N.15W.20.313	35.517	108.449	11/06/69	.1	NA	NA	NA	NA	NA
400	Psa	Stone	15N.15W.20.313	35.517	108.449	07/01/70	.6	NA	NA	NA	NA	NA
401	Psa	Stone	15N.15W.20.313	35.517	108.449	12/08/70	.6	NA	NA	NA	NA	NA
402	Psa	Stone	15N.15W.20.313	35.517	108.449	03/16/72	.3	NA	NA	NA	NA	NA
403	Psa	Stone	15N.16W.23.3132	35.517	108.503	05/03/50	.3	NA	NA	NA	NA	NA
404	Psa	Stone	15N.16W.23.3132	35.517	108.503	03/23/72	.1	NA	NA	NA	NA	NA
405	Psa	Stone	15N.17W.13.1142	35.531	108.590	08/18/64	1.9	NA	NA	NA	NA	NA
406	Psa	Stone	15N.17W.24.4121	35.517	108.591	02/05/42	.2	NA	NA	NA	NA	NA
407	Psa	Stone	15N.17W.24.4121	35.517	108.591	10/14/55	.2	NA	NA	NA	NA	NA
408	Psa	Stone	15N.17W.24.4121	35.517	108.591	08/25/58	.1	NA	NA	NA	NA	NA
409	Psa	Stone	15N.17W.24.4121	35.517	108.591	10/06/60	.1	NA	NA	NA	NA	NA
410	Psa	Stone	15N.17W.24.4121	35.517	108.591	02/28/63	.1	NA	NA	NA	NA	NA
411	Psa	Stone	15N.17W.24.4121	35.517	108.591	06/05/64	.1	NA	NA	NA	NA	NA
412	Psa	Stone	15N.16W.30.3443	35.502	108.574	10/02/68	.1	NA	NA	NA	NA	NA
413	Psa	Stone	12N.11W.25.213	35.240	107.950	06/22/62	29	NA	NA	NA	NA	NA

*Data sources:

Stone—Stone, W.J., Lyford, F.P., Frenzel, P.F., Mizell, N.H., and Padgett, E.T., 1983, Hydrogeology and water resources of San Juan Basin, New Mexico: Socorro, New Mexico Bureau of Mines and Mineral Resources, Hydrologic Report 6, 70 p.

RHR—Roca Honda Resources, LLC, 2009a, 11-20-2009 Permit application, Phase II of a new mine application—Baseline data report: Permit application to the Mining and Minerals Division of the New Mexico Energy, Minerals, and Natural Resources Department, http://www.emnrd.state.nm.us/MMD/MARP/permits/MARP_Permits.htm.

**Data identifiers: these values are data indicators used by the source to identify the data within the report or database.

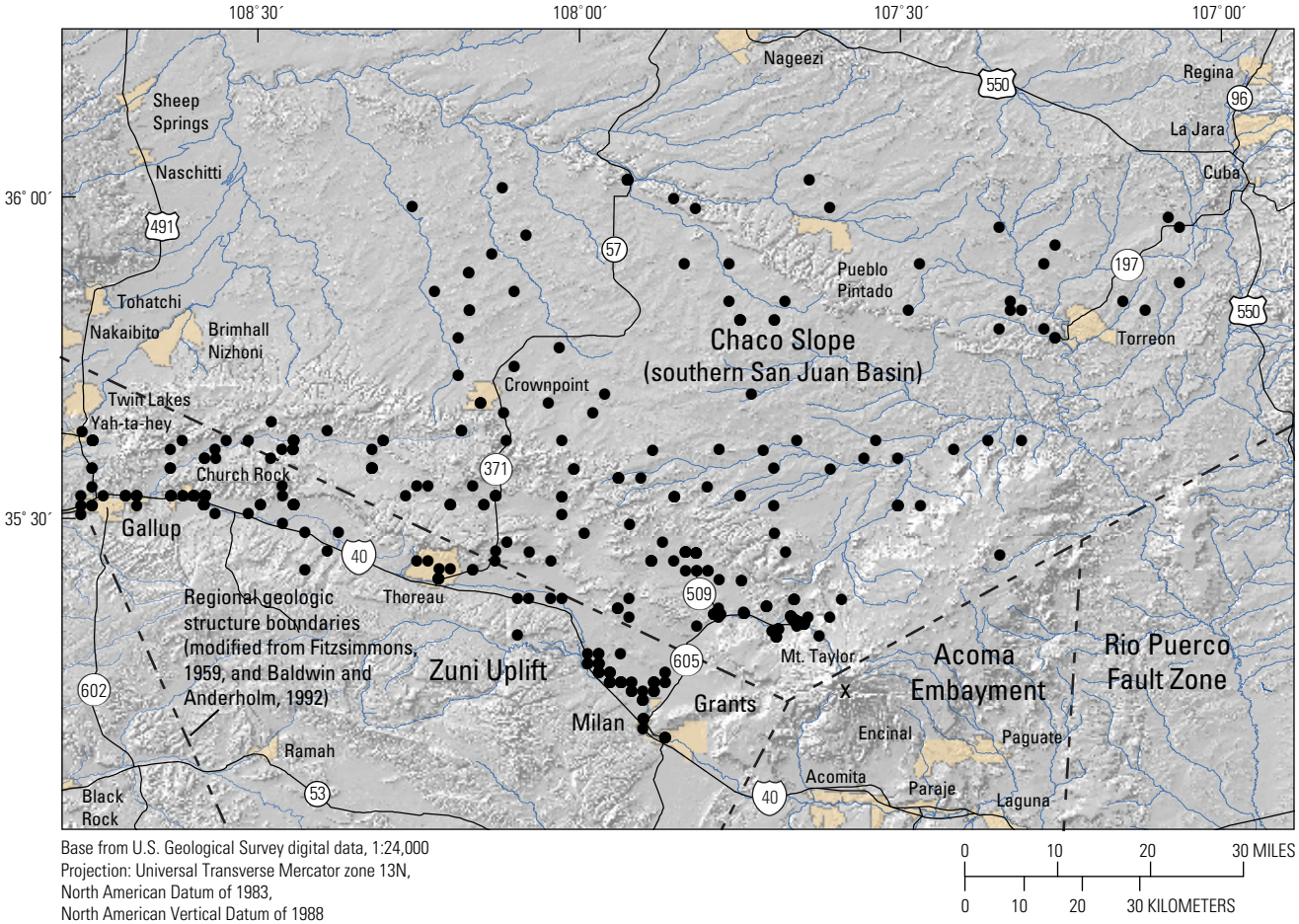

Figure 4-1. Spatial distribution of historical groundwater contaminants-of-concern data in the study area.

Publishing support provided by
Lafayette Publishing Service Center

ISBN 978-1-4113-3359-8

Printed on recycled paper